Universidade do Porto
Faculdade de Engenharia
FEUP

Filipe José Palhares Chaves

Application of Adhesive Bonding in PVC Windows

MDI
Dezembro, 2005

Application of adhesive bonding in PVC windows

by

Filipe José Palhares Chaves

A dissertation submitted for the Degree of Master of Industrial Design
at the Faculdade de Engenharia da Universidade do Porto
and Escola Superior de Artes e Design, 2005.

Abstract

Structural adhesives have been used in many industrial applications throughout the last few decades. Despite its traditional nature, the buildings constructor sector has also been using structural adhesives. For example, the windowframe PVC industry is evolving rapidly, driven by the market growth. Hence it is only logical to search for applications of structural adhesives in this emerging industry, avid for better performances in sealing and production quality.
Having this in mind, this study seeks a new technology for joining the transom to the windowframe. At the moment screw fastening is the standard, but in the near future a mechanical fastening joint of some complexity will be used.

Trying to understand if an adhesive bonded joint will perform as well as the industry standard joint techniques is the goal of this investigation. Firstly, there is the need to consider all the factors inherent to the window transom joint properties in usage. Then the joint design is studied to comply with those factors and perform as well as it is supposed to. One critical step is a proper adhesive selection, which will determine the outcome of the joint performance. The adherends and loads at stake are taken in consideration throughout this selection process. This process is also aided by predicting the joint stress values, using the finite element analysis. Tensile tests of the adhesive bulk and single lap joint specimens are done in order to validate the adhesive selection and the numerical analysis accuracy. The adhesive's glass transition temperature is also determined to establish its temperature range.

Another major concern is the joint resistance with time as function of weather and load usage conditions. To answer this ageing question, an artificial weathering process (60ºC and 80% RH) is promoted inside an environmental chamber during 105 days (more than 3 months).

Finally a process and cost analysis is done to determine whether this new T-joint adhesive bonded proposal is acceptable for industrial purposes and has any economical advantages when compared with the other available solutions.

Acknowledgments

I would like to thank:

Prof. Lucas Filipe M. da Silva and Prof. Paulo Tavares de Castro for their supervision throughout this investigation and for their patience.

Prof. José Chousal for his contribution in the correlation image analysis.

Prof. Pedro Camanho who provided his camera to obtain the best photos for the correlation image analysis, and also for the help with the finite element analysis provided by him and his co-workers.

Prof. António Torres Marques for its contribution with the Tg determination at Instituto de Engenharia e Gestão Industrial (INEGI) and his support to the industrial design cause.

Prof. José Luis Esteves for his help and some useful discussions about structural adhesives.

The technical staff of the Laboratório de Ensaios Tecnológicos (LET) who provided advice and assistance, particularly Mr. Rui Martins da Silva, Mr. José Francisco Moreira and Eng. Miguel Figueiredo.

Eng. Paulo Neves for his help in providing the mould drawings and some other technical information.

Eng. Manuel Gomes Ferreira for his help in the mechanical analysis, for the many discussions about this study details and his friendship.

The staff of Decafil who manufactured and supplied all the specimens used in this study, particularly Mr. Vitor Alexandre Lage.

Madrid's Deceuninck Iberica staff for supplying the best technical information available on PVC windows manufacture. A special thanks to Mr. António Coelho (the Portuguese Deceuninck representative) D. Francisco García García and D. Raúl Alcaina Díaz for their friendship and support.

Mr. Carlos Pinto from Huntsman® who supplied all the information about Araldite's® adhesives and discussed the best solutions for this investigation.

Mrs. Rosario from Reciplás who always supplied the Araldite adhesive batches in due time.

My family for their constant support and tolerance.

Last but not least, all my friends that bared my lack of time and despite my bad humor have been comprehensive and helpful throughout all the time of this work. A special thanks to Ana and her mother because they have always been there for me.

Contents

List of tables

List of figures

Glossary

Cold pressing - A bonding operation in which an assembly is subjected to pressure without the application of heat.

FEM – Finite Element Method. Numerical analysis of the stresses and displacements as a result of applied forces – usually done using computer.

Handling strength - state in which the resin is hard enough for the joint to be handled.

Pot-life - The maximum time from mixing to application of the adhesive system.

Setting time - the period of time during which an assembly is subjected to heat or pressure, or both, to set or cure the adhesive.

Shelf life - Maximum time from mixing the hardener into the resin (done by the adhesive manufacturer) to application, of the adhesive. This time is dependent on the storage conditions.

Isotropic – Considered to have the same properties distribution in any direction.

Resilience – The ability of a material to absorb energy when deformed elastically and to return it when unloaded.

Transom – fixed support profile which separates two different window parts (sashes).

Young's Modulus – It is a mechanical propriety that is characteristic of each material and relates to its elastic behavior.

Notation

- E ► Young's modulus
- f ► Natural frequency
- G ► Shear modulus
- I ► Second moment of area
- k ► Bending moment factor
- l ► Length
- M ► Bending moment on the adherend at the end of the overlap
- F ► Applied load
- R ► Universal gas constant
- RH ► RelativeHumidty
- T ► Temperature
- t ► Thickness
- T_g ► Glass transition temperature
- δ ► Loss angle
- ε ► Tensile strain
- γ ► Shear strain
- j ► Geometric factor
- ν ► Poisson's ratio
- ρ ► Density
- σ ► Tensile stress
- σ_y ► Tensile yield stress
- τ ► Shear stress

Chapter one

INTRODUCTION

1.1 Industrial design perspective

Throughout an industrial design development, there is the need to incorporate new technical solutions and breakthroughs which will either improve or create products and new ways to manufacture them. This development leads to innovations and increases the knowledge in technological, economical and social terms.

Bruno Munari defines a problem as a need to be satisfied [1]. He also draws a possible path that will drive the designer towards a solution as shown in figure 1.

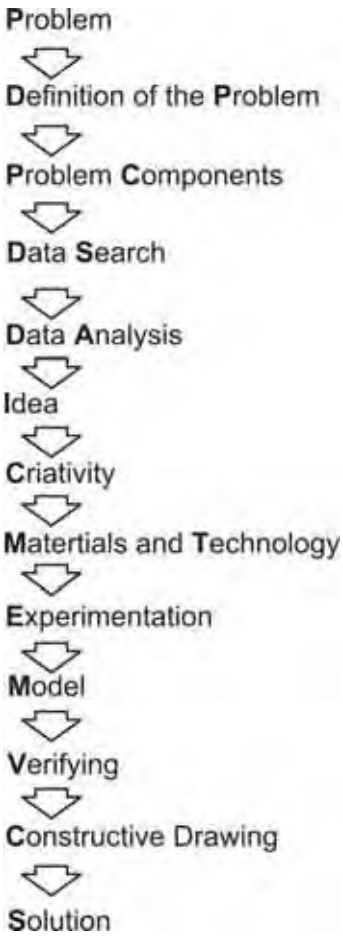

Figure 1. Path representation that drives a problem to its solution [1].

1.2 Industrial context

The windowframe industry is growing, mostly to satisfy the customer demand for better sealing solutions and thermal efficient buildings. In the past, materials like wood, steel and aluminum were used, but the market trend leads to new materials, namely composites like PVC reinforced with steel which is leading several European construction markets.

In order to build a window or door, there is the need to use tools and equipments that are in constant evolution. For PVC windowframe there are specific technologies, like welding and fastening [2].

1.2.1 PVC window manufacturing technology

PVC windowframe technology was developed in the past century, near 1950's. Deceuninck® Plastic Industries has strongly contributed in this technological development, starting its PVC-U window profile extrusion in 1965.

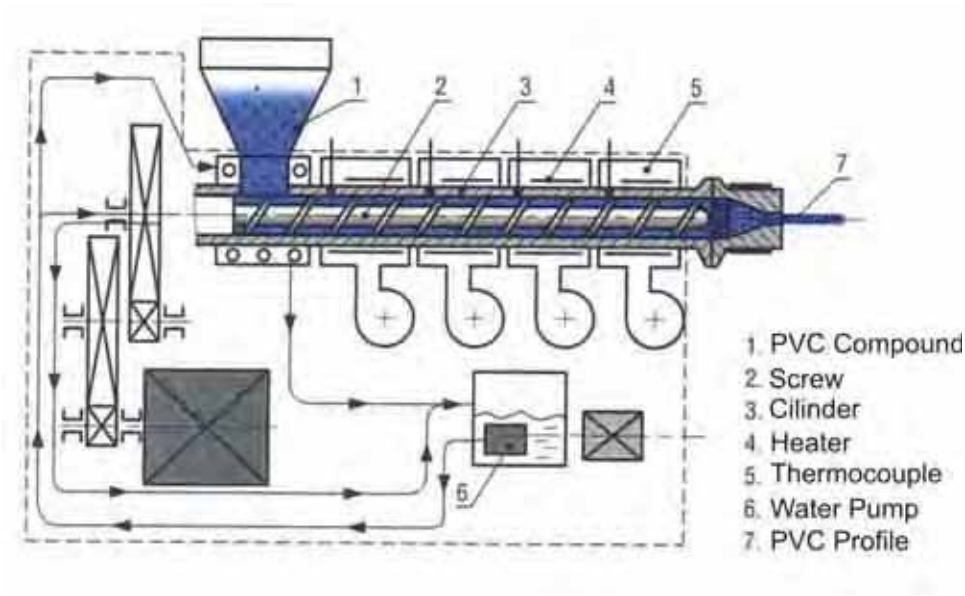

Figure 2. Extrusion machine.

In figure 2 an extrusion machine schematic drawing illustrates the production process of the PVC profile. This process introduces some surface stress on the PVC profiles, as result of the screw, the cylinder and finally the die which will

draw the profile geometry. The PVC compound DECOM1010 plays an important role in this study because it is the substrate of the studied T-joint.

Building a PVC window is a process which involves some technology, and is done following the next steps:

1. Cut the supplied 6 meters PVC profiles and steel reinforcements to the specified window size;
2. Fasten the steel reinforcements inside the PVC profiles;
3. Open the water and air channels;
4. Weld window corners in the welding machine (see figure 3), and fasten mechanical joints to transoms.
5. Clean the excess of material in the corners (figure 4);
6. Install the rubber sealants and the hardware (locks and hinges) gathering the several components;
7. Install the glass.

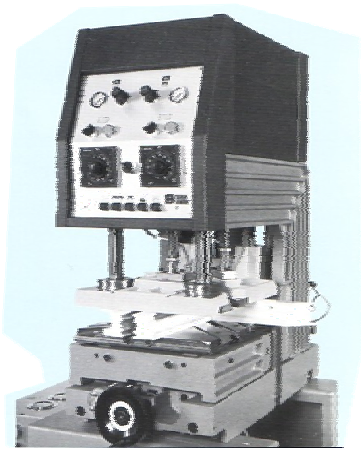

Figure 3. Welding machine.

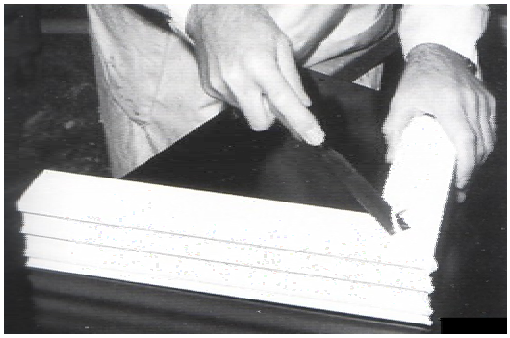

Figure 4. Manual corner cleaning.

The welding process is interesting to understand the PVC bonding technology. The next figure shows a diagram of the welding process.

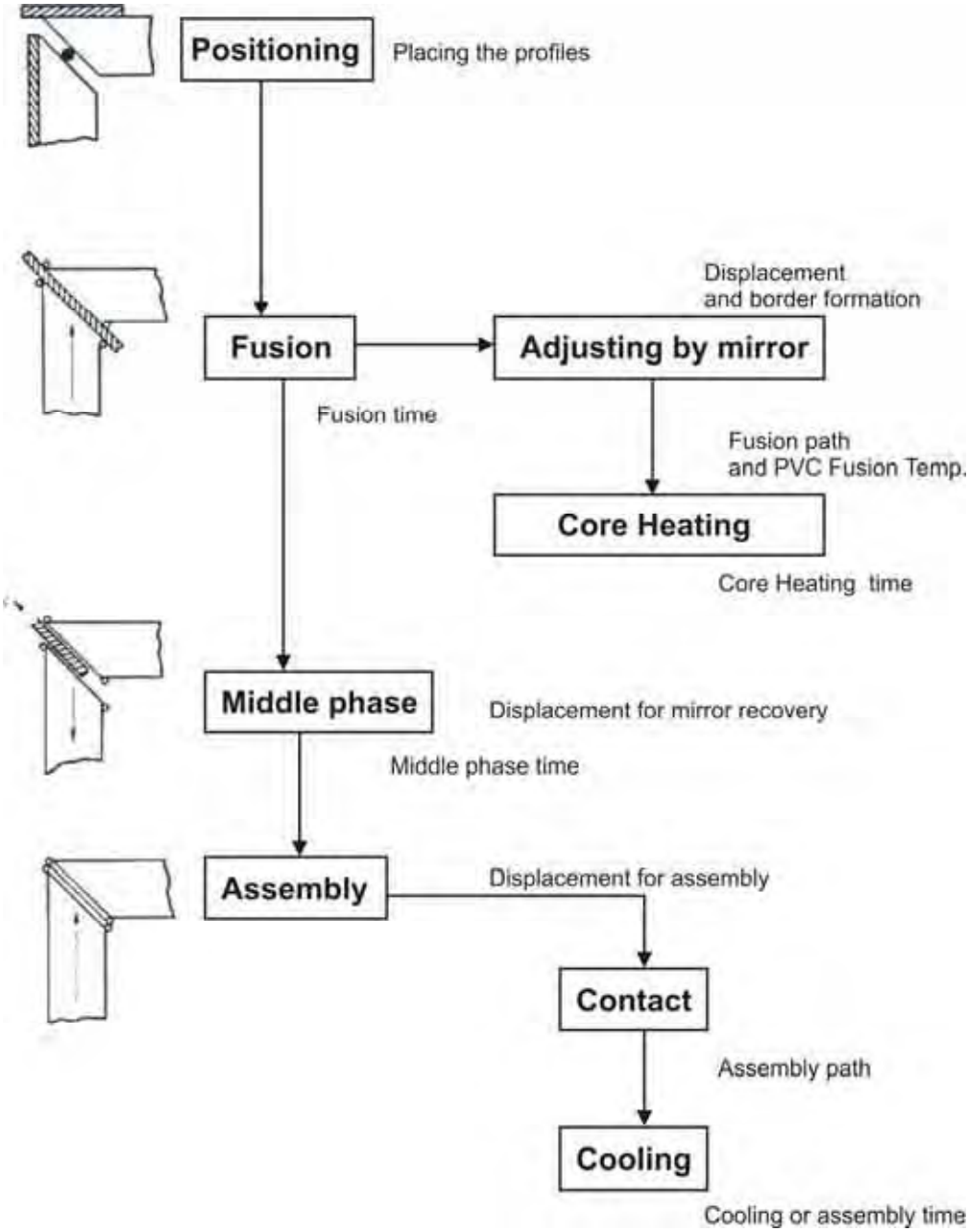

Figure 5. PVC window welding technological process schematic [3].

The PVC fusion temperature referred in figure 5 is 240-260ºC and it is adjustable in the welding machine as well as the different process times (variables of the process).

Despite the welding process advantages (figure 6), it is not such a very good process for transom bonding. This is due to a major technological manufacture complexity and the introduction of surface stresses at the interface and thermal stresses when the material is cooling. Therefore mechanical processes were developed like those shown in figures 7 and 8.

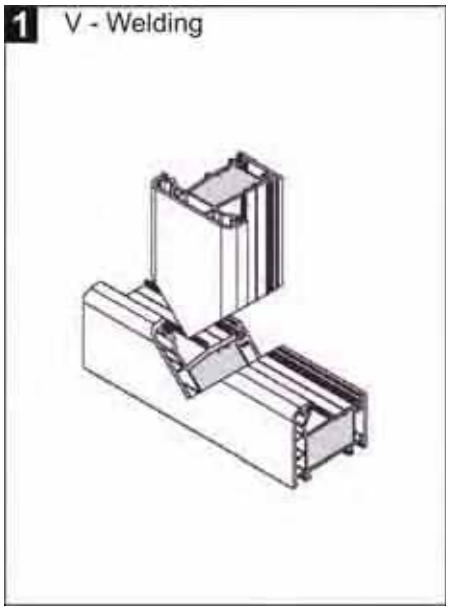

Figure 6. Transom V – welding.

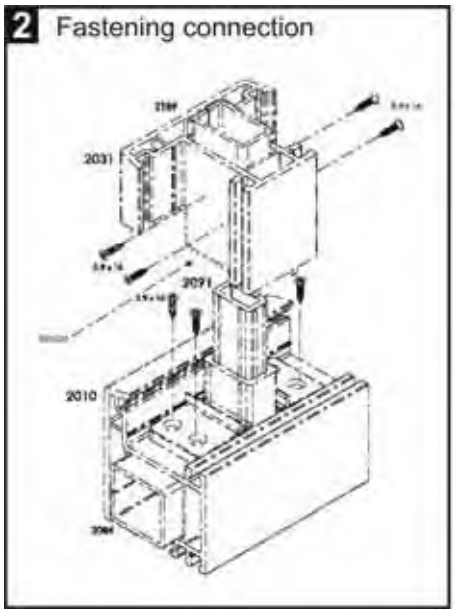

Figure 7. P2090/P2091 Fastening connection.

The fastening connection described in figure 7 uses a T profile (P2090/P2091) which is fastened through the PVC profile to the steel reinforcements. This fastening method is widely used in the industry. It needs extra finishing for optimal sealing with the deposition of silicone.

The new industry trends are mechanical connections, with structural tightening connectors and specific tools to install them. These are good solutions, despite being costly when compared to the previous case. As shown in figure 8, first the holes are drilled with the help of a proper rig (a), then the structural connector (P3270/P3273/P3274) is tightened to the transom extremities (b), after that, sealing caps are applied in the screw hole (c), then the transom is adjusted to the exterior window frame with the aid of a special tool (P3276) and fastened to stay in place (e).

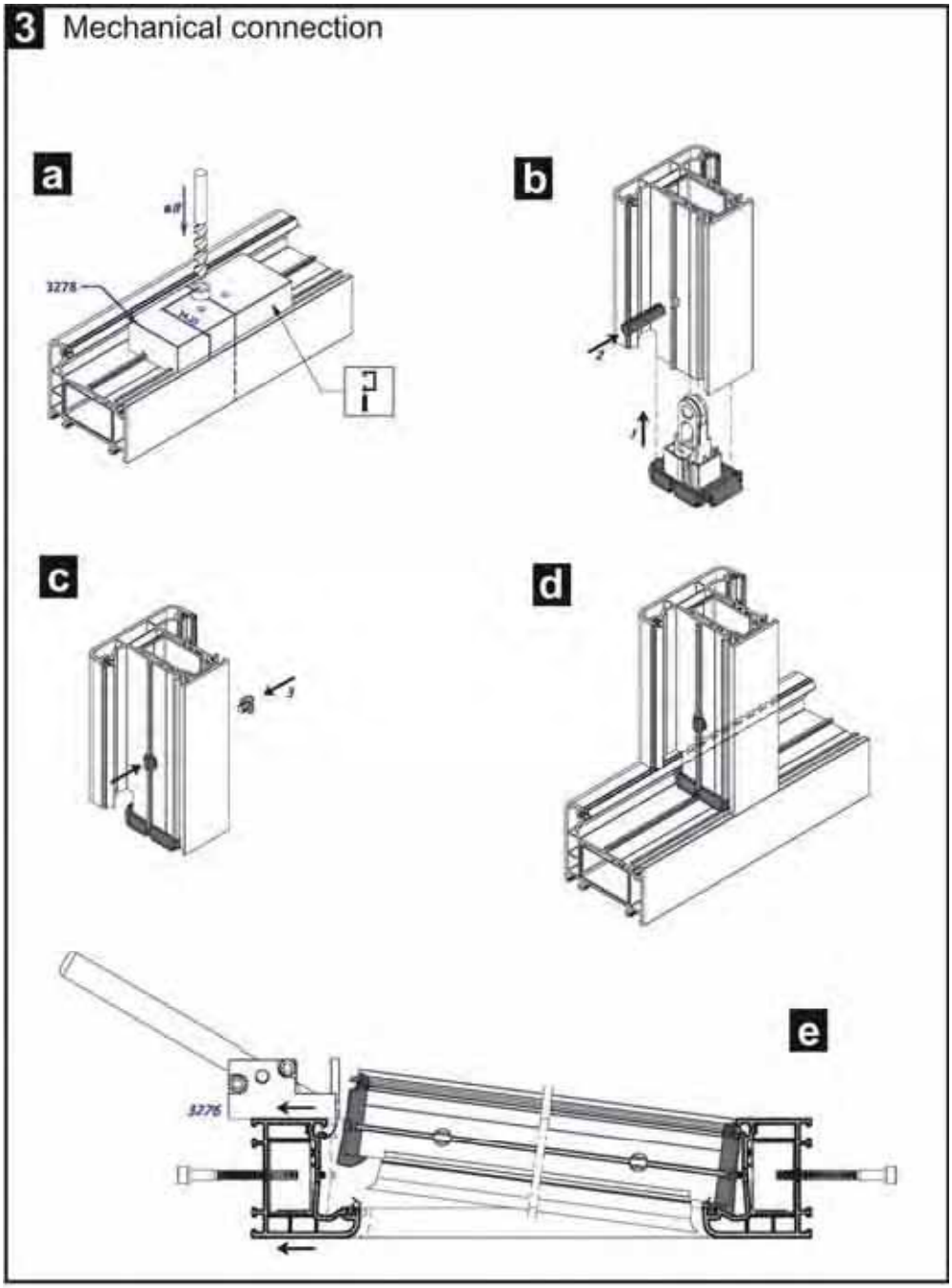

Figure 8. Mechanical connection with P3270/P3273/P3274 [4].

1.2 Definition of problem

Welding is the standard procedure for the corners of windows or doors, but when we are talking about the transom, there are some production inefficiencies and technological considerations such as the manufacturing process and the residual stress. In the last years, mechanical bonding with fasteners was the preferred method. New solutions with more sophisticated mechanical joints are now available to improve the final solution in terms of mechanical properties, visual aspect and ease of production. However, these solutions are costly.

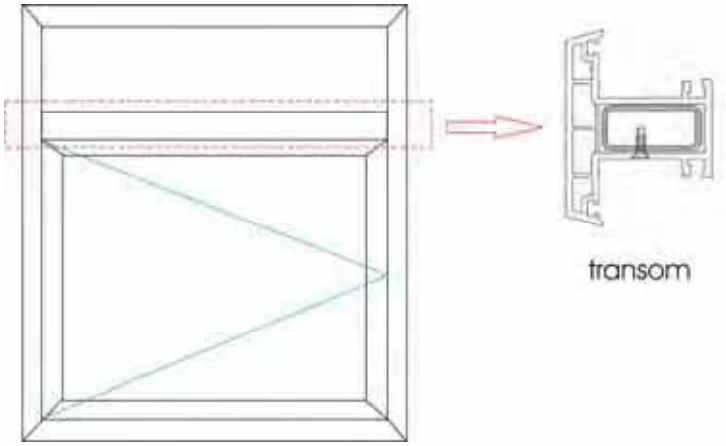

Figure 9. Transom in a window.

A transom is a structural element of a windowframe. It is supposed to be resistant to imposed forces during its use [5]. These forces are:

a. The supported weight (figure 10 a);
b. The pressure from the building interior atmosphere and exterior winds (figure 10 b);
c. The force due to closing the window against the transom (figure 10 c).

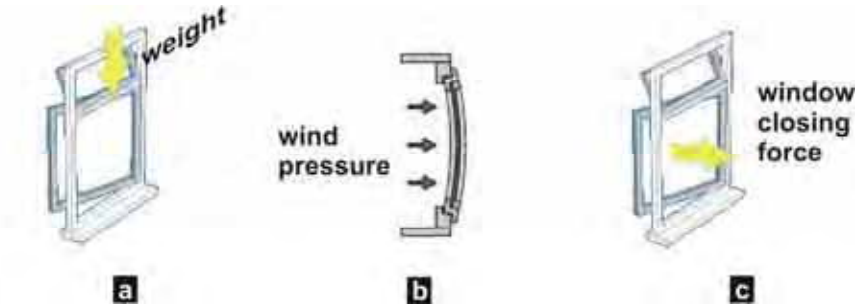

Figure 10. (a) Weight from the above sash and glass weight; (b) wind or interior atmosphere pressure; (c) window closing force.

The mechanical behavior of the windowframe must be in accordance with UNE 85220 standard, which establishes the mechanical resistance of its components.

Another important transom feature is its contribution for the air and water impermeability of the window as a sealing element (figure 11).

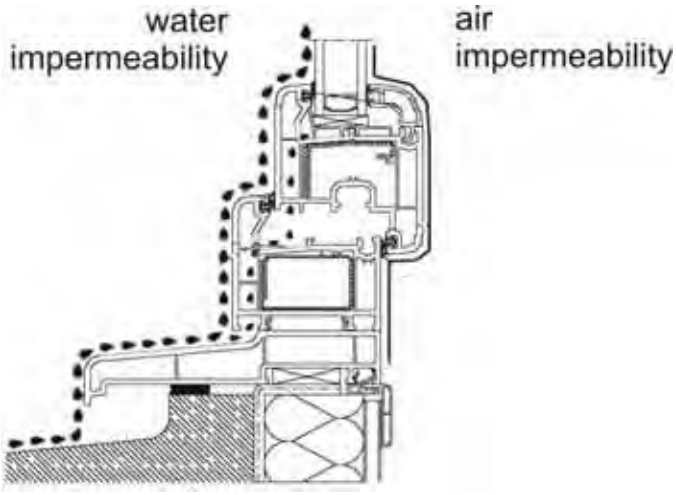

Figure 11. Windowframe water and air impermeability [4].

1.4 Solution

This study intends to investigate the possibility of using a structural adhesive for the transom bonding in a PVC windowframe. Instead of using fasteners the joint is to be bonded with an adhesive. The manufacture is studied and optimised in order to obtain the best joint strength and ease of processing.

The investigation is structured as follows:

i. a survey of structural adhesive technology;
ii. adhesive selection and testing;
iii. preliminary transom/windowframe joint tests;
iv. finite element analysis to predict the stress distribution and optimize the joint geometry;
v. cost analysis.

1.5 Historical background

Adhesion is a concept present in humankind life since the very beginnings. While studying pre-historical tribal graveyards, archeologists discovered near skeletons, clay pottery fragments glued together with resins from tree sap. Ancient Babylon temple statues with eye globes glued to eye cavities were also discovered with some kind of tar resisting to 6000 years weathering degradation.

A good example of early adhesive use is the Ícarus legend and his wings built by his father Dedalus with feathers glued together with wax that melted when Ícarus got dangerously near to the Sun.

Paintings and murals from 1500 to 1000 B.C. figure wood gluing. In the Egyptian civilization animal origin glues were used to seal the tombs. However the first bibliographic reference about adhesives and the art of adhesion dates to 200 B.C.

Circa 1 and 1500 A.C., the Greeks and Romans developed an ornamentation technique by gluing small noble wood layers. To do so, they used animal origin glues, mostly fish glue, egg whites, blood, bones, milk, cheese and some vegetables glue. In naval industry Romans used bee wax and tar in order to joint wood segments and to obtain waterproof decks.

During the following centuries gluing was a standard procedure in almost every object, from furniture to Stradivarius violins. However it was only in the eighteenth century (circa 1700) that the first industrial glue factory was settled in the Netherlands.

In England, the first patent attributed to an adhesive was about 1750, and consisted of fish glue. The following patents were for natural rubber, milk, casein and gum glues. In the early years of the twenty century, there were innumerous glue factories all over the World. Throughout the First World War,

casein adhesives were used to build wood airplanes and by the Second World War modified phenolic resins were used to promote structural connection, once again in the aeronautic industry.

Despite the fact that the knowledge and common use of adhesives remounts to early ages (4000 B.C.), it is just after the twentieth century, when polymers were developed following the industrial expansion, that we observe a sustainable, science supported, and technically based adhesive developments, enriching the knowledge database. This development was also due to the availability of a great variety of formulations improving the adhesion performance of the adhesives, by controlling mechanical properties, curing time, service temperatures and chemical resistance. A good example is the plywood industry that boosted the development of phenolic adhesives and phenolic bakelite.

Figure 12. Superglue [6].

Dr. Harry Cover, in 1942, working for Kodak, produced the cyanoacrylate used later in 1951 by Dr. Fred Joyner and Coover in Eastman under the code name Eastman n. 910 compound known as super glue (figure 12), which was a commercial hit.

These and other adhesives were and are being used in the industry as they enable better solutions and newer applications. Nowadays, they are used in the automotive, aerospace, aeronautic and other industries, in critical and high responsibility applications, due to the specific advantages of structural adhesion.


Figure 13. Notaden Frog glue [7].

Even in medicine, adhesives are used in substitution of common scar sewing to close wounds with cyanoacrylate. In dental restoration, light and UV adhesives and sealants are used. At this very moment, Adelaide University in association with the CSIRO Molecular Science Company are studying a natural glue from *Notaden* gender Australian frog which is biocompatible and wet resistant (figure 13) [7].

A chronological line of adhesive development is shown in the following table.

Table 1. Historical development of adhesives and sealants.

Approximate decade of commercial availability	Adhesive
Pre 1910	Glue from animal bones Fish glue Vegetable adhesives
1910	Phenol-formaldehyde Casein glues
1920	Cellulose ester Alkyd Resin Cyclized rubber in adhesives Polychloroprene (Neoprene) Soybean adhesives
1930	Urea-formaldehyde Pressure sensitive tapes Phenolic resin adhesive films Polyvinyl acetate wood glues
1940	Nitrile-phenolic Chlorinated rubber Melamine formaldehyde Vinyl-phenolic Acrylic Polyurethanes
1950	Epoxies Cyanoacrylates Anaerobics Epoxy alloys
1960	Polyimide Polybenzimidazole Polyquinoxaline
1970	Second-generation acrylic Acrylic pressure sensitive Structural polyurethanes
1980	Tougheners for thermoset resins Waterborne epoxies Waterborne contact adhesives Formable and foamed hot melts Polyaromatic High temperature resins
1990	Polyurethane modified epoxy Curable hot melts UV and light cure systems

1.6 Adhesive Market

In 1995 the adhesive market represented about 26 billion dollars and was growing 3% every year (8-9% in emergent Asiatic markets).

The market segmentation is represented in the following figures [8]. General purpose adhesives represent the major part of the market (51%), followed by binders, hot melts and engineering adhesives. Figure 14 shows that "packaging" and industrial assembly are the two leading end-use markets for adhesives, followed closely by wood and its related products.

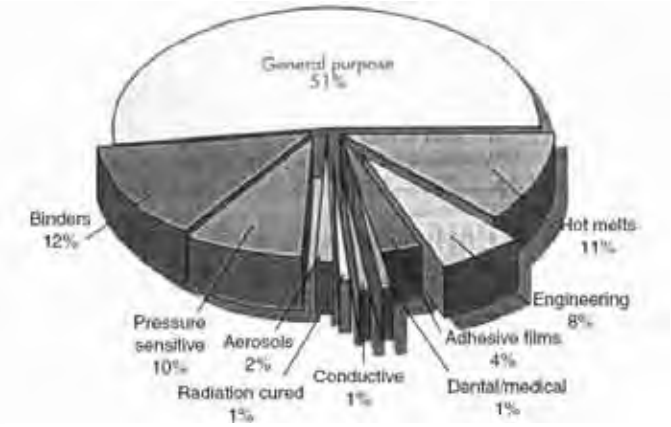

Figure 15. Leading Adhesives and Sealants Products 1995 - Basis: $9.2 Billion [8].

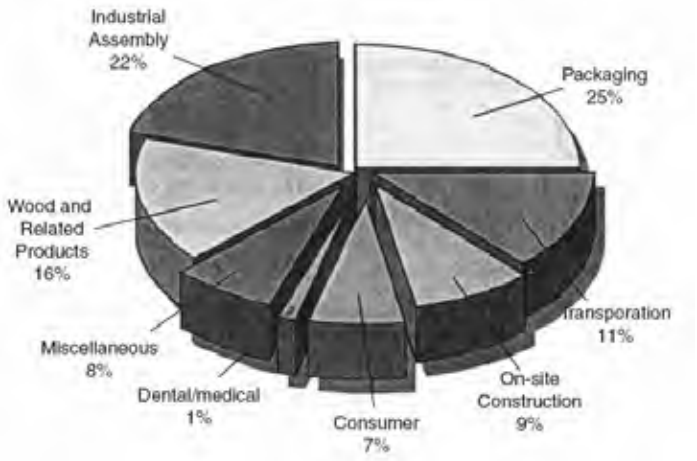

Figure 14. Leading Adhesives and Sealants End-Use Markets 1995 - Basis: $9.2 Billion [8].

Geographically, the market distribution was analysed in 2000 by the ChemQuest Group and is distributed as shown in figure 16. Europe and U.S.A are the two leading markets for adhesives. Recently the Asian market is becoming more relevant because of the Chinese industrial booming.

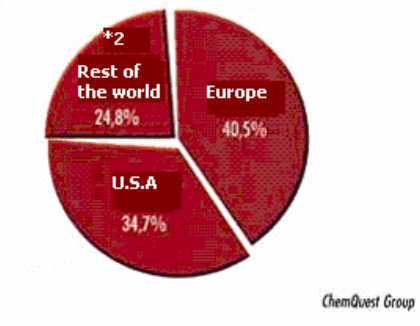

*2 Asia, Lat. América, Africa.

Figure 16. World adhesive markets.

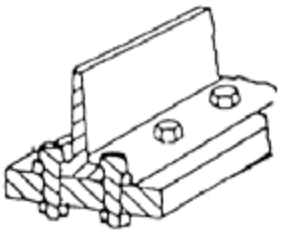

Figure 17. Periodic – Rivets; Screws; Spot welding.

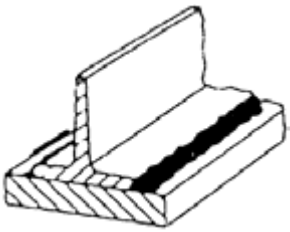

Figure 18. Linear – Welding.

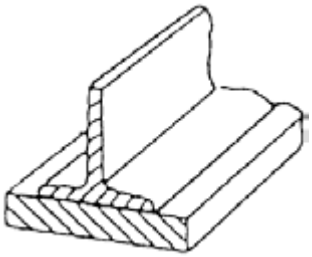

Figure 19. Area – Soldering; Brazing; Bonding.

1.7 Joining Methods Comparison

There are several competitive joining methods such as mechanical fastening, welding and adhesive bonding. The advantages and disadvantages of each technique are presented in the next page (table 2). In this table we can see a comparison between several aspects of the joining technology and production aspects.

There are three general joining methods that differ significantly from each other:

1. Periodic – occasionaly some holes are made in the two components to join with fasteners or other mechanisms (figure 17);
2. Linear – edges bead junction (occasionaly or continuously) just like a weld line (figure 18);
3. Area – this is characterized by a full face contact of the components surfaces to attach togethter (figure 19).

Adhesives may be used in periodic or linear joining methods, but the best attachment performance is achieved by the area joining method. This aspect is illustrated in figure 20, where adhesive bonded joints have a uniform stress distribution while the periodical methods add high stress points near the rivets, fasteners or spot welds. Another important point is the stiffening effect due to a wider bonded area in adhesive joints, reducing the unstiffened area, as shown in figure 21.

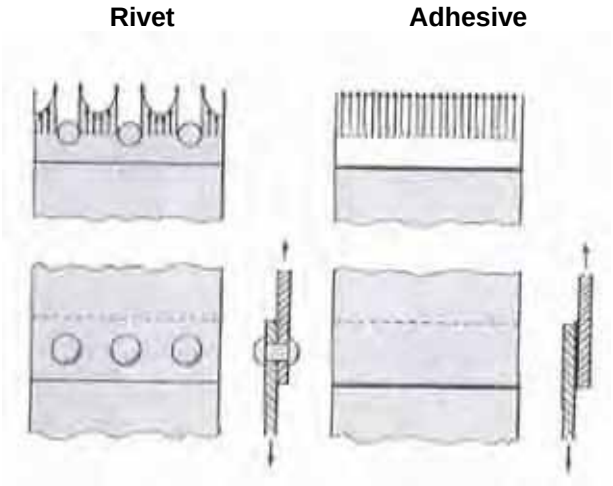

Figure 20. Stress distribution in loaded joints [9].

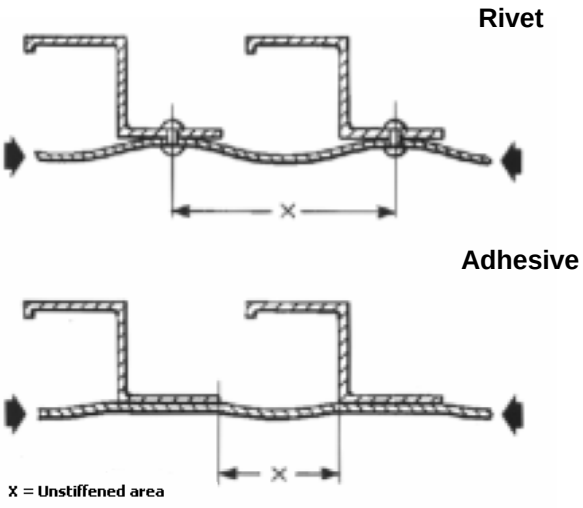

Figure 21. Stiffening effect [9].

	Welding	Brazing and Soldering	Mechanical Fastening	Adhesive Bonding
Joint Features				
Permanance	Permanent joints.	Usually permanent (soldering may be nonpermanent).	Threaded fasteners permit disassembly.	Permanent joints.
Stress Distribution	Local stress points in structure.	Fairly good stress distribution.	Points of high stress at fasteners.	Good uniform load distribution over joint area (except in peel).
Apppearence	Joint appearance usually acceptable. Some dressing necessary for smooth surfaces.	Good appearance joints.	Surface discontinuities sometimes unacceptable.	No surface marking. Joint almost invisible.
Materials Joined	Generally limited to similar material groups.	Some capability of joining dissimilar metals.	Most forms and combinations of materials can be fastened.	Ideal for joining most dissimilar materials.
Temperature Resistance	Very high temperature resistance.	Temperature resistance limited by filler metal.	High temperature resistance.	Poor resistance to elevated temperatures.
Mechanical Resistance	Special provision often necessary to enhance fatigue resistance.	Fairly good resistance to vibration.	Special provision for fatigue and resistance to loosening at joints.	Excellent fatigue properties. Electrical resistance reduces Corrosion.

	Welding	Brazing and Soldering	Mechanical Fastening	Adhesive Bonding
Production Aspects				
Joint preparation	Little or none on thin material. Edge preparation for thick plates.	Prefluxing often required (except for special brazing processes).	Hole preparation and often tapping for threaded fasteners.	Cleaning often necessary.
Post-processing	Heat transfer sometimes Necessary.	Corrosive fluxes must be cleaned off.	Usually no post-processing — occasionally re-tightens in service.	Not often required.
Equipment	Relatively expensive, bulky and often required heavy power supply.	Manual equipment cheap. Special furnaces and automatic unit expensive.	Relatively cheap, portable and "on-site" assembly.	Only large multi-feature, multi-component dispensers are expensive.
Consumables	Wire, rods, etc., fairly cheap.	Some special brazing fillers expensive. Soft solders cheap.	Quite expensive.	Structural adhesives somewhat expensive.
Production rate	Can be very fast.	Automatic processes quite fast.	Joint preparation and manual tightening slow. Mechanized tightening fairly rapid.	Seconds to hours, according to type.
Quality assurance	Non Destructible Test methods applicable to most processes.	Inspection difficult, particularly on soldered electrical joints.	Reasonable confidence in torque control tightening.	NDT methods limited.

Table 2. Joint features and production aspects comparison board [8].

The main disadvantages of adhesive bonding are the peel and cleavage loads, the high temperature limitations, the poor chemical resistance, the curing time, the process controls and the in-service repairs.

Cleavage and peel stresses are undesirable for adhesively bonded joints. Forces at one end of a rigid assembly acting to peel the adherends apart induce cleavage stresses. Peel stresses occur when these forces are applied to one end of a joint where one or both of the adherends are flexible. The flexibility of the adherends results in a greater separation angle for peel than for cleavage.

Adhesives are mostly polymers or synthetic resins, and these materials suffer a transition from glass to rubber properties once they are at high temperatures (generally 100-200ºC) leading to a lower bond strength and posterior failure.

Some adhesives are affected by ambient corrosion factors or surrounding materials causing chemical degradation of the bonded joint.

Most common adhesives require a curing time in order to obtain the maximum resistance. This can represent a disadvantage when compared to mechanical attachments that are immediate.

Once an adhesive joint is badly made it can not be corrected because the joint is difficult to dismantle. The process controls must have high standards and sometimes these are unfamiliar.

Chapter two

MECHANISMS OF ADHESION

2.1 Forces of adhesion

There are several types of forces contributing to the strength of adhesives and the strength of the bonds which they make. The bond types and their corresponding energies are compared in table 3.

2.1.1 Primary or chemical forces

i. Covalent Bonds

These are chemical bonds which promote molecule formation, binding atoms together in two ways:

a. Nonpolar bonds occur when there are two electrons evenly distributed between the two atoms, mainly when identical atoms are bonded together or when the two atoms have similar attractive capacities for electrons (electronegativity);

b. Polar bonds occur when the atoms have different electronegativity and the electrons are attracted to the most electronegative resulting in an electrical dipole.

ii. Ionic Bonds or inter-ionic forces

When two ions of opposite charge are separated by a distance r, a force of attraction is generated, and can be valued by:

$$F = \frac{q_1 q_2}{4\pi\varepsilon_0 k r^2} \qquad \text{Eq. (2.1)}$$

q_1 and q_2	$\Rightarrow$	Ionic charges;
k	$\Rightarrow$	Relative permittivity of the surrounding ions medium.
ε_0	$\Rightarrow$	Permittivity of vacuum

This is the case for oxide surfaces on metals, and it is known that any ion such as $-O^-$ produced on the surface of an epoxy during cure, is strongly attracted to that oxidized metal surface.

Note that because water has a very high permittivity, it easily penetrates in bonded joints, strongly reducing inter-ionic forces. This is a possible explanation for the degradation of adhesive joints by water.

2.1.2 Secondary or physical forces

i. Van der Waals forces

These forces are the result of the interaction between molecule dipoles. There are three types:

a. Dispersion or London forces;
b. Debye forces;
c. Keesom forces.

ii. Hydrogen Bonds

This bonding occurs when an hydrogen atom is chemically bonded to a very electronegative atom, making it very susceptible to establish a bond (hydrogen bond) with another electropositive atom, with a non-bonded pair of electrons. Hydrogen bonds are stronger than Van der Waals forces. For example they are responsible for the high boiling point of water, as shown in figure 22.

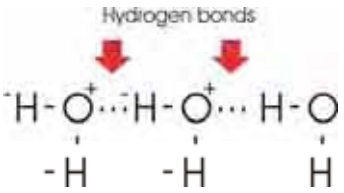

Figure 22. Schematic hydrogen bonds.

iii. Acid-base interactions

These interactions are related to the two definitions of acids and bases, known as:

1. Br∅nsted and Lowry, which define an acid as a proton donor and a base as a proton acceptor;

2. Lewis, which defines an acid as an electron acceptor and a base as an electron donor;

Table 3 shows the bonding types and their bond energies.

Table 3. Bond types and typical bond energies [10].

Bond type		**Energy** [kcal/mol]	**Distance** [Å = 10^{-10} m]
Primary Atomic Bonds			
Chemical Bonds	Ionic	140 to 250	1 to 2
	Covalent	15 to 170	
	Metallic	27 to 85	
Secondary Atomic and Molecular bonds			
Van der Waals bonds	Dispersion (London)	up to 10	4 to 5
	Debye forces	up to 5	3 to 4
	Keesom forces	up to 0,5	4 to 5
Hydrogen bonds		up to 15	3
Donor-acceptor bonds			
	Bronsted acid-base interactions	up to 240	
	Lewis acid-base interactions	up to 20	

The primary and secondary bonding forces will rapidly fall when the distance between the “active points” (bonding forces zones) is greater than 5 Å as shown in the figure 23. That is the reason why adhesives have to be applied in the liquid form to make an “intimate” contact with the adherend and enable the bonding forces to act. After that, the adhesive must harden (cure) to resist separation.

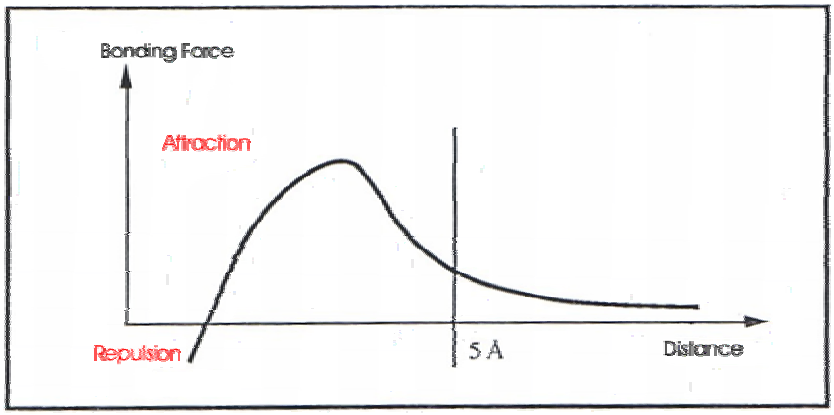

Figure 23. Atomic bonding forces vs. distance.

2.2 Theories of adhesion

The main theories of adhesion are described next:

2.2.1 **Mechanical interlocking theory** – Proposes that the major source of adhesion resides in the interlocking or mechanical keying of the adhesive into the irregularities of the substrate. This requires an uneven surface of the substrate. However Tabor et al. [11,12] and Johnson et al. [13] demonstrated that adhesion can be obtained with smooth surfaces.

A mechanical interlocking is possible with porous surface wood, with honeycomb structure formed on aluminum alloys by etching or anodizing in acid baths.

The surface roughness can be obtained:

Mechanically – Some mechanical abrasion will increase the joint strength, mostly by ensuring that the substrates are free of oil, grease or any other contaminant. There are some other effects like the increase of thermodynamics and kinetics of adhesive wetting, and the wider interfacial bonding area [10].

Chemically – Chemical pretreatments produce a surface topography suitable for mechanical interlocking. There are also some studies that emphasize the different aspects of surface topography dendrites and pyramids [14], as shown in the next table.

Table 4. Peel adhesion of electroformed copper foil to epoxy laminates [14].

Surface topography of copper foil Description	Diagrammatic Representation	Peel Energy kJ/m2
Flat		0.66
Flat + 0.3 μm dendrites		0.67
Flat + 0.3 μm dendrites +oxidation		0.77
3 μm high-angle pyramids		1.0
2 μm low-angle pyramids + 0.3 μm dendrites		1.3
2 μm low-angle pyramids + 0.3 μm dendrites + oxidation		1.5
3 μm low-angle pyramids + 0.3 μm dendrites + oxidation		2.4
Nickel foil with club-headed nodular structures		2.3

Figure 24. Scanning electron micrographs of the fracture surface of polyethylene/copper joints showing the polyethylene remaining on: (a) a smooth chemically polished copper subtsrate, (b) a micro-fibrous cooper substrate [15].

With polymers, a microfibrous surface topography increases the joint strength, as observed by Packam [16] with adhesion of polyethylene (as hot-melted adhesive) to metallic substrates, as shown (figure 24).

2.2.2 Physical adsorption theory – This is the most widely applicable theory, considering that the adhesive and substrate are in intimate molecular contact, and weak attractive forces, known as van der Waals forces (secondary bonds), operate between them. There are two types: the weaker dispersion forces and the somewhat stronger polar forces. Van der Waals forces occur between any two molecules in contact, meaning that they are present in all adhesive bonds. There may be hydrogen and chemical bonds promoting a chemisorption (see table 3).

.

Kusaksa and Suetaka [17], observed the formation of interfacial hydrogen bonds between the carbonyl groups on the cyanoacrylate adhesive and hydroxyl groups on the surface of the aluminium oxide. Pritchard also puts in evidence hydrogen bonding in nylon cords/rubber and resorcinol-formaldehyde [18]. A practical application of this case is the production of tires.

Chemical adsorption theory – According to the chemistry of the interface, several types of primary bonds can be formed across the interface such as covalent or ionic. According to Banks and Rowell [19] these interactions can be formed when adhesives containing isocyanate hardeners are used with surfaces containing active hydrogen atoms, such as hydroxyl groups on wood or glass. Indeed, infrared evidence of covalent primary bonds between a polyurethane adhesive and epoxy based primers was found by Klein et al [20] with the highest joint strengths. It is also known that covalent bonds are formed when silane coupling agents are used in glass [21].

Ionic bonding was observed between polymeric adhesives such as polyacrylic acid and metal oxides, used as filling materials for restoring teeth and for adhesively bonding inlays and crowns [22,23,24]. This ionic bonding between polyacrilic acids and zinc oxide surface is shown schematically by Chu et al. [24] in figure 25.

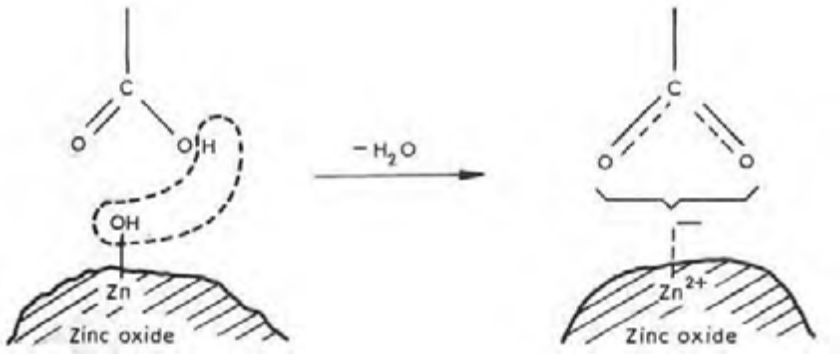

Figure 25. Possible reaction scheme for ionic bonding between a polyacrylic acid and a zinc oxide surface [24].

2.2.3 Electrostatic or electric theory – Implies electron transfer between two surfaces. The force of attraction at the interface is the result of an electrical double layer formed by electrons transferred to balance the energy levels. This seems to be obvious for metals, but not to polymers which do not have conduction bonds. This theory was primarily studied by Deryaguin and co-workers [25] who related this known electron law with the intrinsic adhesion properties. In their studies the adhesive/substrate system was treated as a capacitor which is charged due to the contact of two different materials. Deryaguin [26] proved this theory by conducting peeling experiments on plasticized polyvinyl chloride/glass, natural rubber/glass and natural rubber/steel interfaces in air or argon at different gas pressures.

2.2.4 Diffusion theory – Defined by the inter-diffusion of polymer molecules so that the boundary eventually disappears. Mostly applicable to identical non-crosslinked polymers in contact, such as with contact adhesives, and the solvent-welding of thermoplastics such as polymethylmethacrylate. This theory is not valid for adhesive bonds with metallic materials [27] .

When plastic materials possess similar solubility parameters, inter-diffusion plays an important role in plastic welding technology [28]. Polymer chains in surface layers are given sufficient mobility to inter-diffuse either by the application of heat or a suitable solvent over the regions to be bonded. The solvent is required to plasticize strongly the surface of the polymers, resulting in a large increase in free volume and hence in the chain mobility of the polymer in the interfacial region, increasing the rate and extent of inter-diffusion of the polymer chains. This technique is mostly confined to glassy thermoplastics, such as polycarbonates, acrylic polymers, etc. which have no major structural restrictions of their molecular chains, and weaker crosslinks.

The PVC industry uses an adhesive Deceuninck Decocol (figure 26), which acts as solvent cementing. However this adhesive is not for structural applications. It is used for simple bonding of small parts.

Figure 26. Deceuninck's cement adhesive.

Solvent-cemented joints of similar materials are less sensitive to thermal cycling than joints bonded with conventional adhesives because there is no stress at the interface due to differences in thermal expansion between the adhesive and the substrate.

2.2.5 Weak boundary layer theory – States that clean surfaces are capable of forming strong adhesive bonds, which can be prevented by a layer of contaminant which is cohesively weak such as oils, greases or rust on steel. In some cases the adhesives can dissolve these contaminants. Clean surfaces of most of the materials can form strong adhesive bonds in dry conditions. There are some exceptions, namely low surface energy polymers such as polyethylene, polypropylene, polytetrafluoroethylene and silicones [29] .

The adhesive selected for this study was an acrylate and the substrates are PVC. The surface preparation consists of acetone cleaning (see chapter 4). Therefore, the adhesion forces will be mostly due to physical adsorption with mechanical interlocking because the PVC surface is not perfectly smooth.

Chapter three

ADHESIVES

3.1 Adhesive classification

The adhesion science is sustained by the knowledge of several disciplines. It is a truly wide field of exploration in search for better and better solutions.

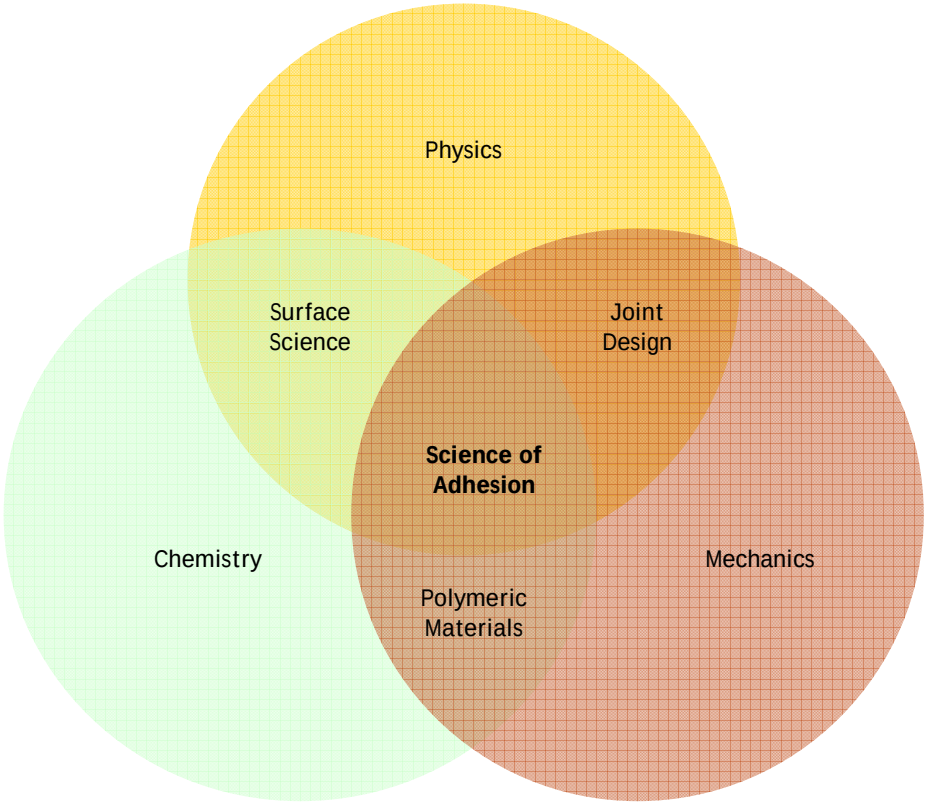

Figure 27. Science of adhesion; Multidisciplinary graph [8].

The aspects of multidisciplinary integration are reflected in figure 27, where the science of adhesion assumes the central position as a result of the integration of other disciplines.

This study will be particularly centered in the joint design, not discarding the other disciplines.

Adhesives may be classified by:

1. Function;
2. Materials to bond;
3. Physical form;
4. Application and cure requirements ;
5. In-service durability;
6. Chemical composition.

These distinctions are all interconnected at some level.

3.1.1 Function

This criterion classifies adhesives in structural and non-structural adhesives. Structural adhesives are supposed to hold together structures and resist high loads in most environments.

If the adhesive has a shear strength value greater than 7 MPa (1000 psi), then it is assumed to be a structural adhesive. In the next table adhesives are listed as structural or not.

Table 5. Several adhesives function/performance classification.

ADHESIVES	
Structural	**Non structural**
Epoxy Epoxy Resins Curing agents	Elastomeric Resins Asphalt Butyl rubber Polyisobutlyene Polyvinyl methyl ether
Epoxic Hybrids Toughened Epoxys Phenolic Epoxys Epoxy nylon Epoxy Polysulfide Epoxy vinyl	Thermoplastic Resins Polyvinyl acetal Polyvinyl acetate Polyvinyl alcohol Ethylene vinyl acetate Polyester (saturated) Polysulfone Phenoxy
Phenolic Modified Phenolic Nitrile Phenolic Vinyl Phenolic Neoprene Phenolic	Inorganic Resins Sodium silicate Phosphate cements Litharge cement Sulfur cement
Acrylic	Natural organic resins Agricultural glues Animal glues
Modified acrylic	
Polyurethane	
Cyanoacrylate	
Aromatic high temperature systems Polyimide Bismaleimide Polybenzimidizole	
Resorcinol and phenolresorcinol formaldehyde	
Melamine and urea formaldehyde	
Polysulfide Silicone	

3.1.2 Materials to bond

The substrate to bond is another way to classify adhesives. Some examples are: metal adhesives, wood adhesives and vinyl adhesives, in accordance to the substrate they will bond.

3.1.3 Physical form

The availability of adhesives assumes different physical forms. The most common are:

- **One part solution (Liquid)** - Free flowing adhesives supplied in a ready to apply solution – not requiring mixing;
- **Solid (tape, film, etc.)** – Do not require metering or mixing, and are easier to handle;
- **One Part solventless (liquid or paste)** – Do not require mixing and therefore give litle waste;
- **Multi Part solventless (liquid or paste)** – Require metering and mixing before application, involving a certain waste.

The difference between liquid and solid adhesives resides on their viscosity and therefore the method of application. The adhesives supplied are initially solid, but will go liquid with temperature to make intimate contact with surface. For instance, pastes need tools like trowels and caulking guns to ensure the best distribution.

The next table shows advantages and remarks of these physical forms.

Table 6. Physical forms advantages and remarks [8].

Type	Remarks	Advantages
Liquid	Most common form; practically every formulation available. Principally solven-dispersed	Easy to apply. Viscosity often under control of user. Major form for hand application
Paste	Wide range of consistencies. Limited formulations; principally solid modified epoxies	Lends itself to high production setups because of less time wait. High shear and creep strengths
Powder	Requires mixing or heating to activate curing	Longer shelf life; mixed in quantities needed
Mastic	Applied with trowel	Void-filling, non flowing
Film, tape	Limited to flat surfaces, wide range of curing ease	Quick and easy application. No waste or run-over; uniform thickness
Other	Rods, supported tapes, precoated copper for printed circuits, etc.	Ease of application and cure for particular use

3.1.4 Application and cure requirements

The application and the way the adhesive reacts or solidifies is another distinction. An adhesive can solidify by:

- **Chemical reaction** - with a hardener or reaction with an outside energy source such as heat, radiation, surface catalyst, etc;
- **Loss of solvent or loss of water** –harden by the evaporation of the carrier (water or solvent) in air or diffusion in porous substrates. The carrier intends to lower the viscosity so it is easily applicable ;
- **Cooling from a melt** – generally thermoplastics that melt when heated and harden when cooled.

Several adhesives require one or more of the above mechanisms to solidify, adding some versatility to its applications.

3.1.5 In-service durability

The durability and the resistance of adhesives also allows to classify them as acid-resistant adhesives, heat-resistant adhesives, and weatherable adhesives, indicating the environments for which each they are best suited.

3.1.6 Chemical composition

The chemical composition of an adhesive tells us if it is a thermoplastic, a thermoset, an elastomer, or an hybrid (composition of two or more also known as alloy).

i. Thermoplastic adhesives

Thermoplastics are polymers with a branched or linear molecular structure, as shown in figure 28, which melt or soften under heat action. Thermoplastic adhesives can be melted with application of heat and then applied to the substrate. The cure process occurs by cooling.

Another option to obtain a flowable adhesive is to use a solvent to dissolve the thermoplastic. The adhesive hardens when the solvent evaporates.

Thermoplastic adhesives can also be applied to a surface waiting for posterior “activation” by moisture, heat or solvent, just like the mailing envelope adhesive.

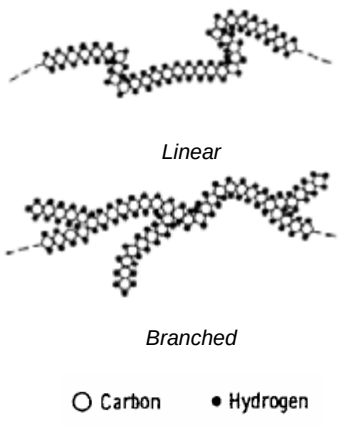

Figure 28. Linear and branched molecular structures (thermoplastic) [8].

ii. Thermosetting adhesives

The major features of thermosetting adhesives reside in their cross-linked molecular structure after cure. Contrary to thermoplastics, these adhesives cannot be softened by heat once cured.

Depending on their typology, thermosetting adhesives cure at room or elevated temperature by an irreversible chemical reaction called crosslinking. It is characterized by two linear polymers linked to form a three dimensional chemical rigid structure (figure 29).

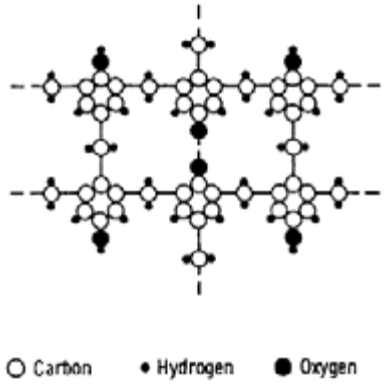

Figure 29. Cross-linked molecules (thermossets) [8].

There are some “room temperature” thermosseting adhesives that cure by internal reactions that provide the curing heat in a process called exotherm.

iii. Elastomeric adhesives

This chemical distinction is due to the rheological properties of elastomeric adhesives. Although elastomeric adhesives can be thermoplastic or thermosetting, the elastomeric resin in which they are based provides high extension and compression capabilities, having a big energy absorption characteristic. This fact makes them a good choice for joint designs with nonuniform loading.

These adhesives are characterized by low modulus, high toughness and a high degree of elongation, making them the best choice to bond substrates with different thermal expansion coefficients.

iv. Hybrid or alloy adhesives

The hybrid adhesive concept aims to combine one or more of the previous adhesive types in order to obtain a mixture improving certain properties. However this has not been easy to obtain, because of the negative impact that some chemical and physical properties have on each adhesive type. Two hybrid systems have been created recently to obtain a better formulation:

1. Reactive hybrids – two liquids that blend and react together in order to cure;
2. Dispersed phase hybrids – discrete flexibilizing particles are incorporated in a resin matrix.

These adhesives are characterized by high peel, impact and shear strengths even at high temperatures and also by a good chemical resistance. In oily substrates, the hybrid adhesives tend to form good bonding because of oil absorption acting as a flexibilizer in the adhesive formulation.

3.2 Adhesive types

There are many adhesives used in bonding processes, but after the last century scientific developments, the industry standard adhesives are:

3.2.1 Epoxy adhesives

Figure 30. 3M® epoxy adhesive film.

Epoxies - These adhesives consist of a formulation composed of an epoxy resin and a hardener. There are many resins and also many different hardeners, allowing a great versatility in formulation. There are epoxy hybrids such as: toughened epoxies, epoxy-phenolics, epoxy-nylon, epoxy-polysulfide and epoxy-vinyl. Their good wetting characteristics offer a high degree of adhesion to almost all substrates resulting in extremely strong durable bonds. These characteristics make them suitable for a wide range of applications.

Epoxy adhesives are available in one-part or two-part .They can be supplied as flowable liquids or highly thixotropic products with gap-filling capability of up to 25 mm, or as films as shown in figure 30.

Epoxy polyamide (epoxy nylon) – The polyamide resin acts as a hardener and a flexible agent. These adhesives have a better flexibility and a large increase in peel strength compared with unmodified epoxy adhesives. In addition, epoxy-nylon adhesives have good fatigue and impact resistance

Epoxy polysulfide – The polysulfide resin contributes for a better chemical resistance. These are good adhesives to bond different substrates, on account of their flexibility that allows different thermal expansions.

Epoxy phenolic – Epoxy temperature resistance is improved by the phenolic resin, allowing to sustain temperatures of 200ºC with good peel properties.

Epoxy vinyl – Certain vinyl resins improve impact and peel strength. However the temperature resistance will be reduced by the lower vinyl glass transition temperature (Tg).

Figure 31 shows the effect of temperature on the tensile shear strength of modified epoxy adhesives tested with aluminum substrates [8].

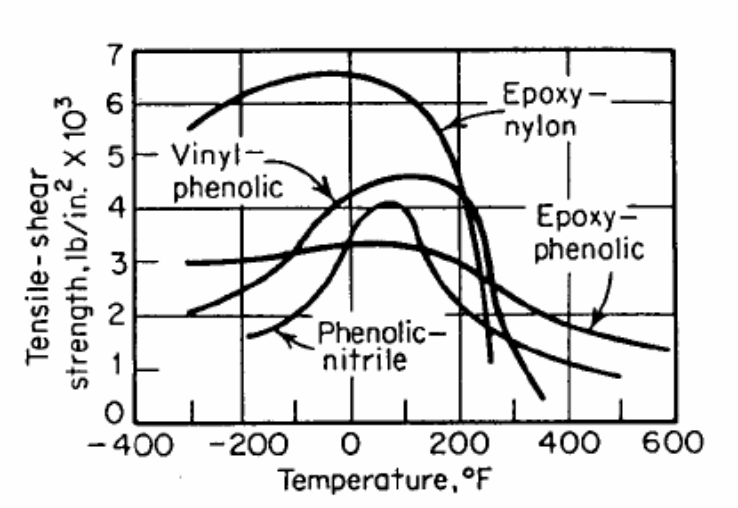

Figure 31. The effect of temperature on the tensile shear strength of modified epoxy adhesives (substrate is aluminum) [8].

3.2.2 Phenolic adhesives

These adhesives were primarily used to bond wood to wood. For structural application they are modified with a vinyl or an elastomer.

Modified phenolics – With a long story of successful use for making high strength metal-to-metal and metal-to-wood joints, they were the first adhesives for metals. These adhesives require heat and pressure for the curing process in order to avoid porosity.

These modified phenolics adhesives are vynil-phenolics, nitrile-phenolics and neoprene-phenolics, and their properties are given in the table 7.

Table 7. Modified phenolics supply forms and properties.

Adhesive	Form	Properties
Vinyl Phenolic	Film 1 part + solvent	Heat resistant (120ºC).
Nitrile Phenolic	Film 1 part + solvent	Chemical resistance and high temperature capability (160ºC); Heat shock resistant; Flexibility.
Neoprene Phenolic	Film 1 part + solvent	Low temperatures resistant (-50ºC).

3.2.3 Acrylic adhesives

There are mainly 3 types of acrylics: the anaerobics, the cyanoacrylates and the methacrylates.

Cyanoacrylates – These adhesives cure through reaction with moisture held on the surfaces to be bonded. Solidifying in seconds, they are commonly used in small plastic parts and rubber. Cyanoacrylates are known to be “crazy glues” and “superglue” like miracle glues having a major commercial success. They are supplied in liquid and thixotropic versions, having a little gap-filling capability. They are based on a special type of acrylic.

Anaerobics – Also known as “locking compounds” or “sealants”, they are used to secure, seal and retain turned, threaded, or similarly close-fitting parts. They harden when the air is excluded from the contact between metal, just like when a screw is fastened in a thread. With a relatively rapid curing, these adhesives do not have gap-filling capability, as a result of their curing process.

Toughened acrylics and methacrylates – The modified acrylics are thermosetting systems that provide high shear strength to joints. Their formulations are based on crosslinked polymethyl methacrylate grafted to vinyl terminated nitrile rubber, in order to improve flexibility and impact resistance. They are known to be weather and moisture resistant.

Usually mixed prior to application, their pot-life should be carefully controlled on account of their fast cure at room temperature. However there are some modified acrylic adhesive systems that allow separate application of the hardener as primer, allowing substrate storage for 6 months [30]. When the part is set to be bonded, only the acrylic resin needs to be applied. There is another particular application that allows applying the hardener to one part face and the acrylic resin to the other part face and when the two faces are bonded together, a fast cure occurs, developing handling strength in 60 seconds [31].

Figure 32. Araldite methacrylates.

Edward M. Petrie states that the fast cure and variety of application alternatives make this adhesive valuable in many production processes [8].

Modified acrylics tolerate minimal surface preparation, bonding well to a wide range of materials as reported in table 8 with the PVC line highligted. It is important to notice that the failure occurs in the substrate in most of the polymeric materials, including PVC, which is the ideal situation in a bonded joint.

Table 8. Tensile shear strength of various joints bonded with thermosetting acrylic adhesives [32].

Substrate*	Average lap shear, MPa at 22º C		
	Adhesive A	Adhesive B	Adhesive C
Alclad aluminum, etched	30,54	27,57	37,36
Bare aluminum, etched	29,68	27,48	34,58
Bare aluminum, blasted	23,27	25,48	30,17
Brass, blasted	27,68	21,72	28,09
302 stainless steel, blasted	32,03	32,41	35,65
302 stainless steel, etched	19,58	29,48	18,27
Cold-rolled steel, blasted	14,13	23,34	14,72
Copper, blasted.	20,09	18,89	22,44
Polyvinyl chloride, solvent wiped	9,48 ♦	8,62 ♦	8,62 ♦
Polymethyl methacrylate, solvent wiped	10,69 ♦	7,99 ♦	5,96 ♦
Polycarbonate, solvent wiped	17,72 ♦	6,62	17,72 ♦
ABS, solvent wiped	11,10 ♦	11,27 ♦	8,83 ♦
Alclad aluminum-PVC	8,14 ♦		
Plywood, 5⁄8-in. exterior glued (lb / in.)	5,53 ♦	6,74 ♦	
AFG-01 gap fill (1⁄16-in.) (lb / in.)	…	7,47 ♦	

* Metals solvent cleaned and degreased before etching or blasting

♦ Substrate failure

3.2.4 Polyurethane adhesives

Polyurethane adhesives are commonly supplied in one part moisture curing or two-part as liquids with a gap-filling capability of up to 25 mm and can be made with a variable range of curing times. They are used to bond certain thermoplastic materials and GFRP (glass fiber reinforced plastics).

3.2.5 UV curable adhesives

Their main characteristic is a very quick cure by exposure to UV radiation. These adhesives are modified acrylic and epoxy adhesives, but while acrylic UV adhesives require one substrate to be UV transparent, the UV initiated epoxy adhesives can be irradiated before closing the bondline, curing in a few hours at ambient temperature.

3.2.6 Aromatic adhesives

Polyaromatic adhesives are known for their outstanding thermal resistance (200-300ºC). There are several polyaromatic resins such as polyimide, bismaleimide, and polybenzimidazole, developed for aeronautical and electronic industry in order to bear high temperatures.

3.2.7 Polyesters (unsaturated)

Thermoset adhesives that have a significant volume reduction when curing, making them unsuitable for industrial application. They are suitable for high temperature bonding.

Structural adhesive properties are summarized in table 9.

Table 9. Structural adhesive properties [33].

Adhesives	Supply Form	Yield strength [MPa]	Max. Service temperature [ºC]	Peeling resistance	Impact resistance	Chemical resistance
Vinyl phenolic	1 liquid component Liquid + Powder Film	17 - 35	100 -130	Average	Good	Poor
Nitrile phenolic	1 liquid component Film	15 -30	140 – 170	Average	Good	Good
Anaerobic (Acrylic)	1 liquid component	10 - 40	120 – 150	Good	Good	Average
Cyanoacrylate	1 liquid component	10 - 35	80	poor	Bad	Bad
Polyurethane	2 liquid components	8 - 15	90	Average	Good	Good
Polyimide	Film	10 - 15	250 – 300	Good	Poor	Good
Epoxy	Various	15 - 45	80 – 150	Good	Bad	Good
Epoxy polyamide	2 component liquid	15 - 45	80	Poor	Good	Poor
Epoxy polysulfide	2 component liquid	15 – 25	80	Good	Good	Good
Epoxy phenol	1 component liquid Film	20	200-250	Poor	Bad	Good
Epoxy nitrile	Film	10-46	100 - 120	Average	Good	Good

3.2.8 Rubber adhesives (elastomers)

These adhesives are not suitable for sustained loading. They are based on solutions of latexes, solidifying through loss of solvent or water.

Silicone adhesives – These are great sealants of joints with different thermal expansions. They resist temperatures up to 250ºC.

Polychloroprene (neoprene) – Commercially known as neoprene, these are contact adhesives with good mechanical properties and good resistance to water, salt spray, commonly encountered chemicals, and biodeterioration.

Polysulfide adhesives – These adhesives are best known as sealants rather than adhesives because of their low strength and high degree of elongation.

3.2.9 Thermoplastic adhesives

Hot melts - Based on modern polymers, they are used for the fast assembly of structures requiring little mechanical resistance. Usually solid polymers that melt when heated, and then form a quick connection upon cooling.

Plastisols – Requiring heat to harden, their joints are resilient and tough. They are based on modified PVC. Used in automotive industry with phenol or epoxy resins.

Polyvinyl acetates (PVAs) – Mostly used to bond porous materials, such as wood, paper and packaging. These adhesives are based on a vinyl acetate emulsion.

Pressure-sensitive adhesives – They are not suitable for sustained loading, but are able to withstand adverse environments. Supplied on tapes and labels, these adhesives do not solidify.

In table 10, the adhesives are summarized by type, and related to some of their applications.

Table 10. Adhesive applications [33].

Type	Adhesive	Substrates	Applications
Natural	Amide, Dextrine Fix Glues Canada Balm, etc	Paper, cork, Textiles, Wood Some polymers and Metals	Domestic appliances and packaging.
Thermoplastic	Cellulose Polyvinyl acetate Polyvinyl Alcohols EVA, Acrylic Polyethylene Polyamides	Metals, Wood, Leather, Textile, and Paper.	Low load bonds.
Thermosets aromatic	Melamine Formaldehyde Polyesters Epoxies Phenolics	Metal, Wood, Ceramic, and Glass.	Metal or wood structural bonds, sustaining considerable loads.
Elastomers	Natural rubber Synthetic rubber Polyurethane Polychloroprene Nitrile	Polymers, Rubbers, Fabrics and Leather	Flexible bonds, with low loads
Two polymer adhesives	Nitrile Phenolic Neoprene Phenolic Vinyl Phenolic Epoxy Polyamide Epoxy Polysulfide Epoxy Phenol Epoxy Polyurethane Epoxy Silicone Epoxy Nitrile	Metals, Ceramics, Glass, and thermoset resins.	High loads and weather exposed structures.

Chapter 4

JOINT DESIGN

4.1 Introduction

The design of the adhesive joint will play a significant role in the joint resistance to applied mechanical loads and environment. Although it may be tempting to use joints originally intended for other methods of fastening, adhesives require special design considerations for optimum properties.

4.2 Joint stresses overview

It is also important to understand and determine the types of stress that may be present in an adhesive joint, such as:

- Tensile;
- Compressive;
- Shear;
- Cleavage;
- Peel.

Tensile Stress: A tensile stress tends to pull an object apart. The stress also tends to elongate an object.

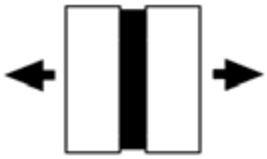

Figure 33. Schematic of tensile stress.

Compressive Stress: A compressive stress, on the other hand, tends to squeeze an object together.

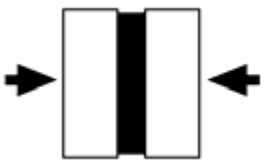

Figure 34. Schematic of compressive stress.

Shear Stress: A shear stress results in two surfaces sliding over one another.

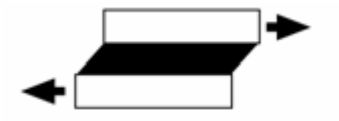

Figure 35. Schematic of shear stress.

Cleavage Stress: A cleavage stress occurs when a joint is being opened at one end.

Figure 36. Schematic of cleavage stress.

Peel Stress: A peel stress occurs when a flexible substrate is being lifted or peeled from the other substrate.

Figure 37. Schematic of peel stress.

Peel and cleavage stress must be avoided and the joint design philosophy is to reduce to a minimum these stress components.

Single lap joints are very easy to manufacture and are found in many applications. Several closed form analysis have been developed to determine the stresses present in this joint. The first approach is supposing the adherend to be rigid and the adhesive to deform only in shear (figure 38), τ :

$$\tau = \frac{P}{wl} \qquad \text{Eq. 4.1}$$

where:

P $\Rightarrow$ applied load
w $\Rightarrow$ joint width
l $\Rightarrow$ joint length

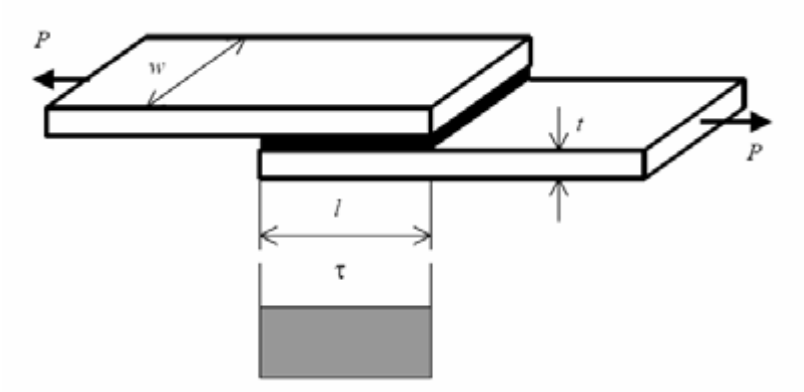

Figure 38. Shear stress in the SLJ: simplest analysis [34].

Volkersen [35] improved this analysis by introducing the differential straining concept as shown in figure 39, where the parallelograms (figure 39a) become distorted to new shapes shown (figure 39b) when loaded. Applying Volkersen's equations allows plotting the shear stresses in the overlap shown in figure 39c. The shear stress peaks at the ends of the overlap and is minimum in the middle.

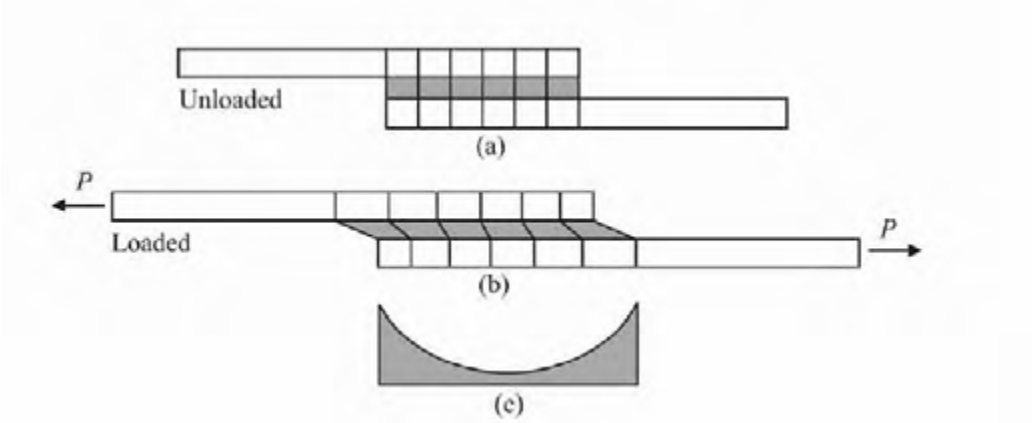

Figure 39. Volkersen analysis; (a) unloaded; (b) loaded; (c) shear stresses [34].

However, this analysis did not consider the rotation of the joint that occurs with the bending moment resulting from the non collinear forces. This means that there is a geometric non-linearity. Having this in mind, Goland and Reissner [36] introduced the bending moment factor k, relating the bending moment on the adherend at the end of the overlap, *M*, to the in-plane loading by:

$$M = k \cdot P \frac{t}{2} \qquad \text{Eq. 4.2}$$

where:

P ⇒ applied load
t ⇒ adherend thickness (adhesive layer thickness was neglected)
k ⇒ bending moment factor

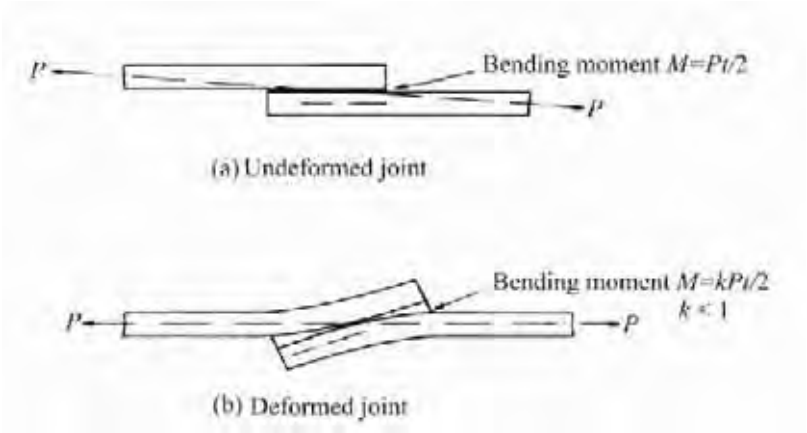

Figure 40. Geometrical representation of Goland and Reissner bending moment factor [34].

When the load is very small, there is no rotation and the bending moment factor is $k = 1$, resulting a moment $M = P\frac{t}{2}$ as shown in figure 40a. The Goland and Reissner mode gives shear stresses similar to those of the Volkersen analysis, but it also gives the transverse tearing (peel) stresses in the adhesive as shown in figure 41.

However these two analyses are based in an elastic behavior, when the adhesive and adherend may become non-linear or plastic. Considering the plastic behavior of the adhesive, Hart-Smith [37] developed the Volkersen and Goland and

Reissner theories. The adhesive characterization is done assuming an elastic/perfectly plastic model such that the total area under the stress-strain curve is equal to that under the true stress-strain curve and that the failure stress and failure strain are the same. Hart-Smith found that the plasticity of the adhesive increases the joint failure strength above the predictions of purely elastic analyses. A ductile adhesive will yield and sustain further load until eventually its shear strain to failure is attained as shown in figure 42. It is preferable to have a joint with a ductile adhesive such as toughened epoxies. Besides being stronger, it is safer as it yields before fracture, redistributing and reducing the peak shear strains.

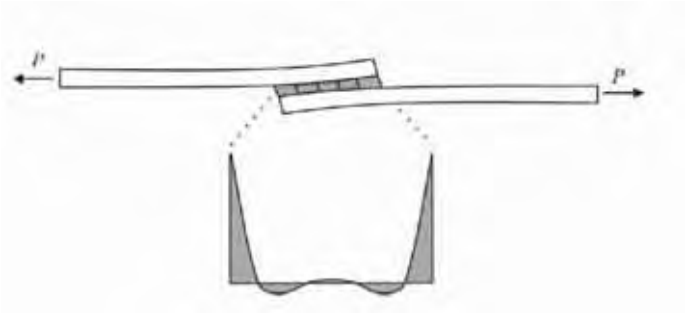

Figure 41. Peel stresses in a single lap joint [34].

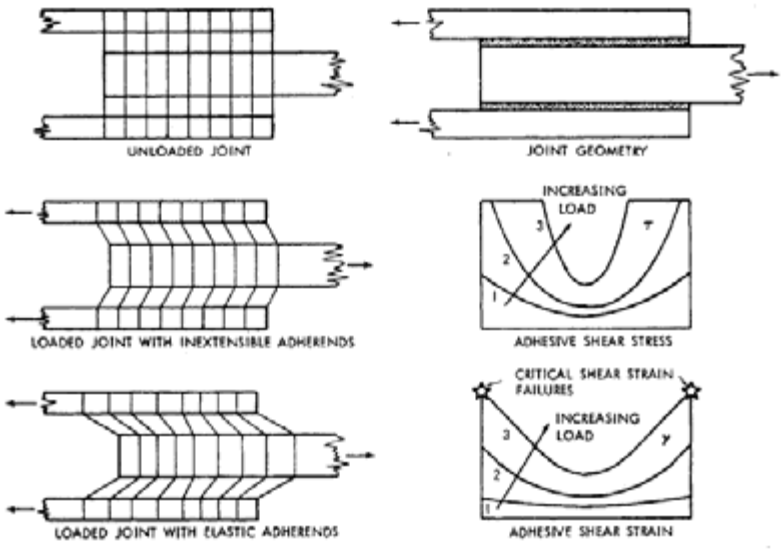

Figure 42. Schematic explanation of shearing in adhesive [38].

More closed-form analysis have been developed with an increasing degree of complexity such as those of Renton and Vinson [39], Allman [40] and Adams and Mallick [41] considering a zero value for the shear stress in the joint extremity. Ojalvo and Eidinoff [42] considered the shear stress variation through the adhesive thickness. Frostig et al. [43] used higher-order theory to analyze single lap joints with an adhesive fillet. Adams and Peppiatt [44] considered the Poissin effect in the width direction.

4.3 T-joint design

The design of the transom joint is like a t-joint. A theoretical analysis with the finite element method of this type of joint have already been published by Apalak et al. [45], and there is also an interesting work by da Silva and Adams [46], but in both of them steel adherends are used. In a recent work published by Broughton et al. [47], aluminum and glass reinforced plastics (GRPs) were used. There is also a study about T-joints for marine applications using polyester/glass laminated composite and plywood as adherends by Marcadon et al. [48]. However PVC T-joints have not yet been studied.

Figure 43 makes clearly visible that the poorest results are obtained with tensile transverse (peel) stresses, while compressive forces, such as N, generally do not cause faillure unless buckle occurs in figure 43i. In this study a joint simmilar to figure 43h is studied.

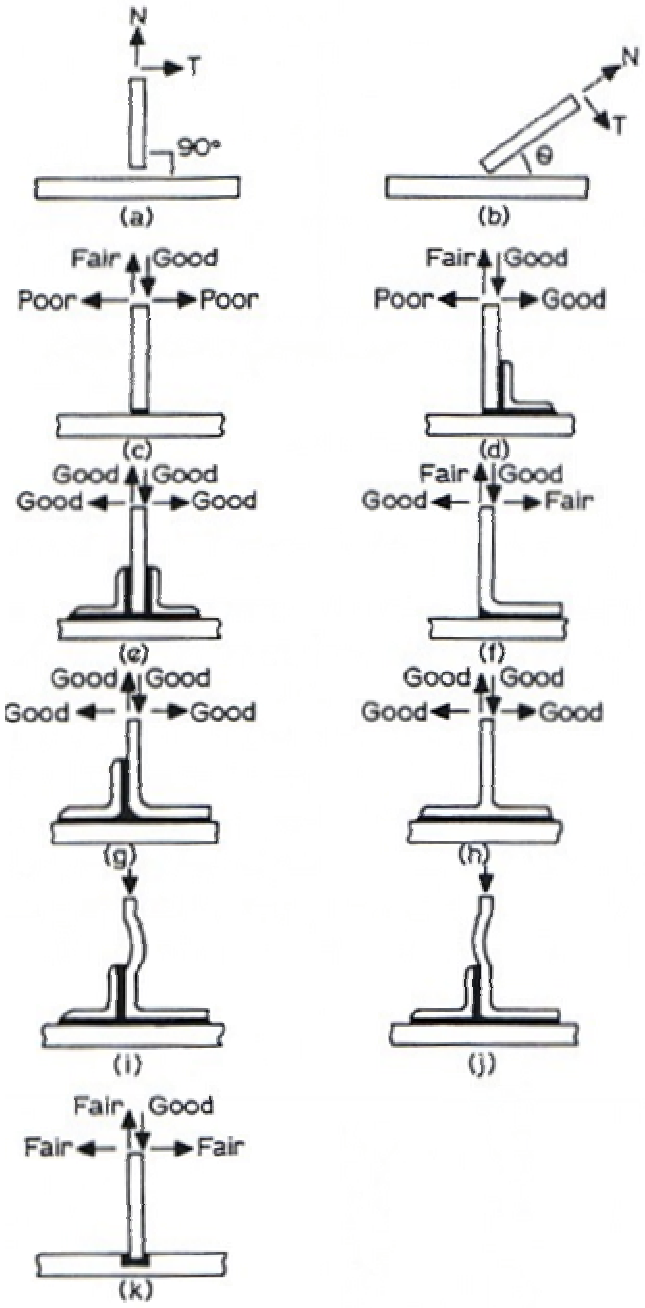

Figure 43. Possible T- Joints [49].

4.4 Joint strength improvement

It is known that critical points of geometric discontinuity generate stress concentration leading to failure. Attempting to optimize the geometry of the joint Adams et al. [50] proposed some improvements like filleting, outside taper and inside taper as shown in figure 44.

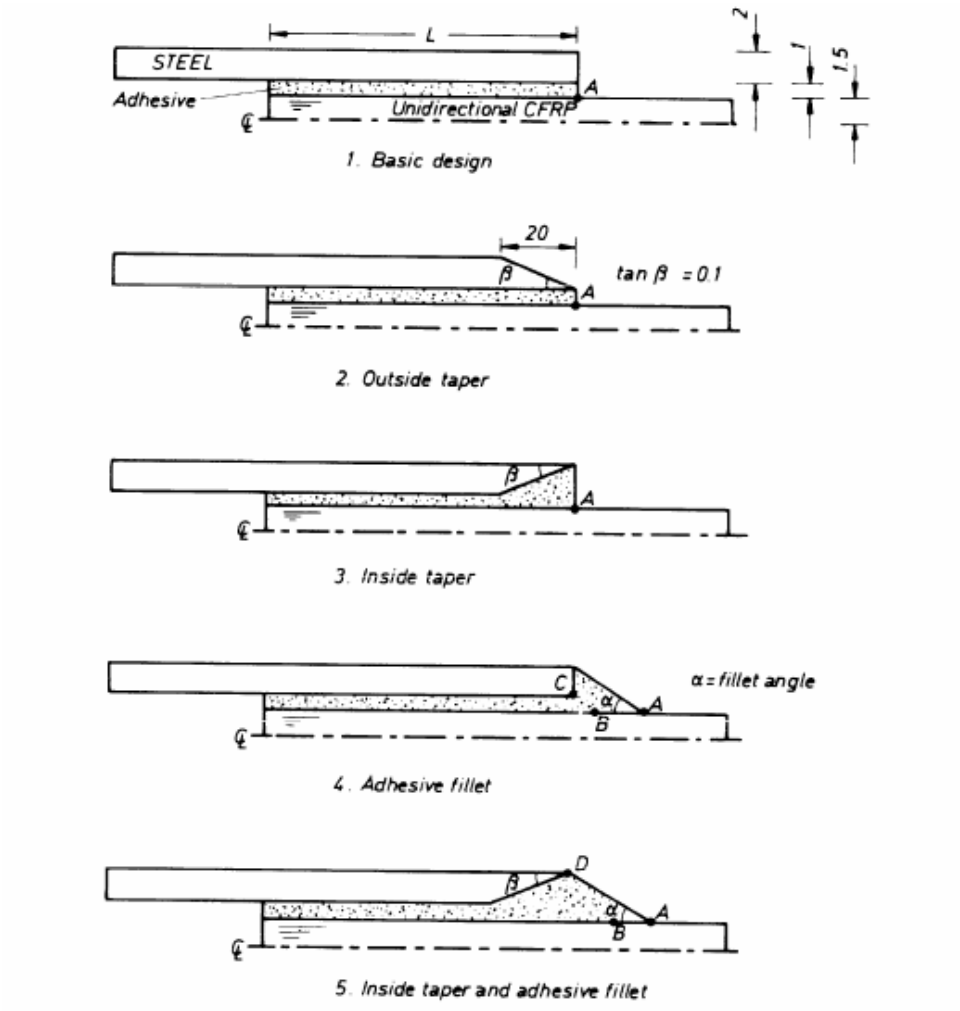

Figure 44. Designs of double-lap joints considered (dimensions in mm) [50].

Modification of the adherend to reduce the peel stress have also been studied by Hildebrand [51], Groth and Nordlund [52], Potter et al [53] and Kaye and Heller [54].

4.6 Bonded joint failure

The nature of joint failure must be taken into account to design a good joint. Joints may fail in adhesion or cohesion modes or by some combination of the two (figure 45).

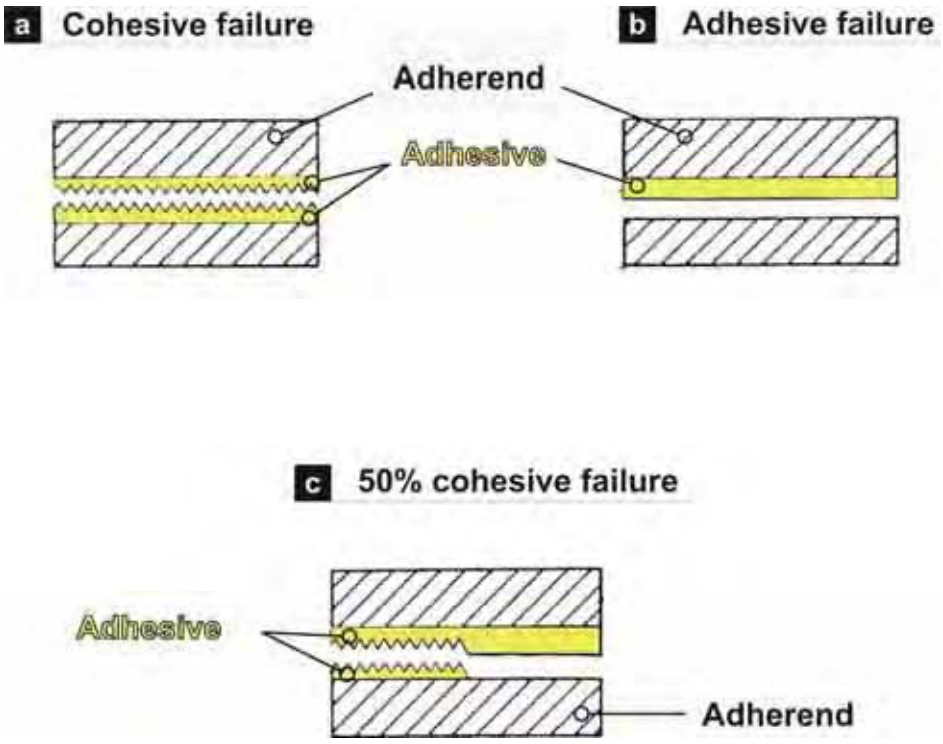

Figure 45. Examples of adhesive and cohesive failure [8].

Figure 45b shows an interfacial bond failure between the adhesive and adherend defined as adhesive failure. In this case the bulk cohesive strength of the adhesive material can be assumed to be greater than the intermolecular strength of adhesion.

Cohesive failure occurs when the failure is such that a layer of adhesive remains on the adherend (figure 45a).

Figure 46 shows a cohesive failure of the adherend occurring when the adherend fails before the adhesive. In this case the bond strength is stronger than the forces holding the bulk together. This type of failure is the ideal

situation because the joint is stronger than the adherends being loaded, i.e., the joint is not the weak link.

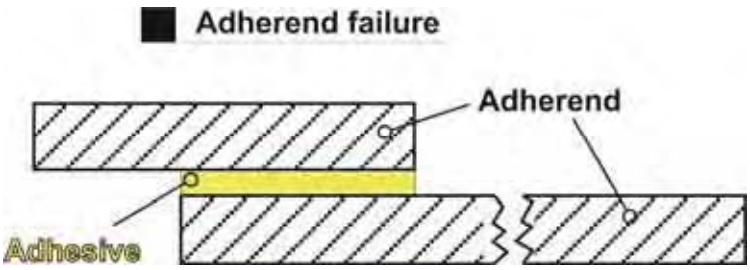

Figure 46. Cohesive failure of the adherend.

An adhesive failure indicates the presence of a weak boundary layer or improper surface preparation as registered in table 11. Cohesive failure is the most common type of failure but the ultimate goal is failure in the adherend.

Table 11. Failure mode as an interference to bond quality [8].

Failure mode	Inference	
Adhesive failure (interfacial)	Cohesive strength > interfacial strength	Weak boundary layer
Cohesive failure (bulk)	Interfacial strength > cohesive strength	
Adhesive/Cohesive failure (mixed failure mode)	Interfacial strength ≈ cohesive strength	Improper surface preparation

4.7 Joint design considerations

In summary, there are several rules that the designer should consider when designing an adhesive joint [8], such as:

1. Keep the stress in the bond-line to a minimum;
2. Whenever possible, design the joint so that the operating loads will stress the adhesive in shear;
3. Peel and cleavage stresses should be minimized;
4. Distribute the stress as uniformly as possible over the entire bonded area;
5. Adhesive strength is directly proportional to bond width. Increasing width will always increase bond strength. Increasing the depth of overlap does not always increase strength;
6. Generally, rigid adhesives are better in shear, and flexible adhesives are better in peel;
7. Although typically a stronger adhesive material may produce a stronger joint, a high elongation adhesive with a lower cohesive strength could produce a stronger joint in applications where the stress is distributed nonuniformly;
8. The stiffness of the adherends and adhesive influence the strength of a joint. In general, the stiffer the adherend with respect to the adhesive, the more uniform the stress distribution in the joint and the higher the bond strength;
9. The higher the $E \cdot t$ (modulus x thickness) of the adherend, the less likely the deformation during load, and the stronger the joint;
10. Within reasonable limits, the adhesive bond-line thickness has not a strong influence on the strength of the joint. More important characteristics are a uniform joint thickness and void free adhesive layer.

Chapter five

SELECTION OF ADHESIVE FOR PVC BONDING

This chapter deals wit the selection of the best adhesive to use in PVC bonding. The previous knowledge about adhesives and joint design was taken into account and a market assessment was done. The selection of the adhesive is a crucial step because it is responsible for all the future steps and results.

5.1 Selection process

The adhesive selection depends primarily on:

- the type and nature of substrates to be bonded;
- the methods of curing that are available and practical;
- the expected environments and stresses that the joint will see in service.

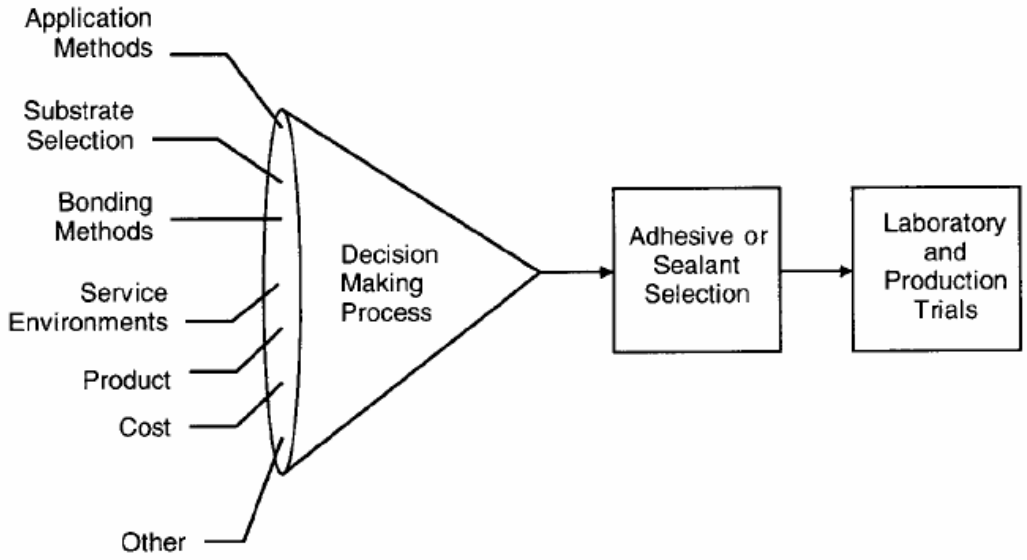

Figure 47. Adhesive and sealant selection considerations [8].

As shown in figure 47, the selection is done in three stages:

1. The decision making process is the point where the several inputs, normally inherent to the problem, are taken in account and used as metrics to evaluate each adhesive.
2. After evaluating the adhesives, the selection is done by choosing the one that best fits the purpose. This selection will determine the success of the next stage.
3. In the last stage, the selection is experimentally validated. Laboratory tests will determine the performance of the adhesive and joint.

5.1.1 Plastic bonding – substrate selection

The design of joints for plastics and elastomers generally follows the same practice as for metal. However, the designer should be aware of certain characteristics for these materials that require special consideration. Such characteristics include flexibility, low modulus, high thermal expansion coefficients, thin section availability, and anisotropy. These characteristics tend to produce significant non-uniform stress distribution in the joint. Thus, tough, flexible adhesives are usually recommended to bond plastic or elastomer substrates [8].

There is no benefit in using high modulus adhesives on low modulus substrates as PVC, because the load transfer is less efficient than with closer matched modulus. Rigid adhesives result in local stress concentration and crack initiation. Therefore by using adhesive/substrate combinations with similar modulus, improvement in joint strength can be expected [55].

There are also some chemical properties to consider, when working with PVC. The adhesive components shall not migrate to PVC surface or change its properties by dissolution. PVC can be stress cracked by uncured cyanoacrylate adhesives. It is compatible with acrylic adhesives, but can be attacked by their activators before the adhesive has cured. Any excess activator should be removed from the surface of the PVC immediately because it can migrate into PVC and reduce its performance. It is also known that it is incompatible with anaerobic adhesives [56]. PVC is compatible with epoxy and polyurethane adhesives, but the phenolic adhesives can aggressively migrate into PVC and rapidly change its appearance and UV resistance.

5.1.2 Application and bonding methods

The ease of adhesive application is very important to obtain a good acceptability by the industry. In fact, the possibility to automate its application should be a major concern in the adhesive selection.

The surface preparation is another important factor that will define the performance of the bonding joint. With PVC, there is a major advantage because Loctite® has discovered that surface roughening and/or the use of Prism Primer 770 or 7701 resulted in either no statistically significant effect or in the rigid PVC failing at a statistically significant lower bond strength than the untreated PVC [56]. So there are no special surface treatments other than cleaning the bonding surface, making it a very good solution for industry in terms of working hours.

It is also important for the adhesive to have a brief curing time, allowing handling.

5.1.3 Service environments

The adhesive should have weatherability properties similar to those of the PVC. The glass transition temperature (Tg) is very important, because after reaching this temperature the adhesive starts to behave like a rubber [34]. This point is treated in section 5.6.

5.1.4 Cost

Once again the industrial factor plays a major role, because the final price of the product should not be affected. If the adhesive proves to be a less expensive solution, it will have a good acceptance, otherwise its advantages will be of no industrial utility for production. However, this study was not driven by the cost factor, but by the best solution to obtain a bonding joint.

5.1.5 Market

The availability of the adhesive is very important. If the adhesive is available only in certain regions or if it has supply problems it will not be a good solution in industrial context.

Based on the precedent process selection, the following criteria were used for the present application.

Table 12. Criteria used to select the adhesive.

►	Tensile modulus	≈ 2 GPa (near to PVC tensile modulus)
	Ductility	The best ductility possible.
►	Tg	≈ 80ºC (near to PVC Tg)
►	Chemically compatible with PVC	
►	Easy application/automated if possible	
►	Available in the market (good supply)	

The local suppliers were contacted to find the adhesive that best fits the above requirements.

5.2 Adhesive selection

After receiving and screening the different supplier's proposals, two adhesives were selected and tested:

Araldite® 2021 – from Huntsman®;

Table 13. Adhesive supplier properties.

►	**Tensile modulus**	**≈ 1,43 GPa**
►	Ductility	50 – 75 %
►	Tg	no reference
►	Chemically compatible with PVC	
►	Automated (two component cartidge)	
►	Supplied by Reciplás .	

Loctite® 3030 – from Loctite®.

Table 14. Adhesive supplier properties.

►	Tensile modulus	≈ 0,043 GPa
►	**Ductility**	**76 %**
►	Tg	no reference
►	Chemically compatible with PVC	
►	Easy application/automated if possible	
►	Supplied by Sistimetra.	

* although this adhesive has a low tensile modulus (not considered a structural adhesive) it was considered in this study for its high ductility.

The next step is the experimental validation to confirm the adhesive properties and supply the necessary mechanical properties for the FEM analysis. Two types of mechanical tests were done:

- Tensile test of the adhesive in bulk (BS 2782:Part 3). This test allows to determine the adhesive mechanical properties such as the Young's modulus, the strength and the ductility.

- Single lap joint test (ASTM D1002 - 01). This test gives a good indication of the adhesive behaviour in a joint and enables to assess the quality of the surface preparation by the analysis of the type of failure (see section 4.6).

Bulk and single lap joint specimens where tested after exposure to severe environments to evaluate the weatherability of the adhesive.

Tg tests were also carried out to assess the service temperature of the adhesive.

5.3 Adhesive bulk properties

5.3.1 Specimen manufacture

The adhesive properties can be obtained from a tensile test on a bulk specimen using a universal testing machine. The bulk specimen was manufactured using the mould presented in figure 51, designed by Costa and da Silva (2005 PESC project).Figure 48 shows the release agent application to the mould. This must be done before usage. The parts were heated to 45ºC in a hot press to speed up the cure reaction of the release agent.

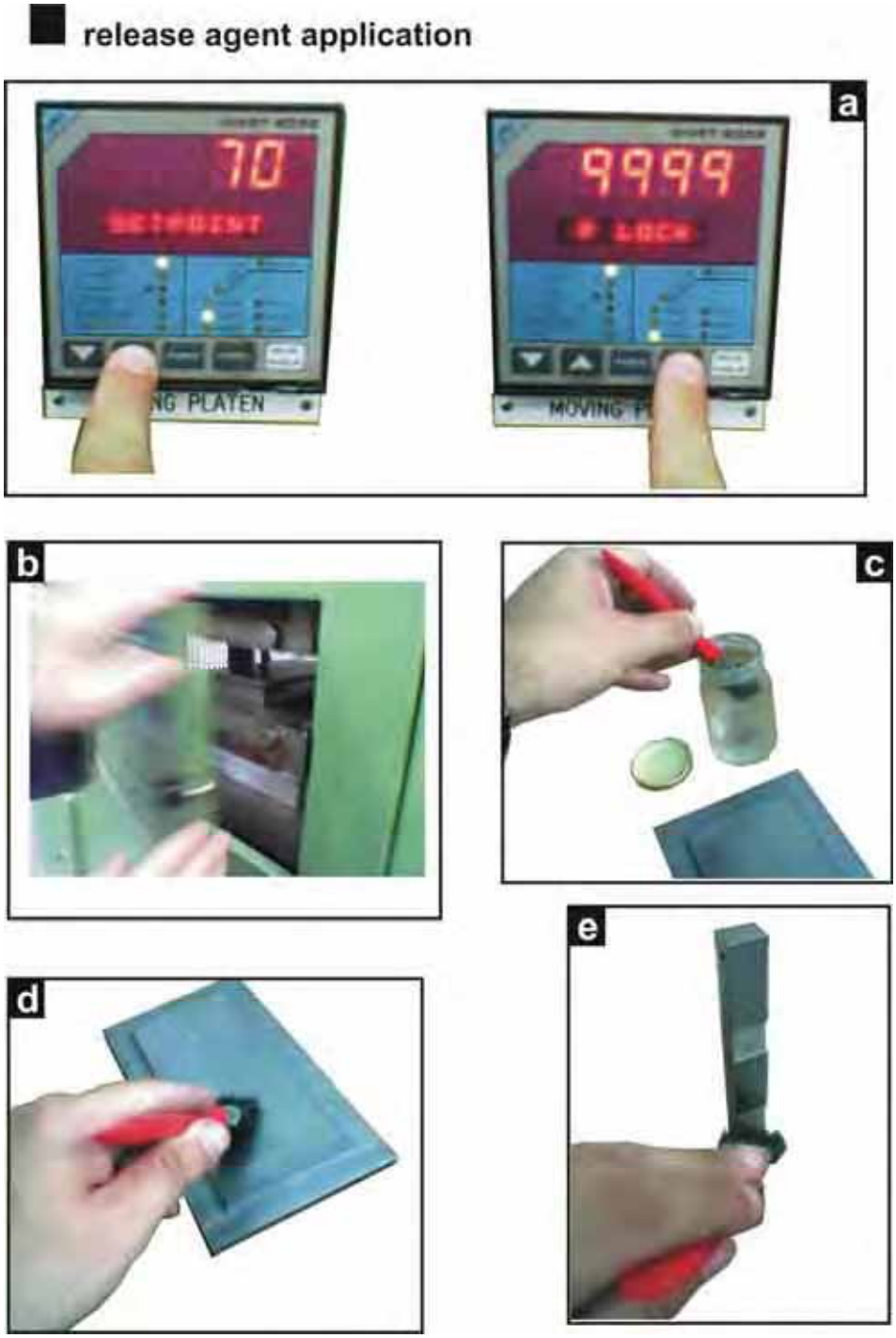

Figure 48. Release agent application.

The various steps of the release agent application are (figure 48): (a) set the temperature controller to 70ºC to allow a rapid warming to 45ºC; (b) insert the parts into the press and warm them until they reach approximately 45ºC; (c) (d)

(e) after removing the parts from the press apply three layers of Loctite® 770NC™.

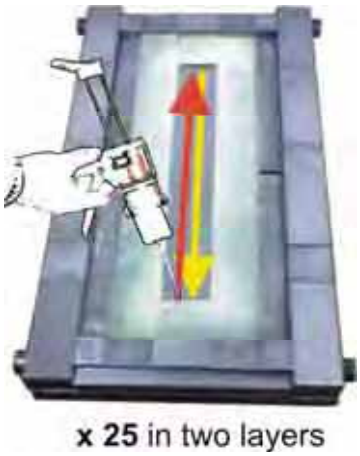

Figure 49. Adhesive application (25 applications of adhesive up – red - and down –yellow).

A major difficulty in the manufacture of adhesive Araldite® 2021 is the pot time of ten minutes. The weighting and pouring had to be done in less than ten minutes, and it was difficult to distribute evenly without voids. To solve this problem, a procedure was established that consisted of applying into the bottom plate of the mould approximately 25 applications of adhesive (up and down) as shown in figure 49 and 50. This method reduces the amount of air entrapment because it eliminates the weighting and enables to pour directly the adhesive on the mould. The number of applications was determined using a digital balance.

The bottom mould plate had a silicone rubber frame (figure 52 and 53) that seals the mould and stops the adhesive flowing out, resulting in a hydrostatic pressure over the adhesive which reduces the voids and promotes a better surface finish as stated by da Silva et al. [57]. The mould is composed of various parts (figure 51).

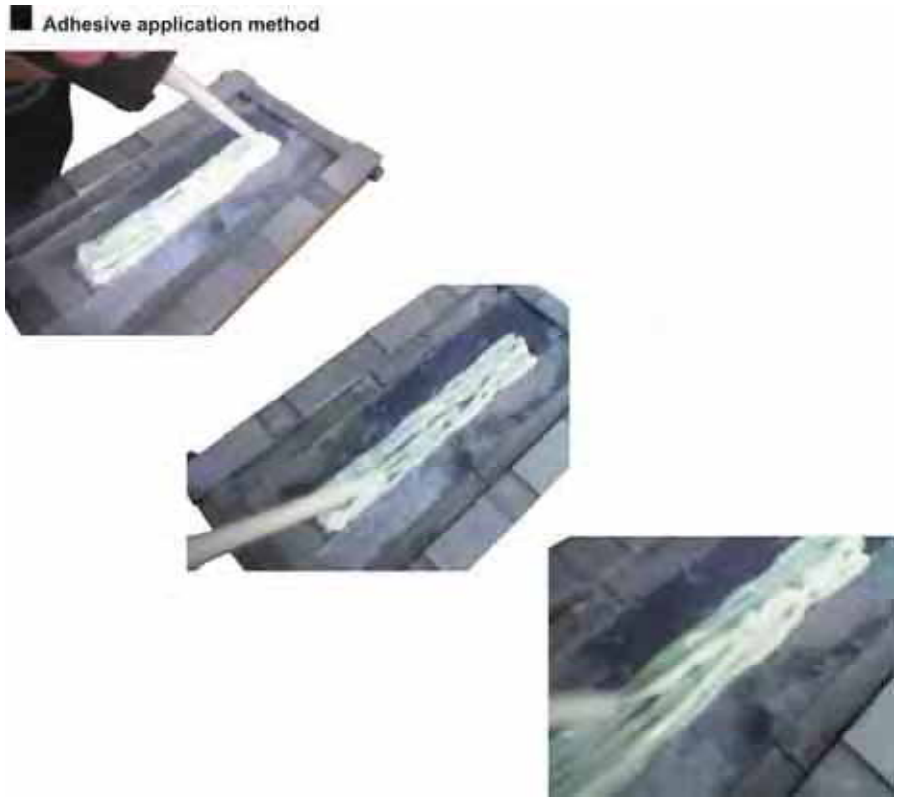

Figure 50. Adhesive application method.

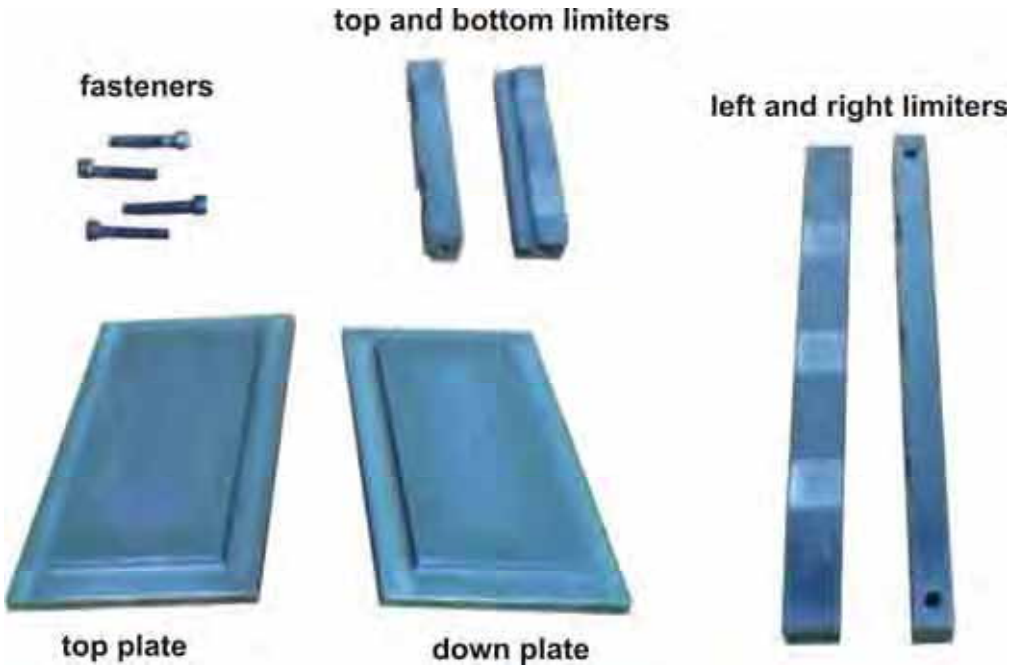

Figure 51. Mould parts.

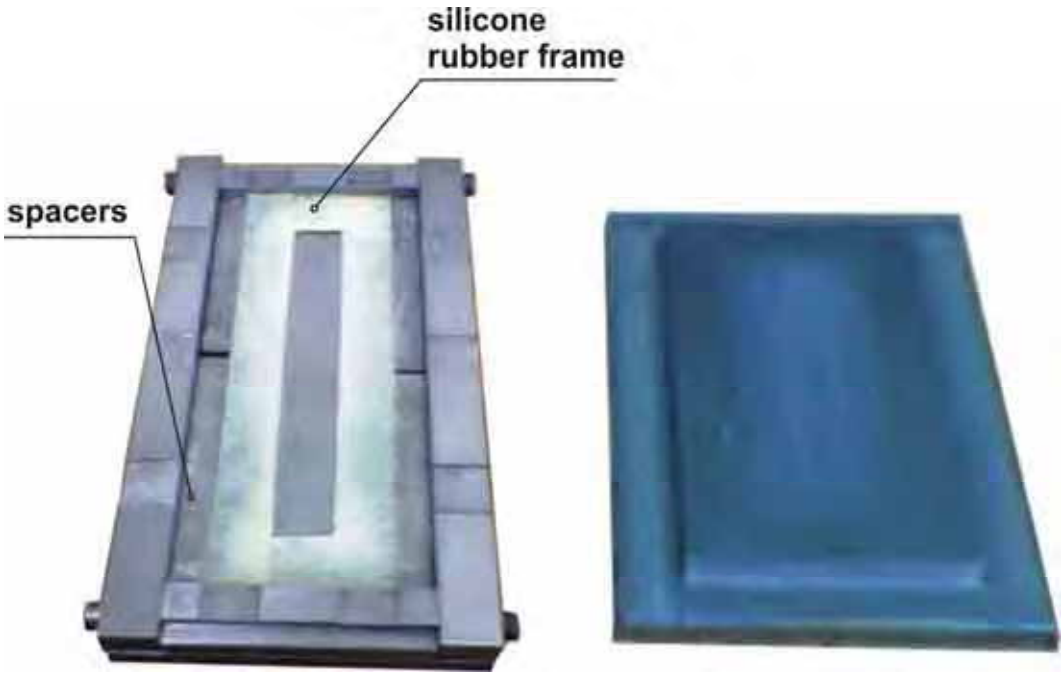

Figure 52. Opened mould with spacers and silicone rubber frame in place.

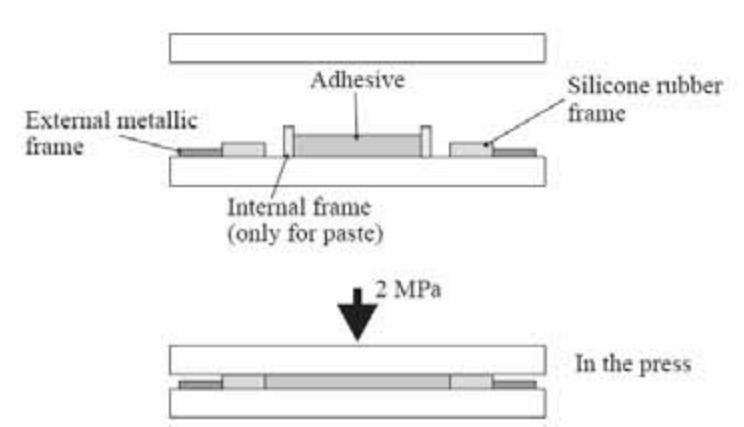

Figure 53. Adhesive plate manufacture according to NF T 76-142 [58].

Figure 54. Bulk adhesive (left) and excess of adhesive (right).

After the top plate application, the mould is placed in a press and subjected to 2 MPa pressure over 30 minutes of setting time at room temperature (25 ºC-28ºC) (cold pressing) . This is visible in figure 58.

All the process preceding the introduction of the mould in the press, must not exceed 10 minutes, otherwise the cure initiation will lead to air entrapment. Some training was needed to get the best results.

Thirty minutes later, the pressure was released and the mould was placed over the work table where it was opened to remove the bulk specimen for posterior machining in order to obtain the test specimen. Figure 54 shows the resulting bulk adhesive and the excess of adhesive that was removed.

The next step is cleaning the mould and tools with acetone.

In summary, there are 8 steps:

1. Apply the release agent;
2. Mount the mould, and place the silicone rubber frame;
3. Apply the adhesive;
4. Close the mould, placing the top plate;
5. Insert the mould in the press machine at 2 MPa and room temperature over 30 minutes;
6. Release the pressure and remove the mould;
7. Open the mould and remove the bulk adhesive;
8. Clean the mould and tools with acetone.

Once the bulk adhesive is obtained, it is machined according to standard BS 2787: Part 3 [59], as shown in figure 55.

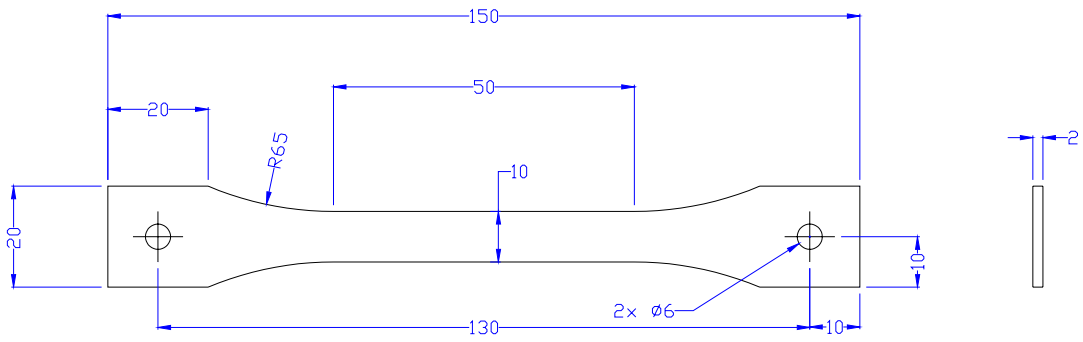

Figure 55. Bulk specimen dimensions (all dimensions in mm).

Figure 56. Intoco press machine.

The pressure application is done with a press machine with heated plates. The heating feature allows to heat the mould parts to apply the release agent.

It has two major control pannels for each function: the heat control pannel and the pressure control pannel with the motion control (see figure 56).

Water is used to promote the press plates cooling . Figure 57 b shows the valve that controls the water flux.

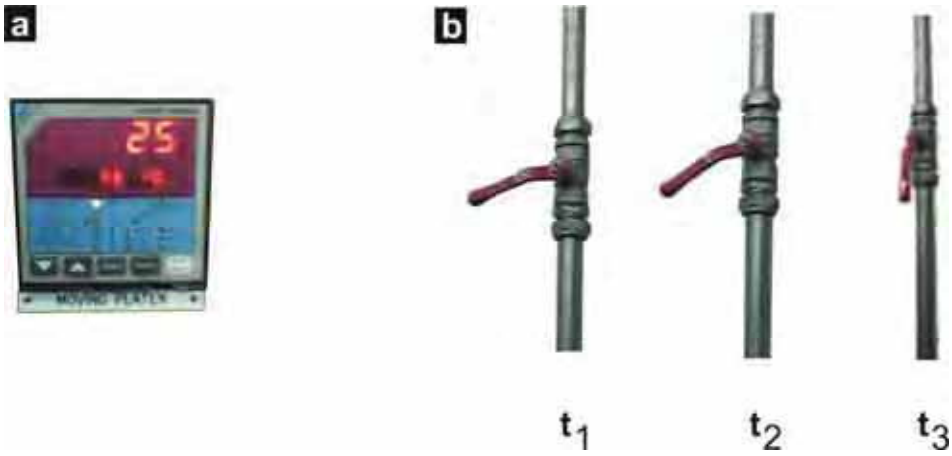

Figure 57. Cooling the press plates. (a) Temperature controller set; (b) water valve opening.

To cool the press plates the temperature controller must be set to 25º C (figure 57a) and the valve which allows water to refrigerate the plates should be progressively opened (figure 57b) to avoid thermal stresses.

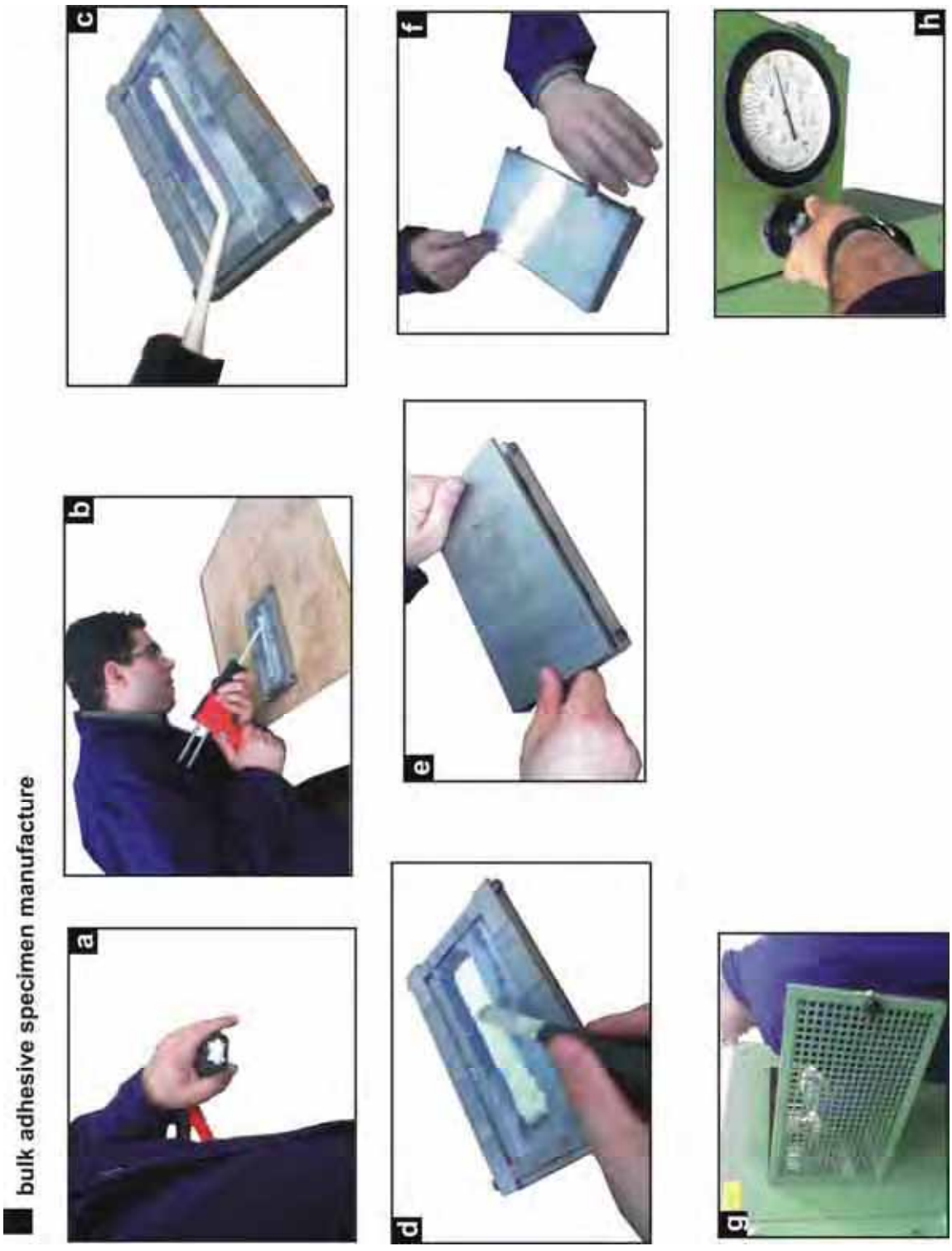

Figure 58. Bulk adhesive specimen manufacture. (a) introduce the adhesive cartridge inside the handgun; (b) and (c) pour the adhesive over the mould; (d) improve the adhesive distribution with a spatula; (e) and (f) insert the mould top plate; (g) insert the mould inside the press; (h) open the pressure gauge valve setting the pressure to 2 MPa.

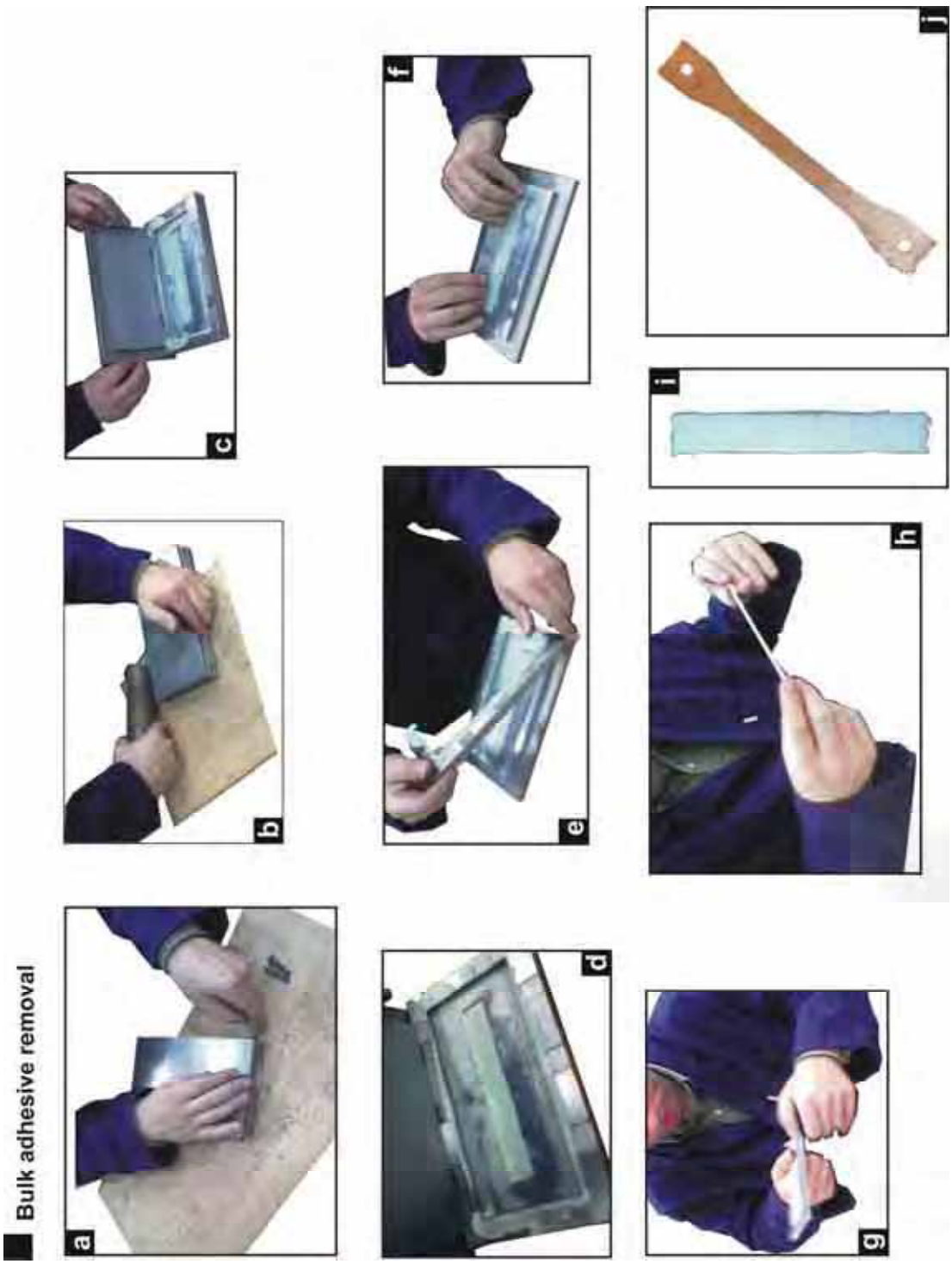

Figure 59. Bulk adhesive removal from the mould. (a) remove the 4 screws ; (b) hammer the mould lightly; (c) and (d) open the top plate; (e) remove the limiters; (f) remove the silicone rubber frame together with the bulk adhesive; (g) remove the bulk adhesive; (h) visual verification of the bulk adhesive; (i) bulk adhesive; (j) dogbone specimen ready to test in the tensile test machine.

Eight adhesive bulk specimens were manufactured, referenced T1 to T8. The first four (T1 to T4) were placed inside an environmental chamber, promoting their weatherability (see section 4.5) together with single lap joint specimens. The last four specimens (T5 to T7) were tested as made in the tensile test machine.

The adhesive cartridges used for the bulk specimen, the single lap joint specimens and the T-joint specimens are registered in table 15 and in figure 60.

Table 15. Adhesive batch number and expiry date.

	Batch number	Expiry date
Araldite® 2021™ cartridges	TA 583643	11/05
	TA 588353	03/06
	TA 590753	06/06

Figure 60. Araldite® 2021™ cartridges with the batch number.

To manufacture the three single lap joint specimens L1, L2 and L3 a Loctite® 3030™ batch was used with the number 4KP373B and, expiry date 11/05 (figure 61).

All the adhesive cartridges were used within the expiring date.

Figure 61. Loctite 3030 cartridge.

Another important detail to register is the adhesive delivery nozzle attached to the cartridge. This delivery nozzle has four different steps at the tip with different exit diameters (figure 62). Cutting it at the best step allows obtaining an optimal flow for each application, as explained in figure 63. The fourth step (smaller diameter) allows a small amount of adhesive to flow with the best accuracy which is used for the single lap joint specimen manufacture. Cut #1 (bigger diameter) allows the highest rate adhesive deposition, used for the bulk specimen manufacture requiring a rapid pouring of the adhesive to avoid premature cure. Cut #2 has an intermediate diameter, allowing a good adhesive flow and also good accuracy, which was used to manufacture the T-joints.

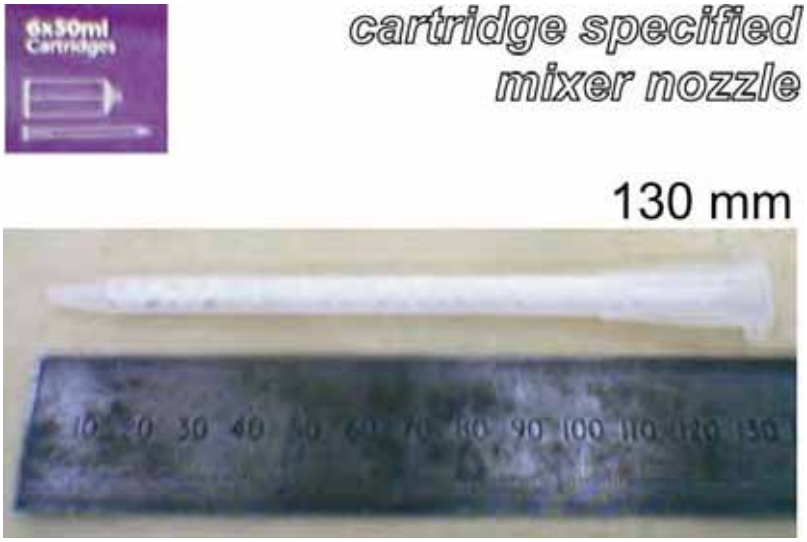

Figure 62. 130 mm Araldite 2021 cartridge pouring nozzle.

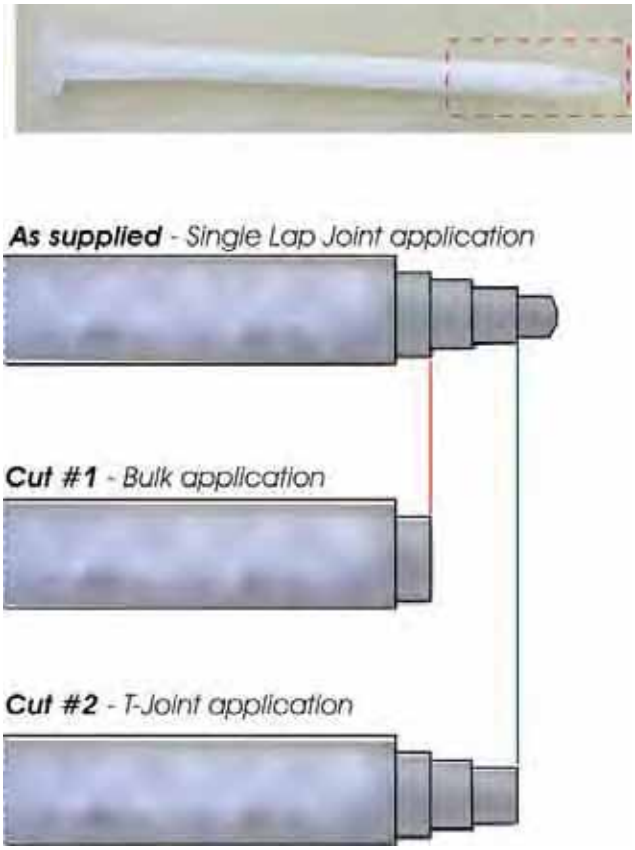

Figure 63. Different cuts for the 130 mm Araldite 2021 cartridge pouring nozzle.

5.3.2 Deformation measurement

To measure the bulk specimen displacement the correlation method developed by Chousal [60] was used.

The bulk specimen was placed in the tensile test machine together with a digital photography camera to register photos in sequence (spaced in time) for each test. This is visible in figure 64a and in the zoomed figure 64b where a background sheet was placed to help posterior image processing.

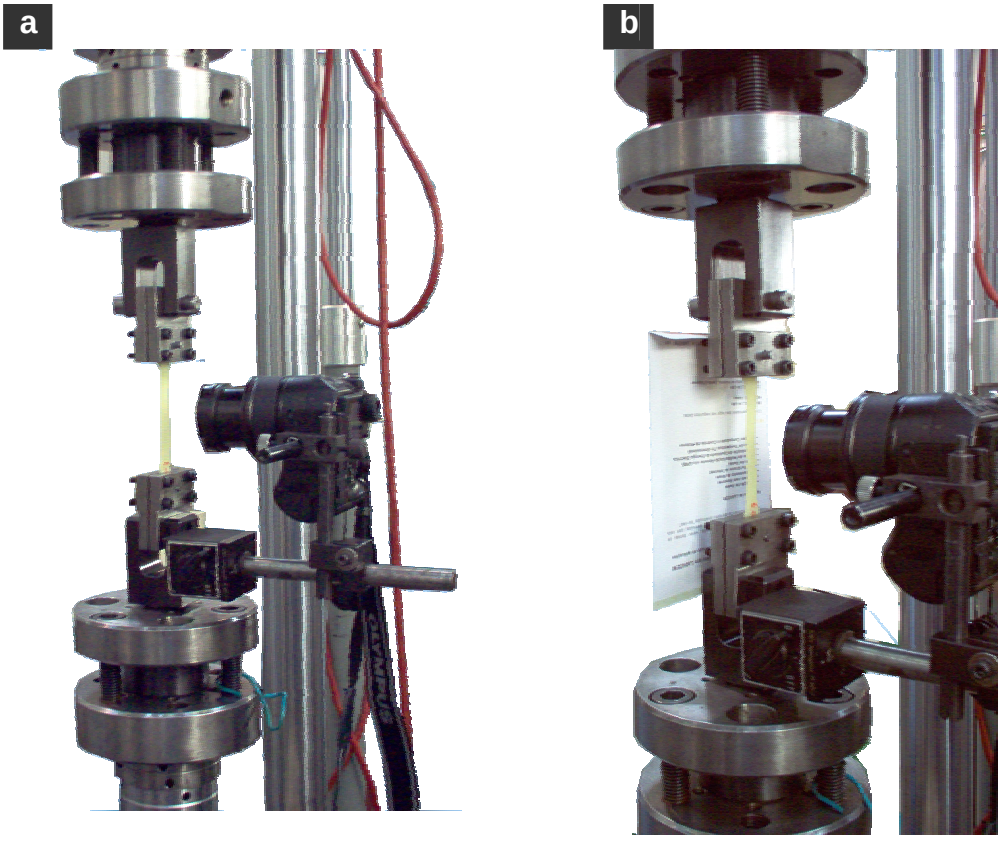

Figure 64. Camera set to register photos of the bulk specimen in the tensile test machine.

The bulk specimen was marked with two points, (figure 65a), used to measure the displacement in the successive photos, (figure 65b).

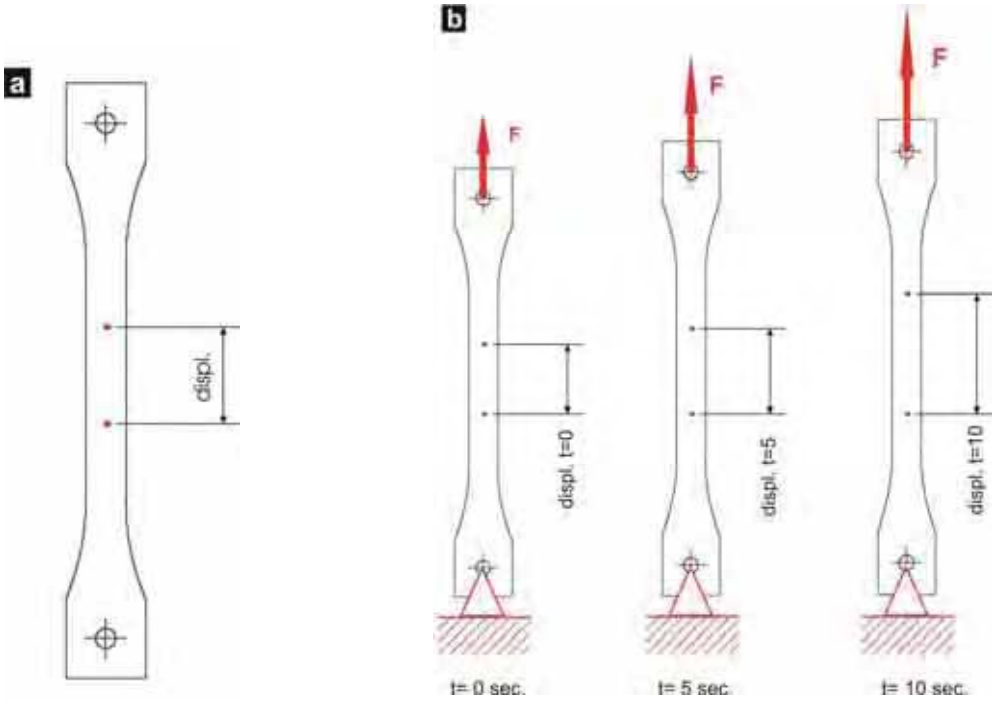

Figure 65. Specimen marked with the two points (a) and displacement while stretching (b).

The small strain measurement using the numerical processing of digital images was done with the help of Prof. Chousal [60] . Basically it is the analysis of a sequence of digital images, taken over the time of the tensile test, which are divided in several sub-images that will be subjected to a Fast process of Fourier Transformations (FFTs – Fast Fourier Transforms), as shown schematically in figure 66. The photo taken in R0 moment suffers a Fourier transformation in order to "normalize" the noise and obtain a clear measure of the point (previously marked). This is compared with photo D0 taken in the next moment to determine the displacement.

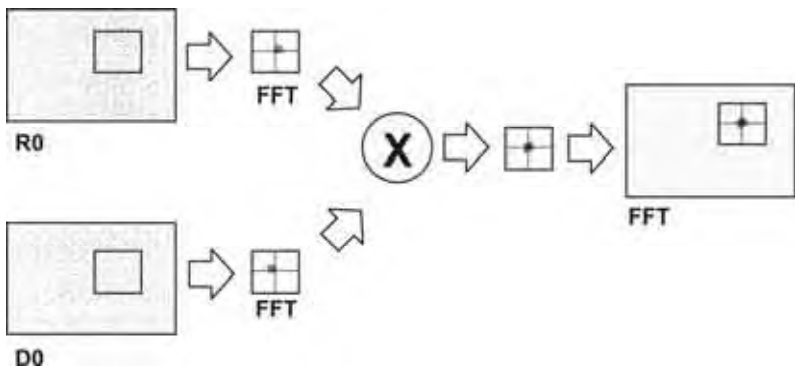

Figure 66. Image processing with Fast Fourier Transforms [60].

5.3.3 Test results and discussion

The bulk specimen test data was recorded into files named after the specimen reference as T#.dat (# - from 1 to 8). These files were imported into spreadsheets to have the stress-strain curves, as shown in figure 67.

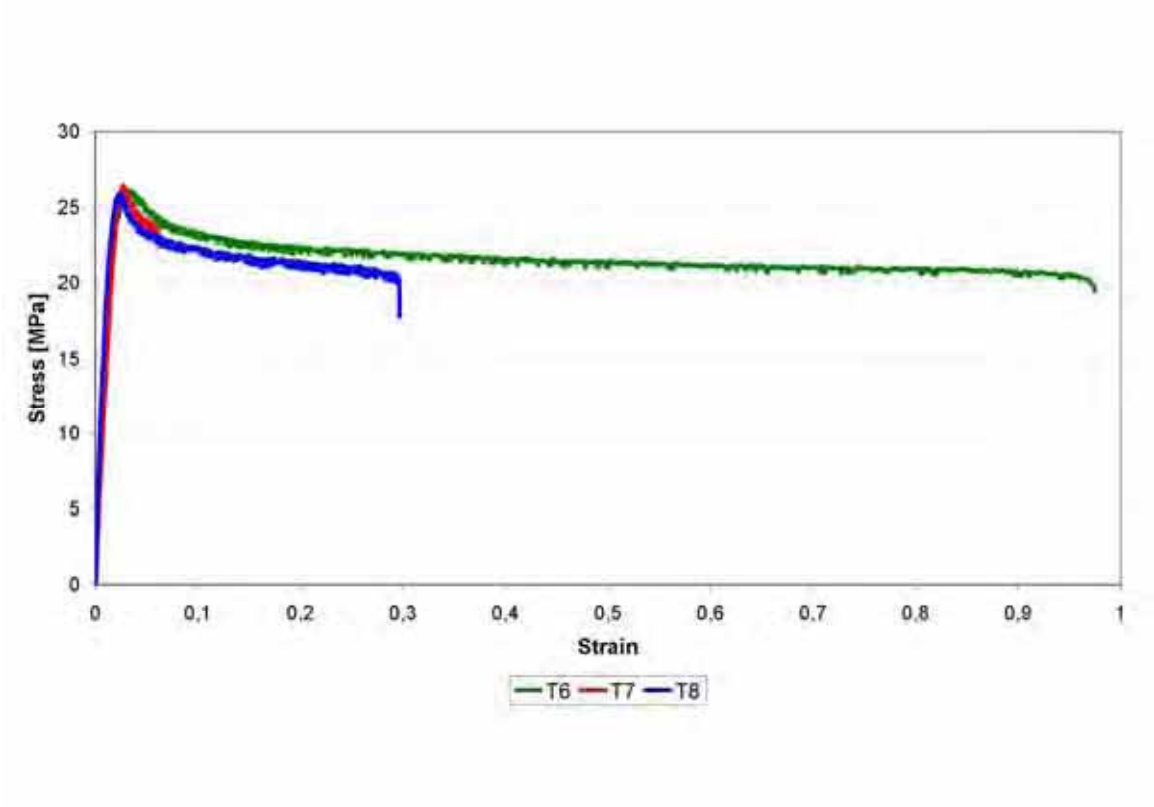

Figure 67. Tensile stress-strain curves (cross-head speed: 1 mm/min) of bulk specimens T6, T7 and T8 (as made) .

The stress-strain curves show a big scatter, especially in terms of ductility. This is probably due to the presence of voids that are difficult to control but have a great influence on the adhesive behavior.

Table 16. Mechanical properties of Araldite® 2021™.

Young's modulus	E	→	1500 MPa
Tensile strenght	σ_r	→	25 MPa
Elongation at break	ε_r	→	40%

The mechanical properties presented in table 16 show that the adhesive is strong and ductile. When compared to a typical epoxy adhesive, Araldite® 2021™ has a lower strength but a higher ductility. The modulus compares well with the supplier data.

5.4 Single lap joints (SLJs)

5.4.1 Manufacture

Figure 68. Fractured Specimen in grip area.

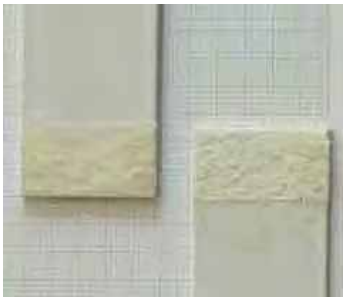

Figure 70. Loctite 3030 overlap showing a 50 % cohesive failure.

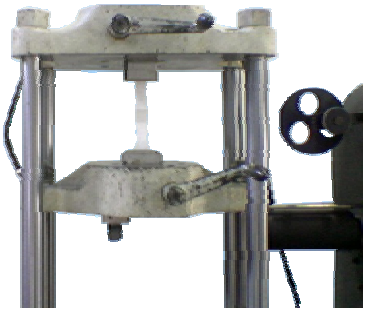

Figure 71. Tinus Olsen test machine with a specimen.

The joint geometry and dimension is presented in figure 69 (ASTM 1002).

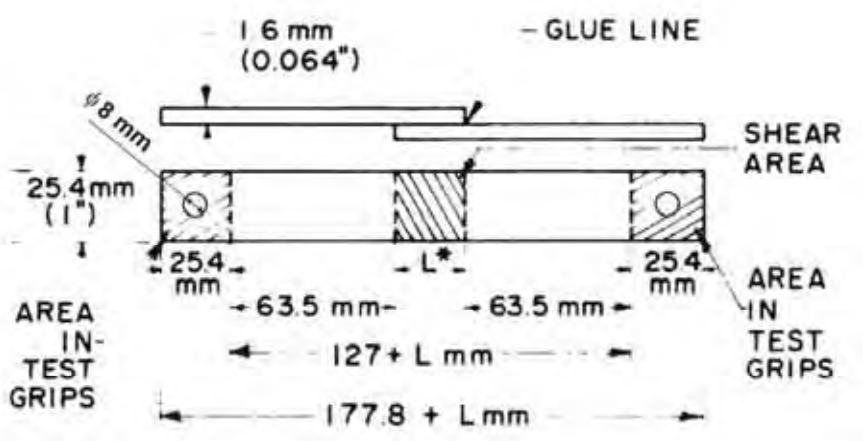

Figure 69. Form and dimensions of the SLJ [61].

One batch of 6 specimens was done using Araldite® 2021™ and Loctite® 3030™ adhesives. The three SLJs with Araldite® 2021™ were referenced A1, A2 and A3 and the other three SLJs with Loctite® 3030™ were referenced L1, L2 and L3.

The first few specimens were tested in a MTS tensile test machine with a grip arrangement that consists of a pin placed in holes of 8 mm in diameter (see figure 69). These specimens (see figure 72) proved to be unworthy because they failed in the grip area due to high stress concentration near the hole for the pin (figure 68).

A different test machine (TINUS OLSEN – figure 71) was used in order to provide a better grip and avoid failure at the hole. This machine uses a different grip

arrangement, consisting of two jaws that grip the specimen uniformly (see figure 71). This time, the specimen fractured in the substrate, away from the grip area. The failure load and failure mode for each test is registered in table 17.

Table 17. Results from the tensile test done with the TINUS OLSEN machine.

	Specimen	Force [N]	Stress [MPa]	Failure
Araldite 2021	A1	1666.0	33.32	Cohesive adherend
	A2	1822.6	36.46	Cohesive adherend
	A3	1832.6	36.65	Cohesive adherend
Loctite® 3030™	L1	656.6	13.13	Cohesive 50%
	L2	656.6	13.13	Cohesive 50%
	L3	1176.0	23.52	Cohesive 50%

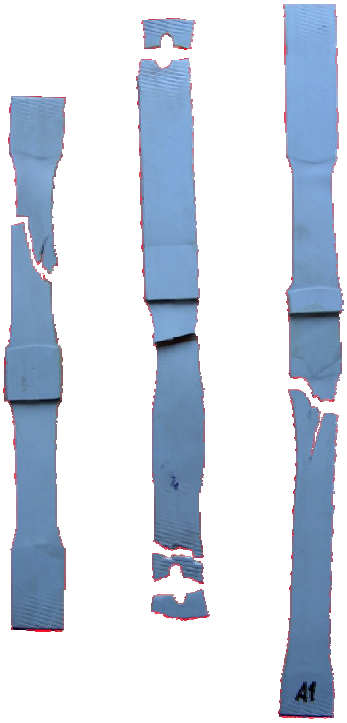

Figure 72. Fractured specimens – substrate cohesive failure.

After the preliminary tests some modifications were made in the geometry of the grip area. Tab ends were used to guarantee that the specimen does not fail in grip area when loaded by the grip arrangement of the MTS machine. This new geometry also reduces the bending moment that occurs in the simple ASTM 1002 specimen. The specimen dimension and geometry is presented in figure 73.

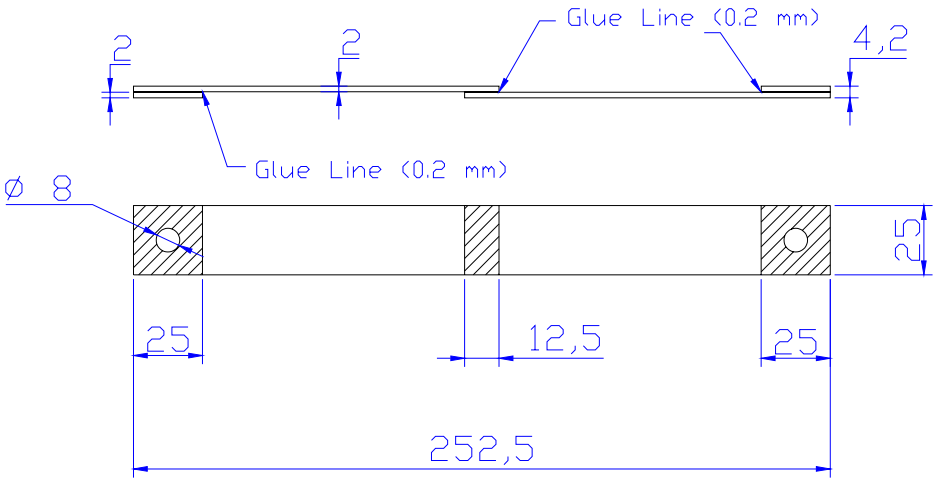

Figure 73. SLJ specimen new version (dimensions in mm).

To manufacture this specimen, a mould was used (figure 75) where packing shims control the glue line thickness and the overlap. Note that before bonding, there is the need to apply the release agent Frekote® 770 NC™ over the entire surface of the mould and the metal shims.

The drawings of the mould are presented in Appendix I.

The procedure used to fabricate the single lap joint specimens was established as follows:

1. Cleaning of the mould with acetone;
2. Application of the Freekote® 770 NC™ release agent (mould is at 45ºC);
3. Cleaning of the PVC adherend surface with acetone (surface preparation);
4. Application of the PVC substrates and tab ends and the 2,2 mm metal skins in the mould;
5. Application of the adhesive in the overlap area (figure 74 a and b);
6. Application of the top substrates;
7. Application of mould lid;
8. Insertion of the mould in the press with a load of 8900 N at room temperature for about 30 minutes;
9. After 30 minutes, release the pressure and remove the mould to the work table;
10. Remove the specimens from the mould.

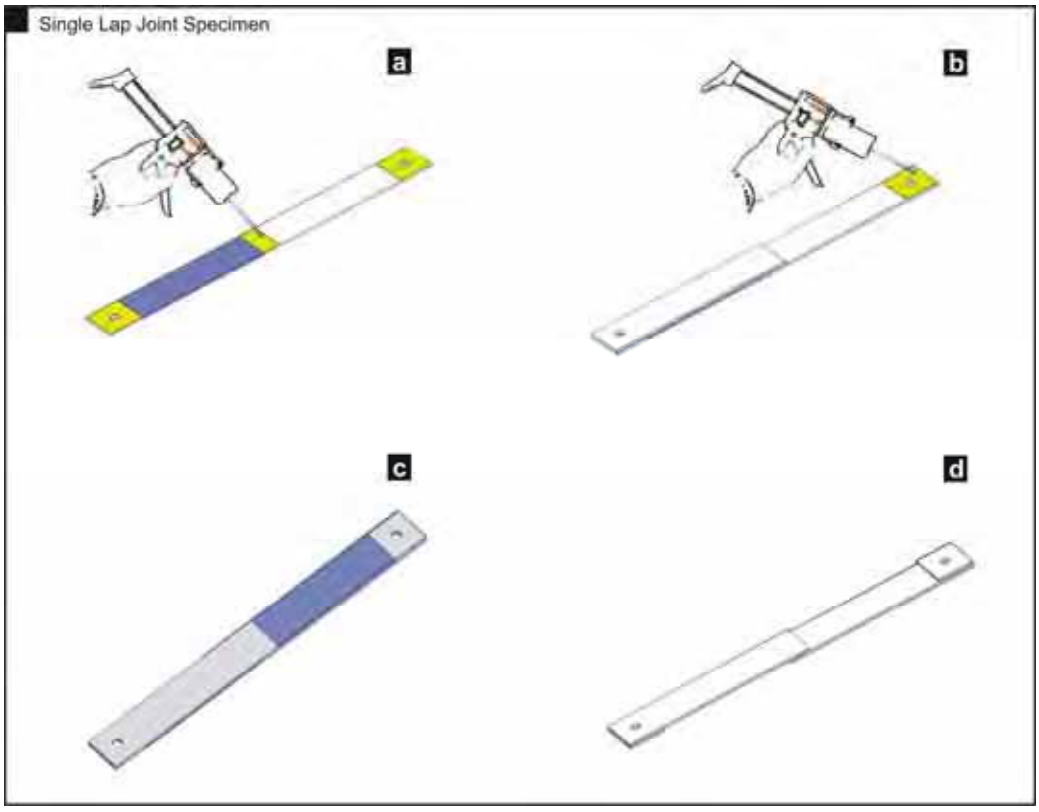

Figure 74. Adhesive application in the SLJ. The yellow parts are the adhesive application areas and the metal shims are represented in blue.

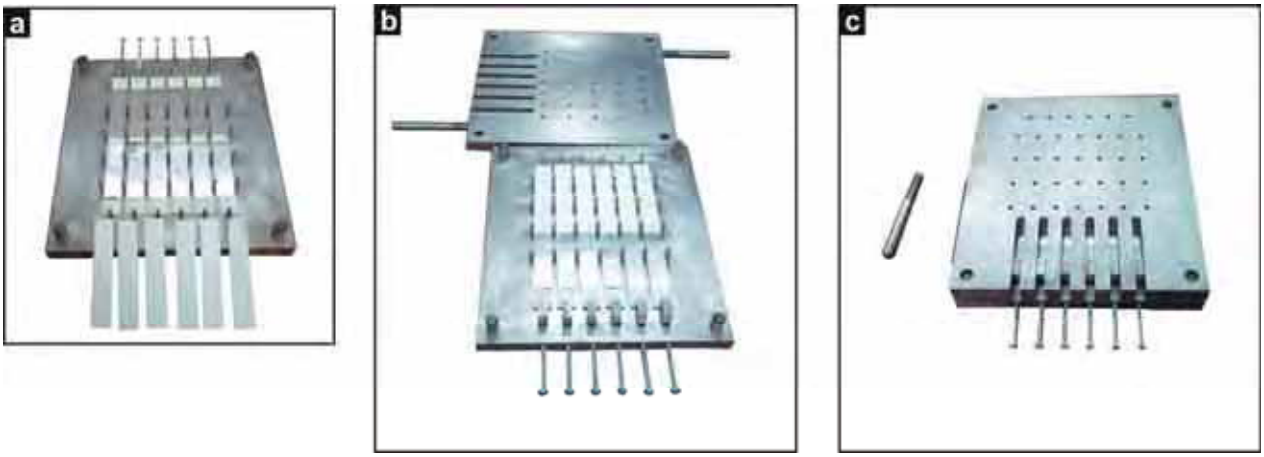

Figure 75. SLJ mould; (a) top PVC substrates ready to be placed; (b) top PVC substrates and skims in place; (c) closed mould ready to insert in the press.

The SLJ specimens obtained were referenced and the dimensions (overlap, glueline thickness) were measured. These measures are registered in Appendix II. Five batches were manufactured and each batch contained six specimens.

The total number of SLJ specimens was thirty referenced LSS1 to LSS30. Four batches of six specimens were placed inside an environmental chamber for the weatherability tests. The last batch of six was tested “as made”.

5.4.2 Test results and discussion

Each specimen was attached to the MTS tensile testing machine (figure 76 a) with an in-house gripping arrangement (figure 76 c). This was prepared over a proper workbench (figure 77) where the screws are fastened to 15 [N.m] and pins were used for proper specimen alignment (figure 76 c).

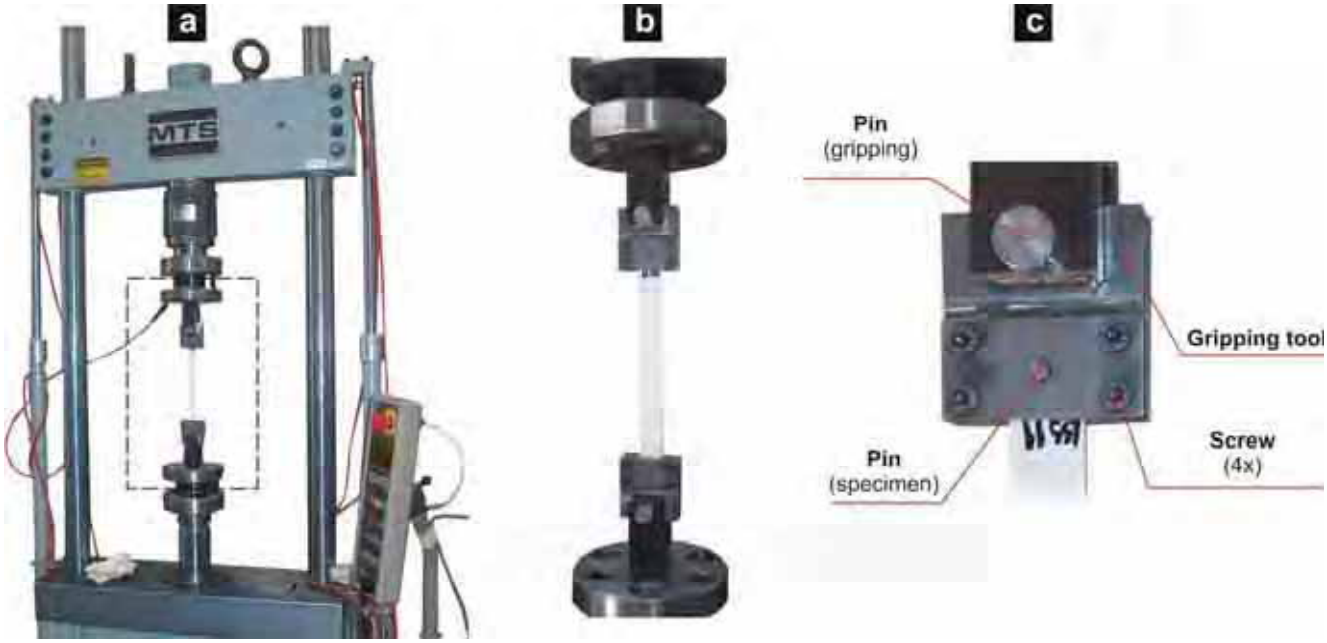

Figure 76. (a) Single lap joint specimen in the tensile test machine (MTS) and zoomed photo of the gripping set (b); (c) In-house gripping tool arrangement in detail.

Figure 77. SLJ specimen grip tool setting for the tensile testing machine.

The lap shear strength test data was recorded into files named after the specimen reference as LSS#.dat (# - from 1 to 30). These files were imported into spreadsheets to plot the load displacement curves (figure 78).

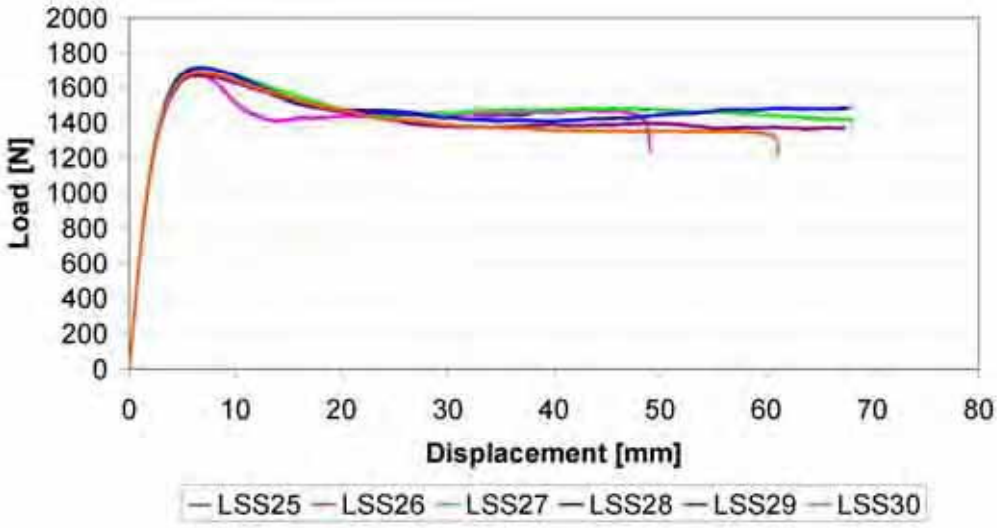

Figure 78. Load – displacement curves of the SLJs test (cross-head speed: 1 mm/min).

The SLJ specimens LSS25 to LSS30 were tested after production, without weathtering.

An elastic zone can be distinguished from 0 N to 1600 N. After 1700 MPa, plastic deformation occurs with the first visible necking which grows until fracture.

The plateau in figure 78 corresponds to the plastic deformation. The specimen begins to create a neck (figure 79) resulting in section reduction and subsequent fracture. The fracture occurs in the substrate away from the overlap, resulting in a cohesive adherend failure. This failure takes place because the bond strength is stronger than the adherend. This SLJ test is like a tensile test of the PVC. It is important to notice that the necking is more visible in the specimens as made, i.e. without weatherability.

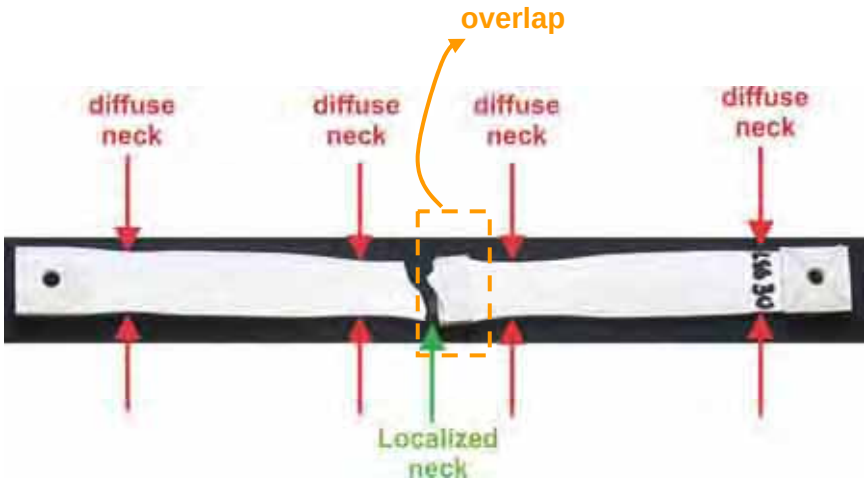

Figure 79. SLJ specimen (LSS30) with diffuse and localized necking.

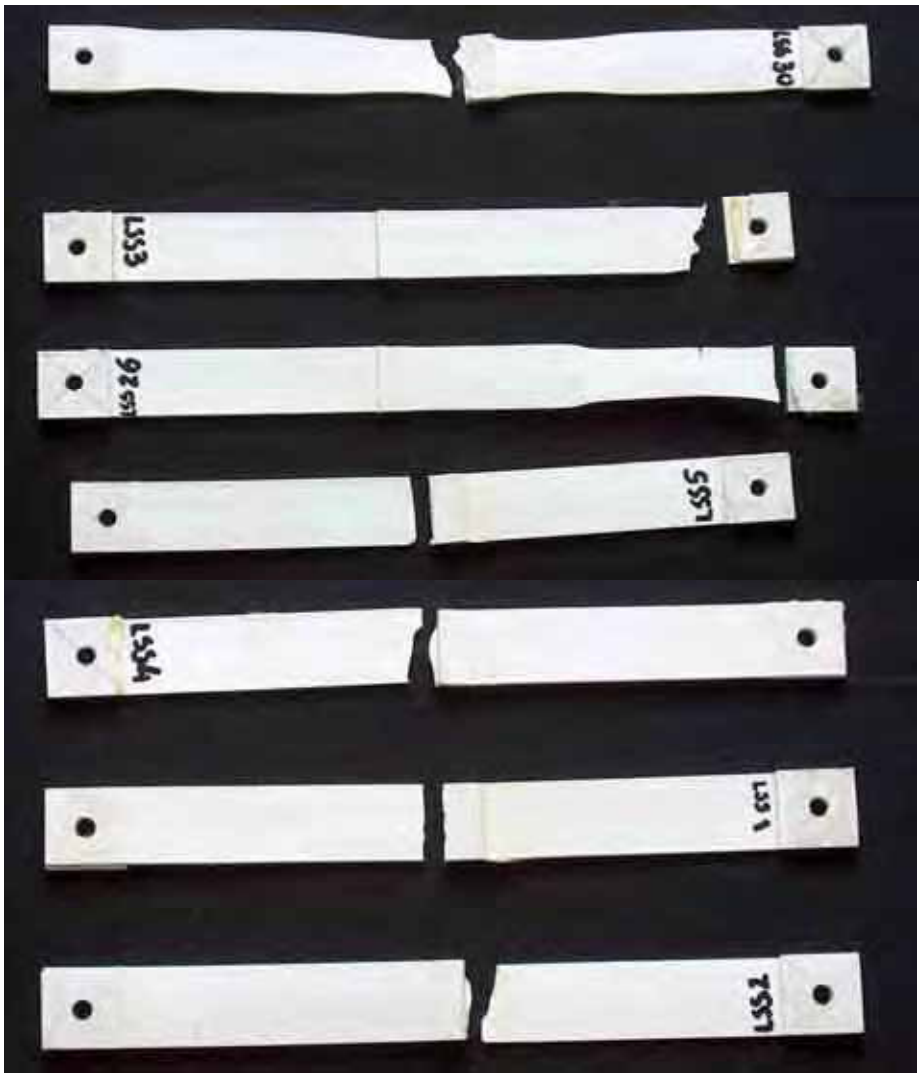

Figure 80. SLJ fractured specimens.

5.4.3 Stress analysis

5.4.3.1 Closed form analysis

There are some closed form models that allow predicting the stress distribution in single lap joints:

- Volkersen (only shear);
- Goland and Reisner (shear and peel);
- Adams and Mallick (shear, peel , longitudinal).

Using a software developed by Adams and co-workers [62] and considering the following entry data, the stress distribution according to each model can easily be obtained.

Table 18. Single lap joint entry data used in V.C. Joint v.1.0.

Geometric parameters	Upper Adherend Thickness (mm) = 2.0000 Adhesive Thickness (mm) = 0.2000 Lower Adherend Thickness (mm) = 2.0000 Overlap Length (mm) = 12.5000 Joint Width (mm) = 25.0000 Load (N) = 1500.0000 Temperature (deg C) = 0.0000
Upper adherend (PVC) Mechanical Properties	Upper Modulus E11 (GPa) = 2.6000 Upper Modulus E22 (GPa) = 2.6000 Upper Modulus g12 (GPa) = 0.9630 Upper Poisson's v11 = 0.3500 Upper Poisson's v12 = 0.3500 Upper Poisson's v22 = 0.3500 Upper Thermal Expansion 11 (per deg C) = 0.0000 Upper Thermal Expansion 22 (per deg C) = 0.0000
Lower adherend (PVC) Mechanical Properties	Lower Modulus E11 (GPa) = 2.6000 Lower Modulus E22 (GPa) = 2.6000 Lower Modulus g12 (GPa) = 0.9630 Lower Poisson's v11 = 0.3500 Lower Poisson's v12 = 0.3500 Lower Poisson's v22 = 0.3500 Lower Thermal Expansion 11 (per deg C) = 0.0000 Lower Thermal Expansion 22 (per deg C) = 0.0000
Adhesive (Araldite 2021) Mechanical Properties	Adhesive Modulus E11 (GPa) = 1.1430 Adhesive Modulus E22 (GPa) = 1.1430 Adhesive Modulus g12 (GPa) = 0.4233 Adhesive Poisson's v11 = 0.3500 Adhesive Poisson's v12 = 0.3500 Adhesive Poisson's v22 = 0.3500 Adhesive Thermal Expansion 11 (per deg C) = 0.0000 Adhesive Thermal Expansion 22 (per deg C) = 0.0000

Figure 81 shows that the adhesive shear stress for this particular loading case (1500 N –value before rupture of the SLJ with Araldite® 2021™ as shown in figure 78) assumes a maximum value of nearly 30 MPa. The mininum value is 0 MPa.

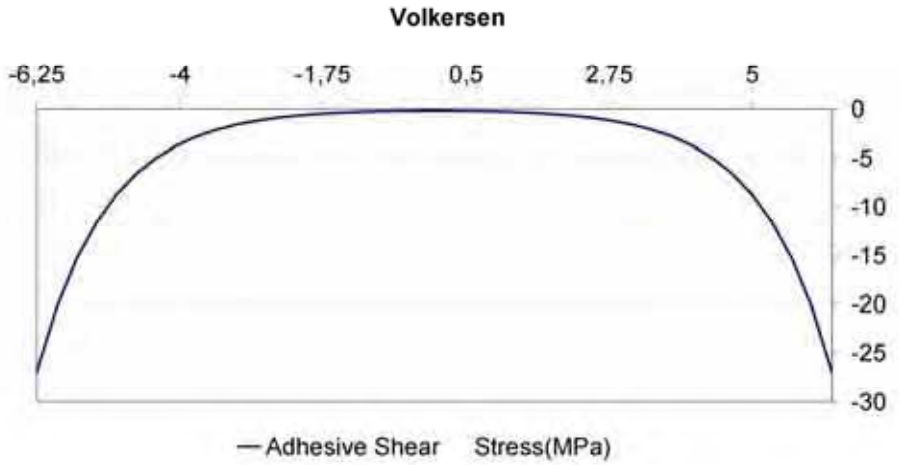

Figure 81. Volkersen analysis.

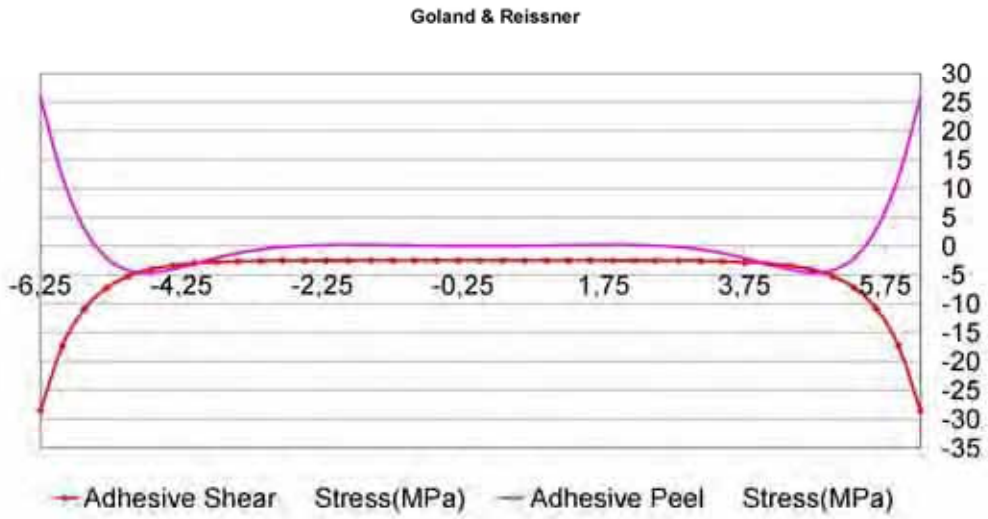

Figure 82. Goland and Reissner analysis.

In figure 82, the maximum value for the adhesive shear stress (red line) is nearly 30 MPa, and the minimum value is very close to 0 MPa. The adhesive peel stress minimum value is 0 MPa and the maximum 27 MPa.

The analytical models are applicable when the adhesive is flexible in relation to the susbtrate, which does not occur in the present case. For example, for the Goland Reissner analysis [36], the range of application is given by:

$$\frac{t_1 G_3}{t_3 G_1} \leq 0.1 \text{ and } \frac{t_1 E_3}{t_3 E_1} \leq 0.1 \qquad \text{Eq. (5.1 and 5.2)}$$

In the present case:

t1 =	2	PVC
t2 =	2	PVC
t3 =	0,2	Araldite 2021
E1 =	2.6	PVC
E2 =	2.6	PVC
E3 =	1.143	Araldite 2021
G1=	0.963	PVC
G2=	0.963	PVC
G3=	0.4233	Araldite 2021

resulting in :

$$\frac{t_1 G_3}{t_3 G_1} = 4{,}396 >> 0.1$$

$$\frac{t_1 E_3}{t_3 E_1} = 4{,}396 >> 0.1$$

$\Rightarrow$ The result is clearly greater than $\frac{1}{10}$, confirming that this single lap joint is out of the application range of the Goland and Reissner model.

Figure 83 shows the results of the Adams & Mallick model. This model enables to have the longitudinal stress in addition to the shear and peel stress.

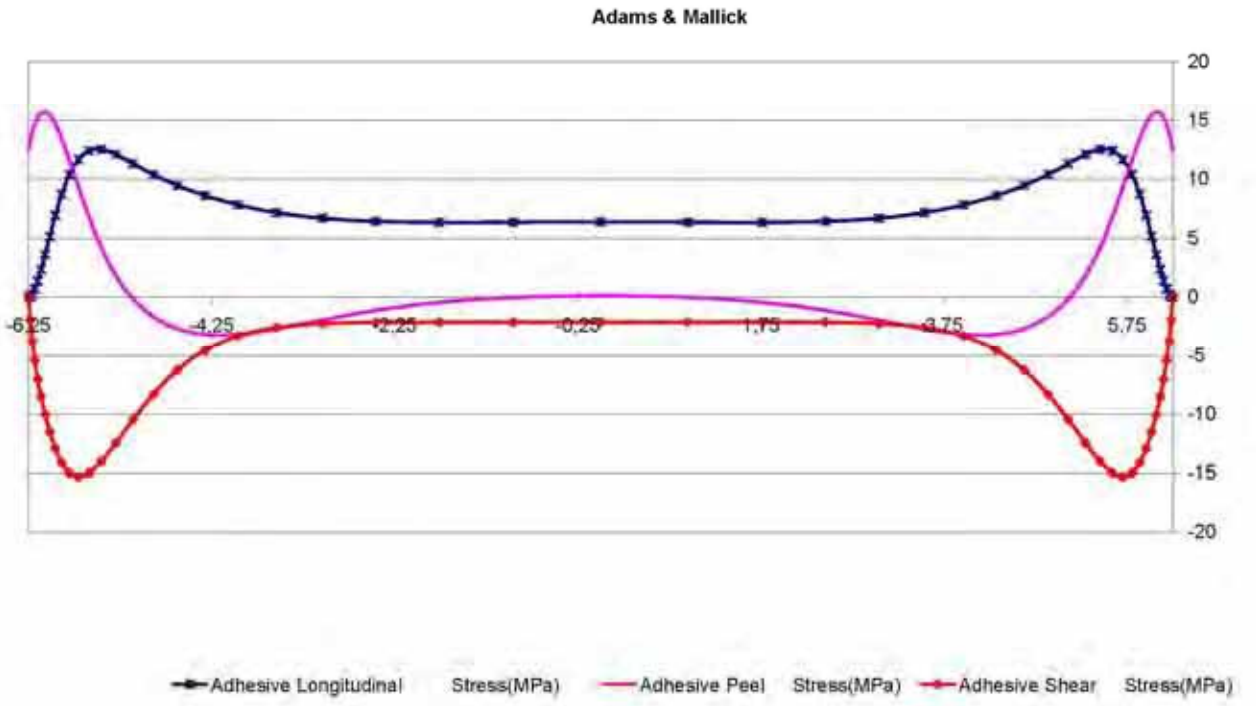

Figure 83. Adams and Mallick analysis graph plot.

The analytical models have the advantage of being easy to manipulate, and are the preferred method of analysis for design purposes. However when they are not applicable in research context, the designer has to use other tools such as the finite element analysis.

5.4.3.2 Numerical analysis (finite element method)

The commercial code ABAQUS/CAE Version 6.5-1 was used to determine the stress distribution.

A model was created with three distinct sections as shown in figure 84.

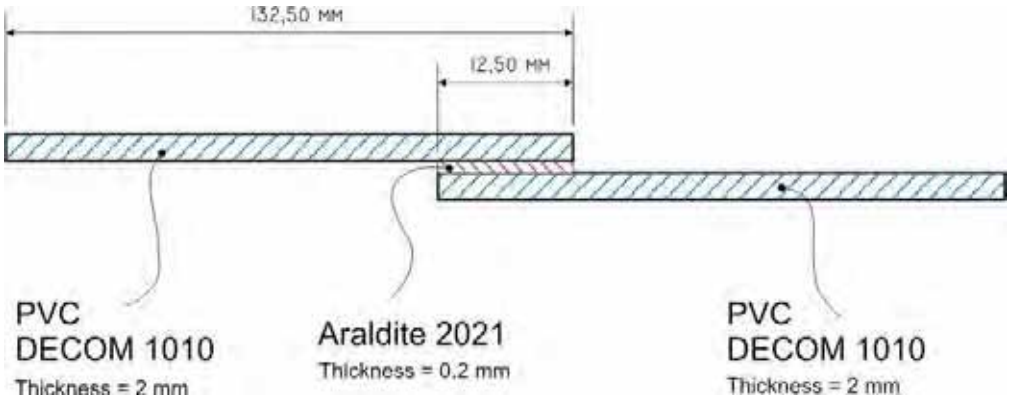

Figure 84. Sections and material attributes of SLJ Specimen - schematic.

The boundary conditions and loading are shown in figure 85, which intend to simulate the experimental test.

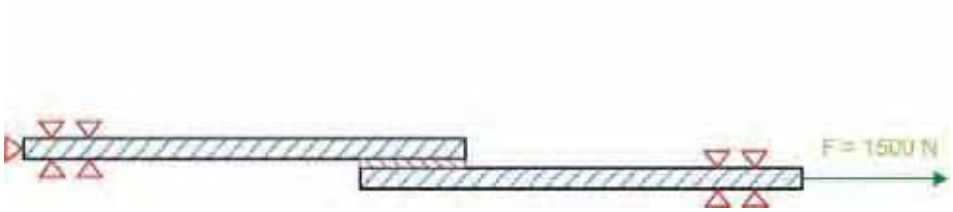

Figure 85. Boundary condition - Schematic.

The mesh density has a big influence on the results. Therefore a convergence analysis was carried out where the mesh density is plotted against the corresponding maximum stress (figure 86 and 87).

Nonlinear geometry (Nlgeom) was considered to include the nonlinear effects present in single lap joints due to the bending caused by the eccentricity of the load (see chapter 4).

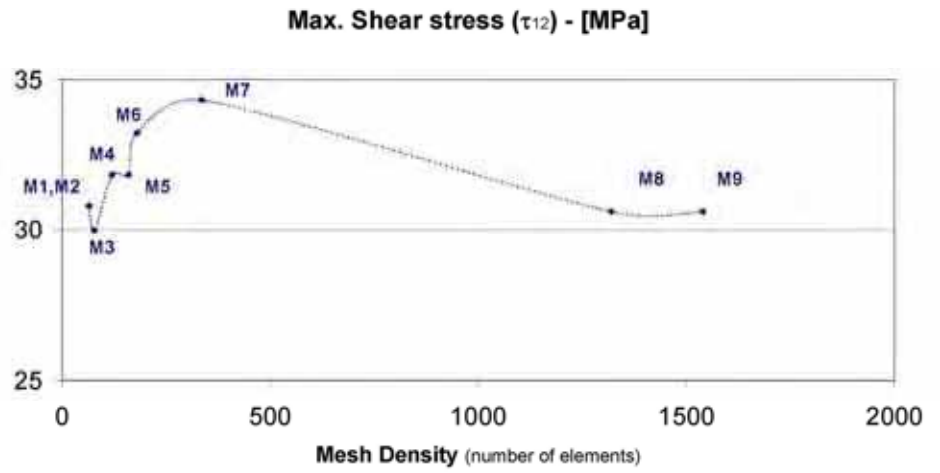

Figure 86. Maximum shear stress versus mesh density (number of elements).

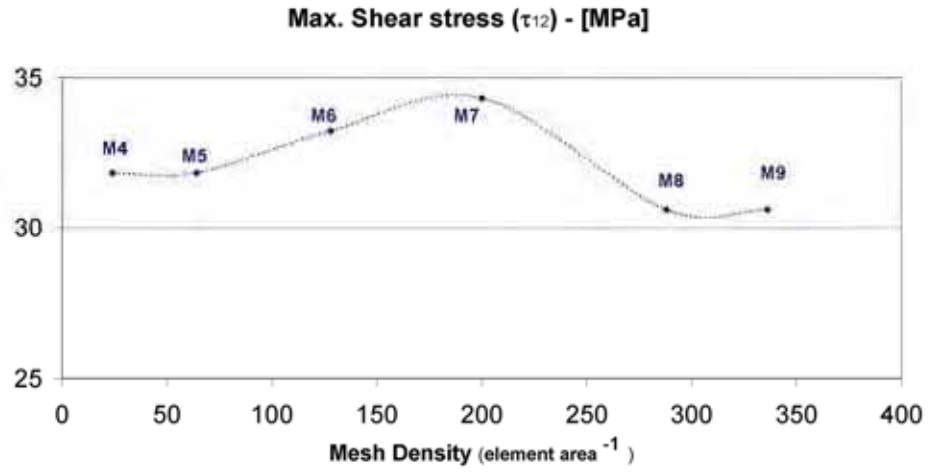

Figure 87. Maximum shear stress versus mesh density (element area^{-1}).

Figure 86 and 87 show that the maximum stress is dependent on the mesh density up to mesh 7. From mesh 8 the stress is more stable and converge for a value of 30 MPa . Mesh 8 is represented in figure 88.

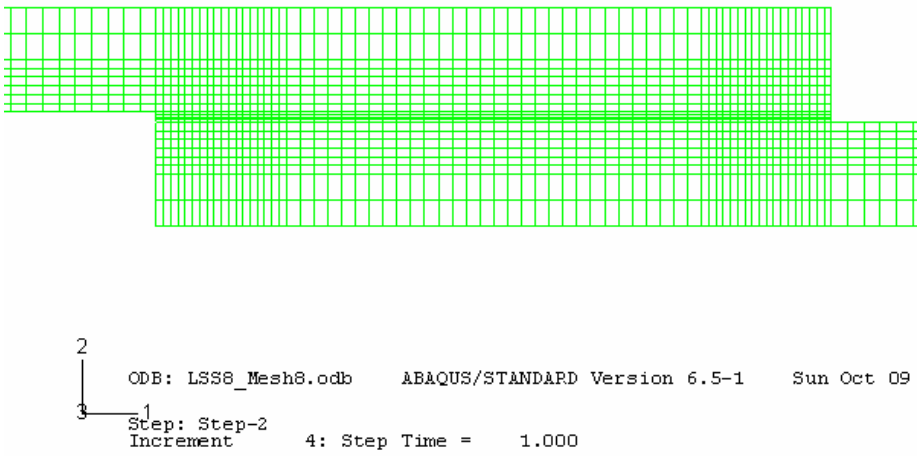

Figure 88. Mesh 8 (overlap).

The adhesive shear and peel stress are represented in figure 89 and 90. It is interesting to note that the maximum stress at the ends of the overlap compare reasonably well with the closed form analysis. However in the middle of the overlap the analytical models are not in accordance with the FEA.

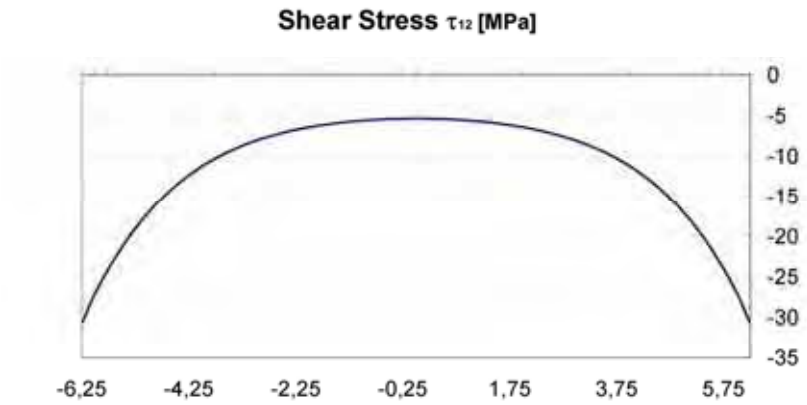

Figure 89. FEA adhesive shear stress distribution.

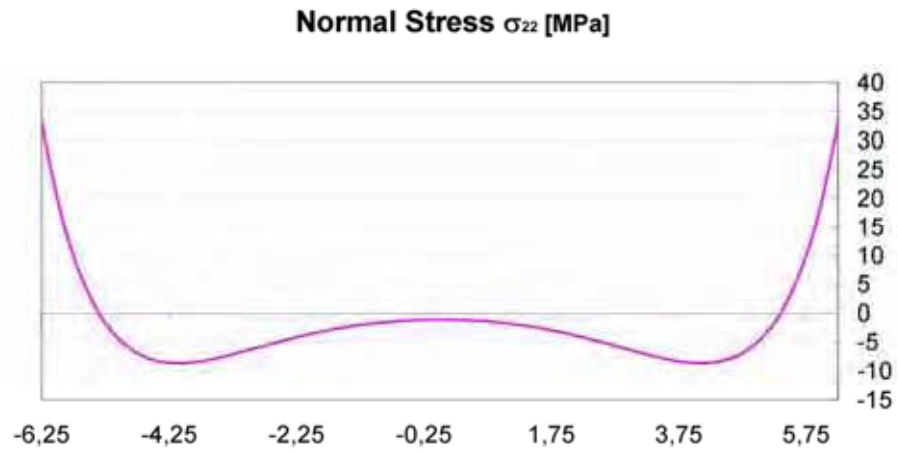

Figure 90. FEA adhesive peel stress distribution.

Figure 90 shows that for 1500 N, the peel stress (σ_{22}) in the adhesive is higher than its ultimate strenght (σ_r = 25 MPa), however the failure occured in the PVC. This is because the tensile test (bulk specimen) was carried out at a strain rate much lower than that experienced by the adhesive when in a single lap joint.

Bulk $$strain\ rate \approx \frac{1\ mm/\min}{50\ mm\ (gauge\ length)} = 0.02\ /\min \qquad \text{(Eq. 5.1)}$$

SLJ $$strain\ rate \approx \frac{1\ mm/\min}{0.2\ mm\ (adhesive\ thickness)} = 5\ /\min \qquad \text{(Eq. 5.2)}$$

The strain rate is much higher in a single lap joint and it is known that the higher the strain rate, the higher the adhesive strenght is, especially for ductile adhesives.

Adhesives are sensitive to strain rate effects and adhesive properties should be determined using the same strain rate that the adhesive will experience in a joint.

The following figures present contour plots of shear and peel stress in the SLJ.

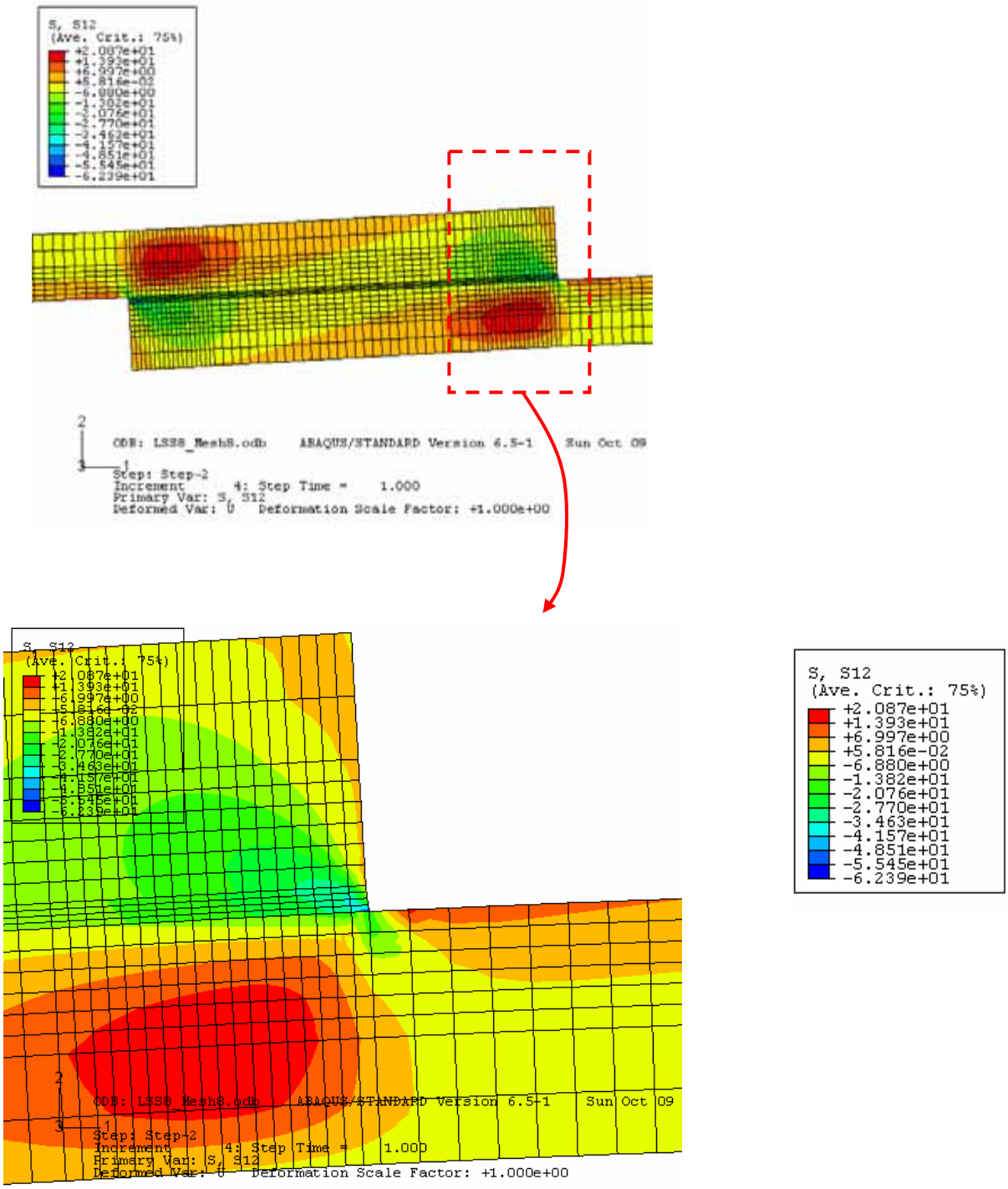

Figure 91. Shear stress contour plot.

The shear and peel stress in the adhesive peak at the ends of the overlap, which is in accordance with the line plots of figure 89.

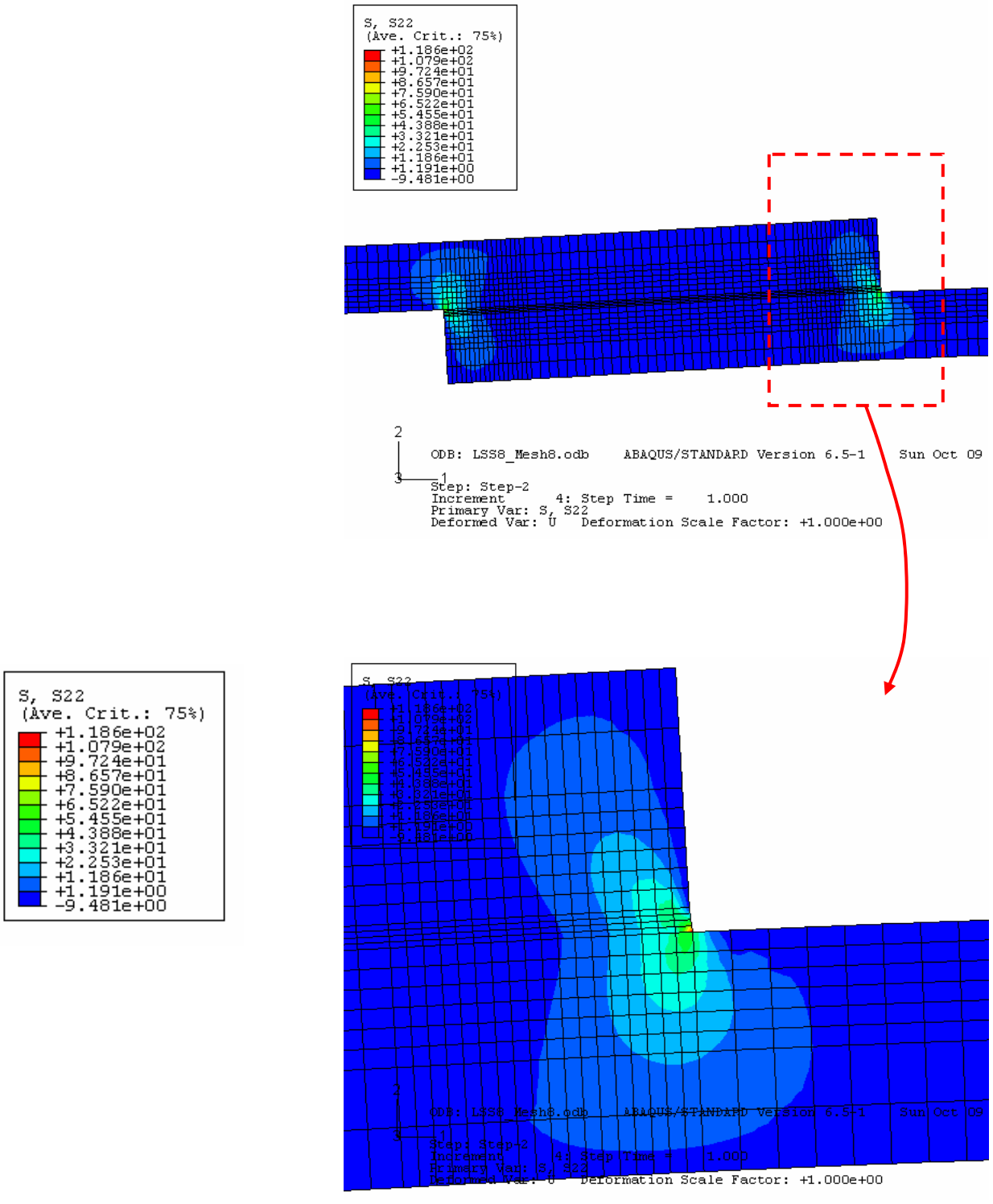

Figure 92. Peel stress contour plot.

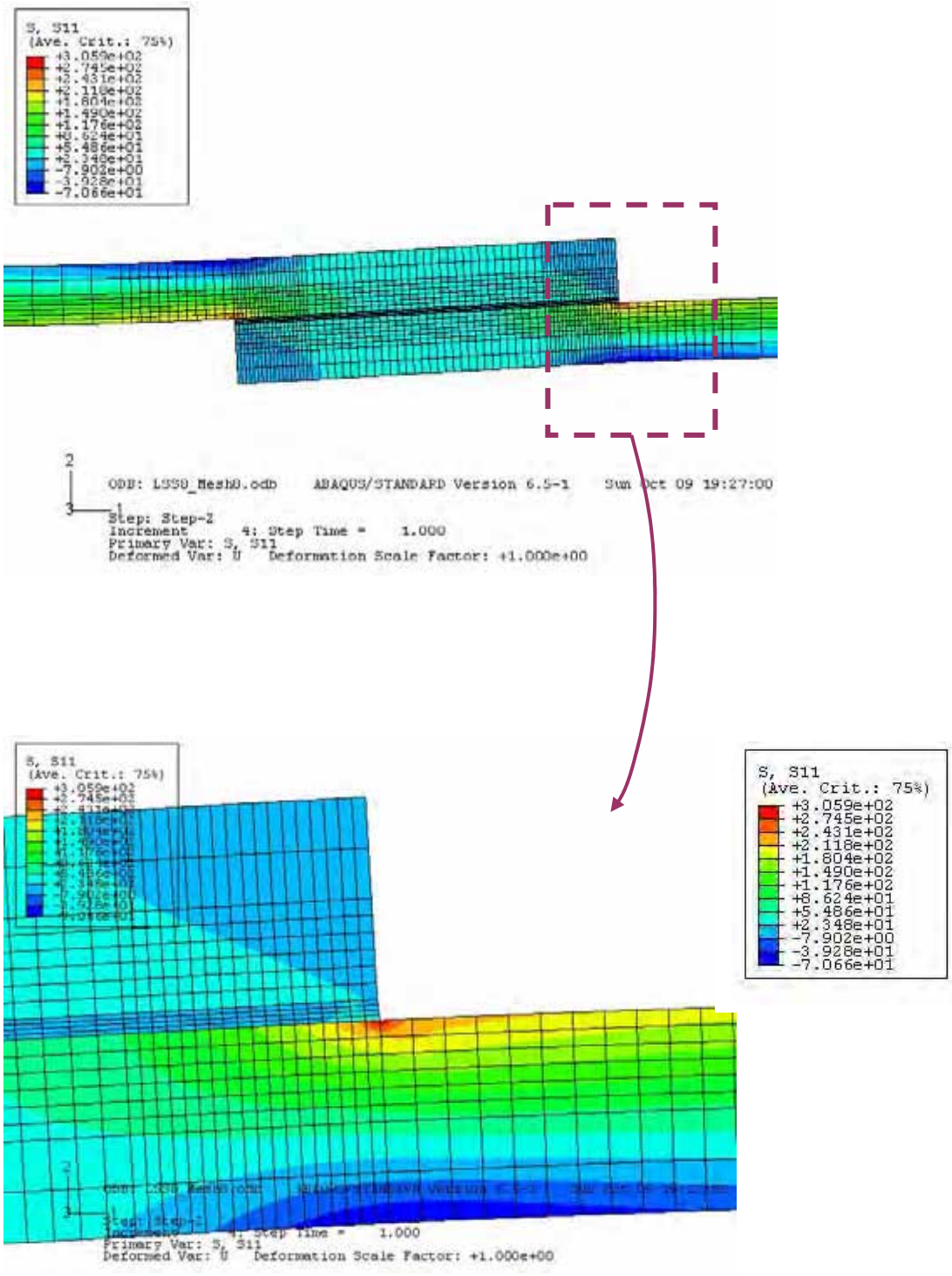

Figure 93. Stress (σ_{11}) contour plot.

Figure 93 shows the critical area (red) in the PVC adherend at the end of the overlap. This confirms the experimental tests results where the PVC failed close to overlap.

5.5 Weatherability

The weatherability is the result of material exposure to the weather. It is a complex phenomenon, dependent on several factors explained in table 19.

Table 19. Degradation parameters or factors of materials [63].

Parameter	Typical range	Comments
UV radiation (sunlight)	295 to 380 nm	UV radiation in this range is found in the sun radiation. UV radiation below 295 nm causes degradation that does not occur in real life
Air temperature	-40 to 40ºC	Air temperature is rarely the same as the material temperature because materials also absorb infrared radiation
Material temperature	-40 to 110ºC	Actual material temperature is a composite of air temperature, effect of infrared radiation, effect of wind, and surface evaporation of water. Material temperature is a parameter which must be selected for testing.
Rain	0 to 2500 mm/year	Rain is important because it washes away material components at its surface (e.g., acid rain).
Relative humidity	10 to 100%	The relative humidity degrades some components of the material and promotes deposition of pollutants.
Pollutants	Variable	Pollutants include carbon oxides, ozone, oxides of sulfur and nitrogen, radicals, dust particles. These pollutants can be deposited by rain to become more aggressive degradants
Stress	Variable	Materials degrade more rapidly under a mechanical stress

Weatherability plays an important role in the mechanical behaviour of a material and in its lifetime. Windows and doors are applied in the house interface to prevent the weather factors (such as hot air in the summer, cold air in winter, rain and sun) to change the optimal climatic conditions inside the house. The effect of the weather agents on these elements should be controlled and minimized.

Due to the polymeric nature of both adherend and adhesive, the weatherability is particulary important and this point should therefore be studied.

5.5.1 Weatherability factors

For polymeric materials, the most relevant factors of degradation are photodegradation, water absorption and temperature.

i. Photodegradtion

This is the most relevant aspect of polymers weatherability. Solar spectra contain substantial ultraviolet radiations (between 0.28 and 0.4 μm in wavelength) shown in figure 94, which carries energy that photoexcites certain polymeric groups with a selective absorption.

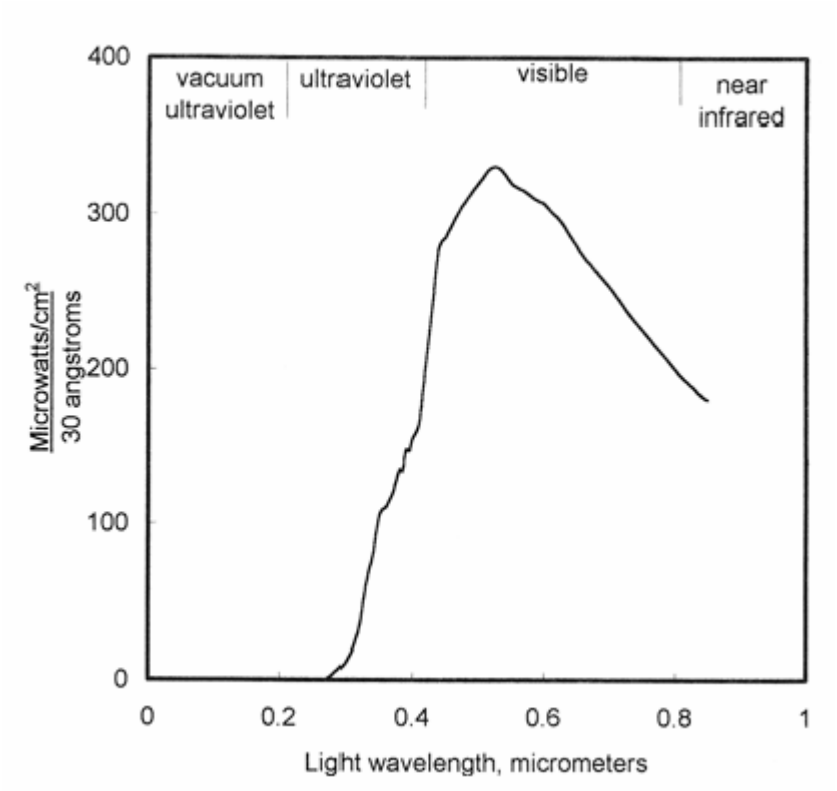

Figure 94. Solar spectrum [64].

Due to UV or oxygen impermeability of the polymer, this weatherability is essentially a surface phenomenon. In most cases there is an oxidation aided by the UV radiation. This oxidation leads to polymer chain rupture, affecting the mechanical properties by reducing the failure strength.

In PVC and polymers with benzenes (polystyrene, polycarbonate, etc.), the photo-oxidation drives to colored structures (yellowing).

ii. Temperature effect

Thermal ageing implies a slow and irreversible evolution of the structure, the composition and the morphology of materials, related to their exposure to higher or lower temperatures. This effect occurs as a result of physical or chemical mechanisms.

The general effect is observed in figure 95 where the lifetime is defined as time versus property with temperature.

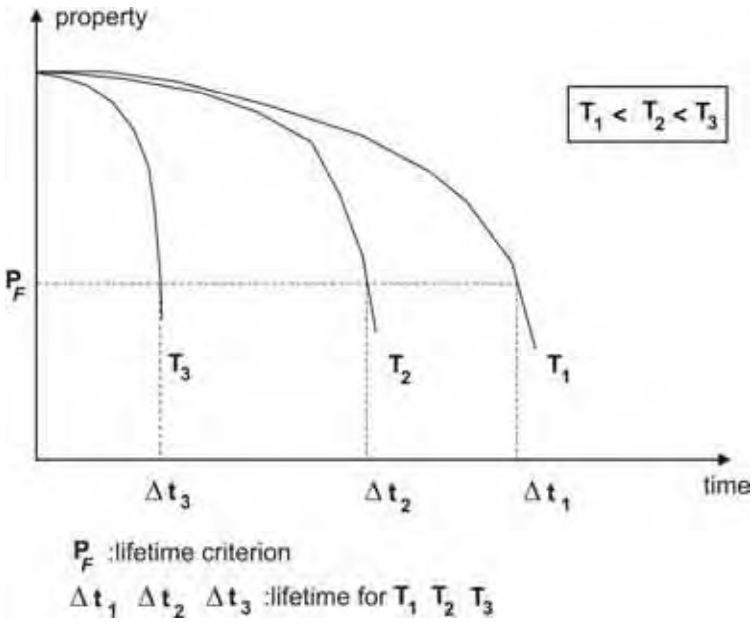

Figure 95. Curves for the development of one property for three different temperatures, with the lifetime determination for a given lifetime criterion (P_F).

iii. Water absorption

Water can easily penetrate inside the macromolecular chains, breaking their interconnection, leading to an increase in mobility. This mobility increase is characterized by an increase in ductility and a reduction in the Young's modulus as shown in figure 96. Normally this is reversible when the polymer dries in an oven.

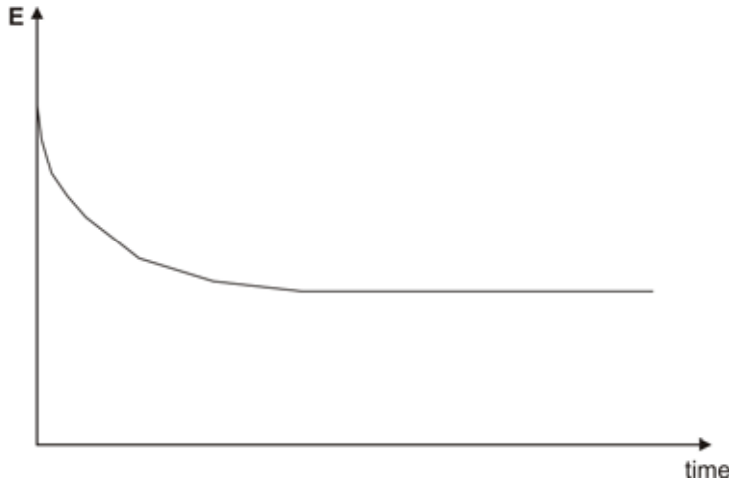

Figure 96. Typical evolution of a Young's modulus when a polymer is immersed in a liquid medium.

iv.Hydrolytic weatherability

Some polymers contain hydrolysable groups in their chains, susceptible to weathering in humid atmosphere or in water immersion. Hydrolytic weatherability occurs when water promotes the split of a chemical bond, often splitting one compound into two. This reaction leads to a chain rupture and an important ductility reduction, making it brittle with time.

The polymer life can be expressed by t_F [65]:

$$t_F = K \cdot (RH)^{-\alpha} \cdot \exp(E_H / RT) \qquad \text{Eq. (5.3)}$$

K $\Rightarrow$ constant
RH $\Rightarrow$ Relative humidity
α $\Rightarrow$ Constant near unity (1)
E_H $\Rightarrow$ Hydrolyses activation energy
R $\Rightarrow$ Perfect gas constant
T $\Rightarrow$ Temperature

Note that water absorption effects have a major impact in weathering than the hydrolysis, but the difference resides in their irreversibility. Water absorption is reversible by drying processes, but hydrolysis is irreversible.

5.5.2 PVC and acrylics weatherability

The two polymers studied in this work are PVC and acrylic. Their weatherability is specified in detail, next.

i. PVC

PVC is susceptible of dehydrochlorination under the action of heat, UV light, oxygen, radiations, etc. This process occurs when a hydrogen and an adjacent chloride atom are subtracted upon heating, to form a double bond that disintegrates the chains with elimination of hydrogen chloride and formation of sequential double carbon-carbon bonds in macromolecules with the appearance of undesirable coloration (from yellow up to black). Some major improvements have been done recently to reduce this effect by using fillers and compounds such as titanium oxide TiO_2 [66,67]. The PVC profiles used in window and door production contain these fillers and compounds and have good resistance to weather degradation.

Elvira B. Rabinovitch [64] states that PVC performs well in both color retention and impact retention compared to other polymers. The buckling strength of PVC profiles were measured as shown in table 20.

Table 20. Additional stress to cause the buckling of polymers in a window profile [64].

Material	Coefficient of linear thermal expansion cm/cm ºC	Heat defelection temperature, ºC	Safety margin (additional stress to cause buckling) in [MPa]	
			White PVC	Brown PVC
Rigid PVC	2.1×10^{-5}	68	6.0	3.5
High heat PVC	1.9×10^{-5}	74	6.9	5.0
Glass Fiber reinforced PVC	0.9×10^{-5}	73	18	15

From the previous table we can conclude that buckling resistance is better with a low coefficient of linear thermal expansion. Elvira also indicates that PVC usually has superior microbial resistance.

The DECOM 1010 PVC studied in this work is near to high heat PVC (white PVC).

ii. Acrylic (PMMA)

PMMA has a good stability to outdoor exposure. In fact its weatherability resistance is referred as one of its most outstanding property [68,56]. However, acrylics are chemically attacked by ketones, esters, aromatic and clorinated hydrocarbons. This should be taken into account when working with these products, mainly the ketone used to clean the surfaces before bonding.

It is also known that the PVC is compatible with acrylic adhesives, but can be attacked by their activators before the adhesive has cured [56]. However, in the case of Araldite®2021™ the activator is mixed with the acrylic resin through a mixing nozzle before contacting the surface of the PVC, avoiding the direct contamination and not allowing this chemical attack.

5.5.3 Testing conditions

Testing for weatherability means subjecting a specimen to the environmental conditions that the joint will normally experience in service. These tests should be done over several months or years. There is however an established time for these tests, of about 10^4 hours (a year and two months), that allows predicting the mechanical properties over a longer period of time by extrapolation of the results obtained for 10^4 hours. There is little variation of the properties after 10^4 hours, and the major degradation of the properties occurs in the first 2000 hours (three months) of the test [33].

In this work, the time available was limited to twelve months, so there was the need to plan accelerated weathering tests. There was also the limitation of the light exposure, because it was done inside an environmental chamber without an UV lamp. However, from previous studies, the two materials (PVC with fillers and PMMA) have a good resistance to U.V. radiation so there should be no problems in this field.

Single lap joint specimens PVC - Araldite® 2021 and Araldite® 2021 bulk specimens were tested for residual strength after weathering. The single lap joint specimens are important to determine the effect of weathering on the adhesion and the bulk specimens enable to assess the direct influence of temperature and relative humidity on the adhesive.

In the Araldite® 2021 product specification sheet, there is a reference to tropical weathering test, using DIN 50015 standard as a reference. The conditions of this tropical weathering are 40 ± 2 ºC and 92 ± 3% of relative humidity.

Figure 97. Door in Quinta do Peral, Alentejo.

However in this study it was decided to use different conditions to simulate the Portuguese climate with a more severe temperature (60ºC maximum and a relative humidity which can reach 80%). The most severe climatic conditions of Portugal were taken into account. The highest values of temperature and moisture were obtained by consulting the Portuguese meteorology authority (Instituto de Meteorologia e Geofísica) internet site. To confirm these values the temperature on some windows applied in the Alentejo region (hottest) was measured on the door surface (figure 97). The value obtained for the exterior surface temperature of the door exposed directly to the sun was of 56ºC in September 10th 2005 with an ambient temperature of 35 º C.

Based on the previous data, the tests were carried out at a temperature of 60ºC and a relative humidity of 80%, as shown in figure 100.

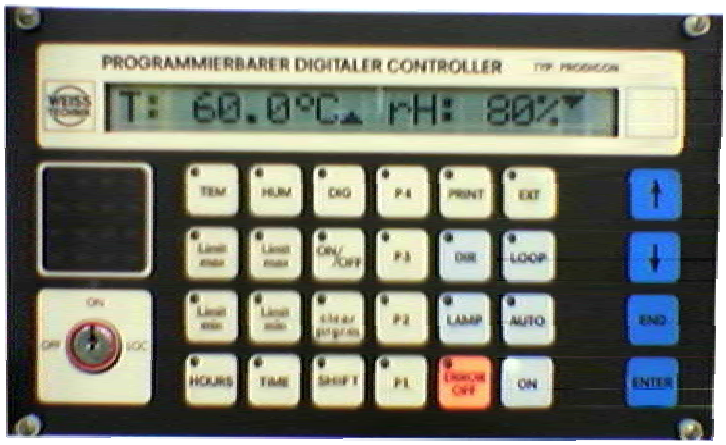

Figure 100. Weiss Technik Digital Controller.

Figure 98. Weiss Technik environmental chamber.

Twenty four single lap joint specimens (4 sets of 6 specimens), and 4 bulk specimens of Araldite® 2021, were placed in the environmental chamber (see figure 98 and 99). The time of exposure of each specimen is indicated in table 21.

Figure 99. Specimens placement inside the environmental chamber.

Table 21. Specimens time of exposure inside the environmental chamber.

Specimen reference	Type of specimen	Days of exposure inside the environmental chamber
LLS1 to LSS6	Single Lap Joint	**11**
T1	Bulk Araldite® 2021	
LSS7 to LSS 12	Single Lap Joint	**49**
T2	Bulk Araldite® 2021	
LSS13 to LSS 18	Single Lap Joint	**79**
T3	Bulk Araldite® 2021	
LSS19 to LSS 24	Single Lap Joint	**105**
T4	Bulk Araldite® 2021	

The weathered specimens were tested a few hours after removal from environmental chamber.

The manufactured Araldite® 2021™ Bulk specimens (T5, T6, T7 and T8) were tested in order to obtain the adhesive mechanical properties. The weathering effects were measured testing T1 (11 days of weathering), T2 (49 days of weathering), T3 (79 days of weathering) and T4 (105 days of weathering) specimens.

5.5.4 Bulk results and discussion

The tensile stress-strain curves of the specimens subjected to temperature and relative humidity are shown in figure 101.

This figure shows T3 (79 days) having the higher value for elongation, T2 (49 days) has the second best elongation value. T1 (11 days) and T4 (105 days) shows a lower elongation value when compared to the other two. The same trend occurs for the tensile strength. T3 specimen gives a tensile strength of 33 MPa, T2 32 MPa, T1 30 MPa and T4 27 MPa.

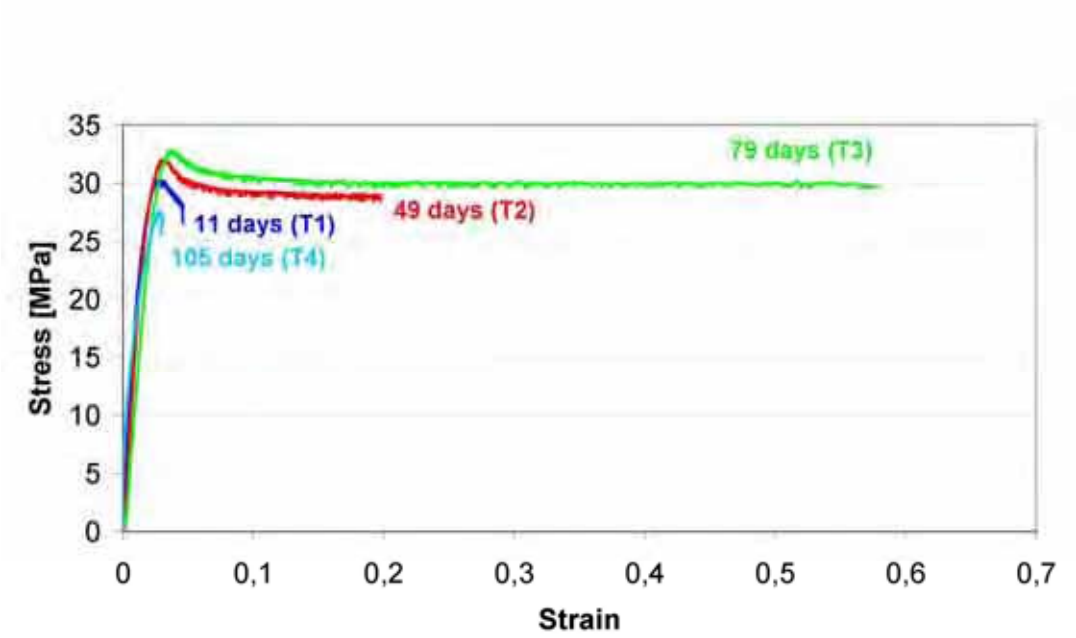

Figure 101. Stress-strain curves (cross-head speed: 1 mm/min) of the adhesive bulk specimens T1 (11 days) , T2 (49 days), T3 (79 days) and T4 (105 days).

These results show that in the first 79 days, the adhesive gets stronger and more ductile. However, after 105 days the effect of weathering is the opposite. It is as if initially the effect of the humidity is dominant (ductility increases) and after a period of time, the temperature effect gets more important (more brittle). The temperature “over cures” the adhesive making it brittle.

Figure 102 includes the tensile stress-strain curve of a specimen without weathering for comparison purposes.

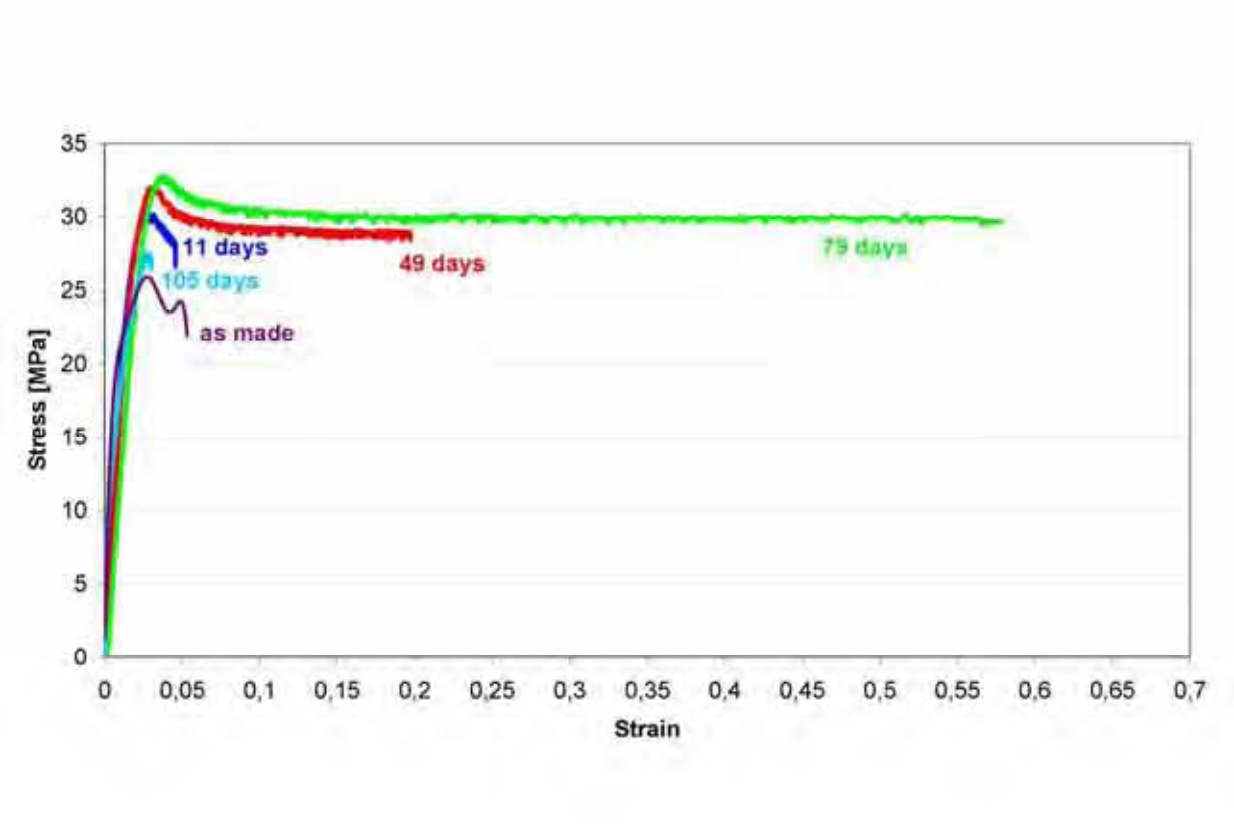

Figure 102. Graph plot of the adhesive bulk specimen tensile tests (cross-head speed: 1 mm/min) before (as made) and after weathering (T1, T2, T3 and T4) .

The weather is clearly favourable up to 79 days but is detrimental after 105 days. However, these results should be analysed with caution because only one specimen was tested for each weathering case. These tests need confirmation with more specimens.

5.5.5 Single lap joint test results

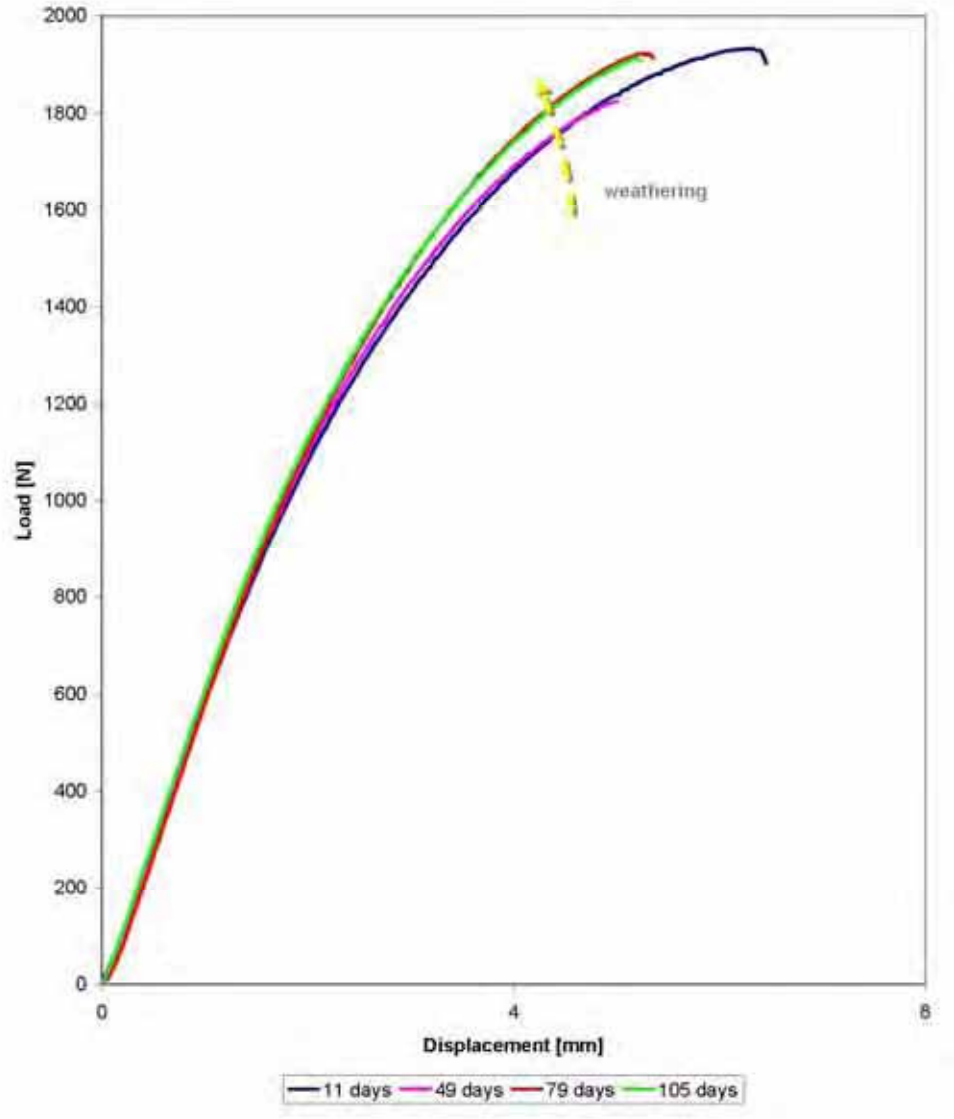

Figure 103. Load-displacement curves of the aged single lap joint specimens (cross-head speed: 1 mm/min).

The results after weathering are shown in figure 103. The load-displacement curves do not differ significantly with the time of ageing.

To assess the effect of weathering, figure 104 presents a graph plot with the weathered specimens and the as made specimens.

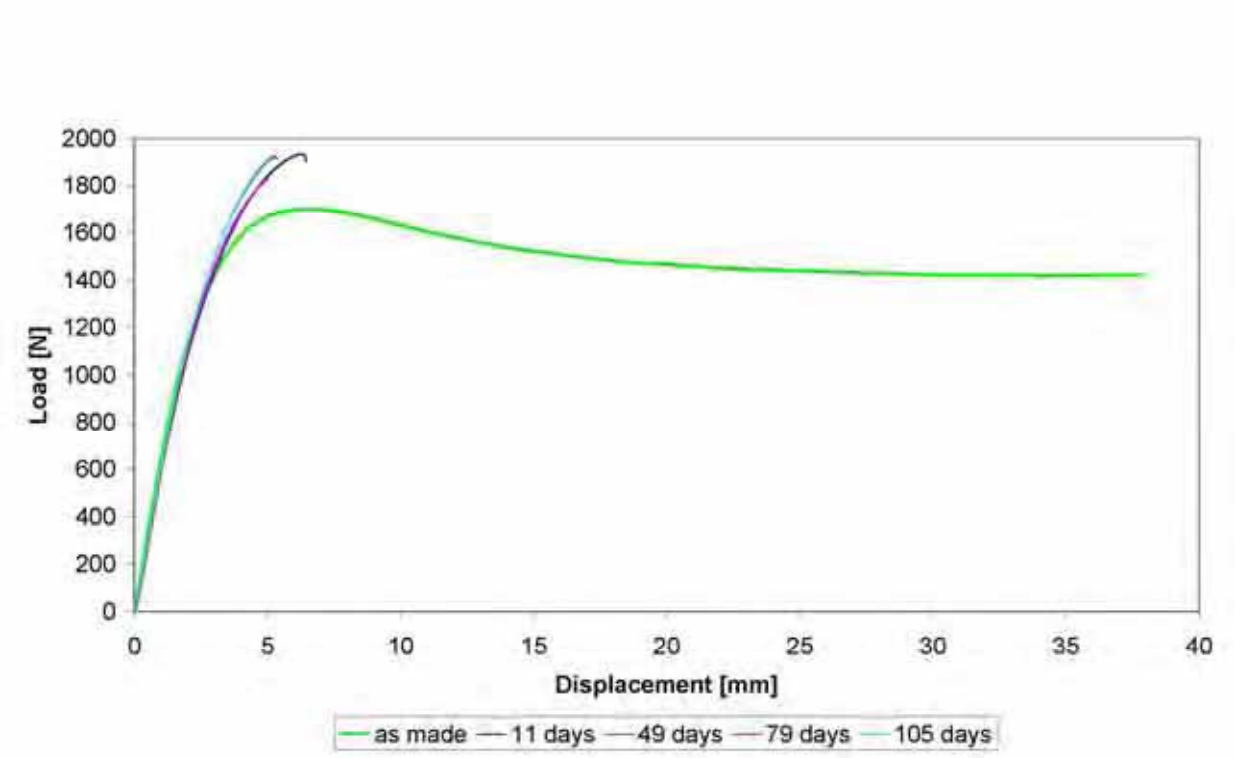

Figure 104. Effects of weathering on the load-displacement curves of single lap joint specimens (cross-head speed: 1 mm/min).

Figure 104 shows that the single lap joint specimen toughness decreases with the weathering effect. A ductility reduction and a rise in the failure load are also observed. The brittleness effect is very visible with the total inexistence of elongation for the weathered specimens in opposition to the high elongation when the specimens are tested as made.

It is important to notice that the failure occurs in the adherend, i.e. the displacement is mostly from the PVC, rather than the adhesive. Therefore the change in mechanical behaviour of the SLJ with exposure to temperature and RH is mostly due to the PVC. The weatherability tests therefore confirm that the adhesive is suitable for this application because the adherends (PVC) are degraded more severely than the adhesive.

5.6 Tg determination

Figure 105. Mould spatial organization.

The glass transition temperature plays an important role in the adhesive mechanical behavior, making crucial its determination because it will output the temperature range suitable for the adhesive to maintain its mechanical properties namely strength (generally decreasing with temperature raising) and ductility (generally increasing with temperature raising).

In this particular case, the adhesive should withstand temperatures ranging from 0º C to 60ºC, so it will work well together with the PVC substrate.

A bulk specimen was first used, but the results were not conclusive due to its low rigidity, not allowing to obtain a good test. To solve this problem, the adhesive was cast over an aluminum bar to increase the rigidity of the specimen, as shown in figure 107.

Figure 106. Silicone rubber frame and the aluminum bases.

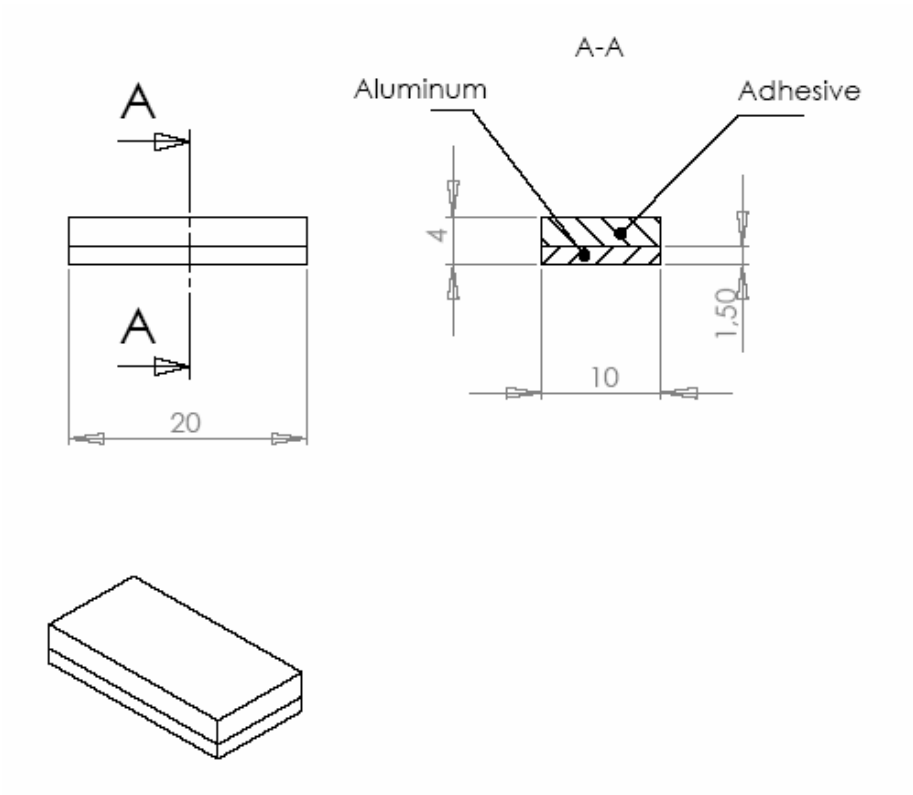

Figure 107. Specimen sketch.

A procedure was improvised to speed up the manufacture of two specimens.

This technical procedure is detailed over next lines:

1. Application of the release agent over the bulk specimen mould surface;
2. Placement of the silicone rubber frame as shown in figures 105 and 106.
3. Shot blasting of the aluminum base and degreasing with acetone;
4. Apply Araldite® 2021™ on the aluminum base;
5. Close the mould;
6. Specimens removal, after 30 minutes of curing time (figure 108).

Figure 108. The result set of the two specimens

Figure 109. Specimens.

Figure 110. Specimens marked with the code PMTg1 and PMTg2.

The specimens were cleaned and referenced (figure 109 and 110), and finally machined in order to obtain the best geometry for placement in the DMTA glass transition temperature test machine. The test was done with the help of Pedro Nóvoa from INEGI.

The method used to determine Tg was the thermo-mechanical analysis which subjects the specimen to a known sinusoidal vibration while the temperature rises. The phase difference, δ, between the two signals (σ -stress and ε -strain) is a measure of the molecular mobility of the polymer. δ (or tan δ) peaks at Tg. The Tg may also be defined by the complex modulus that includes the storage modulus (E') and the loss modulus (E''). The complex modulus is the ratio of the dynamic stress to the dynamic strain. The storage modulus refers to the ability of a material to store energy and is related to the stiffness of the material. The loss modulus represents the heat dissipated by the sample as a result of molecular motions and reflects the damping characteristics of the material. Figure 111 shows E', E'' and tan δ as a function of temperature. E' changes most rapidly with temperature at Tg and E'' peaks at Tg. The Tg given by E' and E'' are very close. However the tan δ peaks at a slightly higher temperature than as E', since $\tan\delta = E''/E'$.

Bellow and above Tg, the damping is low. At Tg there is a peak corresponding to the maximum energy dissipated hence maximum damping. Therefore, if the damping peak can be measured as a function of temperature then Tg can be found [34].

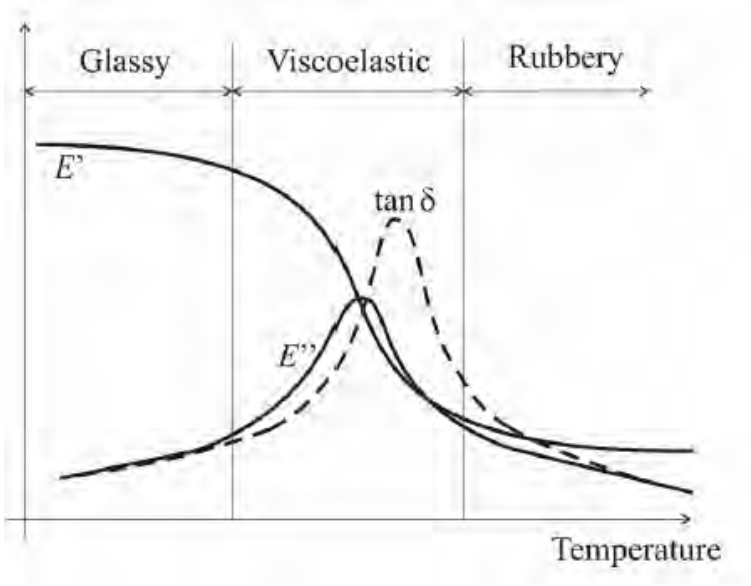

Figure 111. E', E'' as function of temperature [34].

The test results are plotted in figure 112. This graph contains the gain modulus, E', and the loss factor, tan δ, for each specimen. The glass transition temperature (Tg) corresponding to the tan δ peak is approximately 131 ºC.

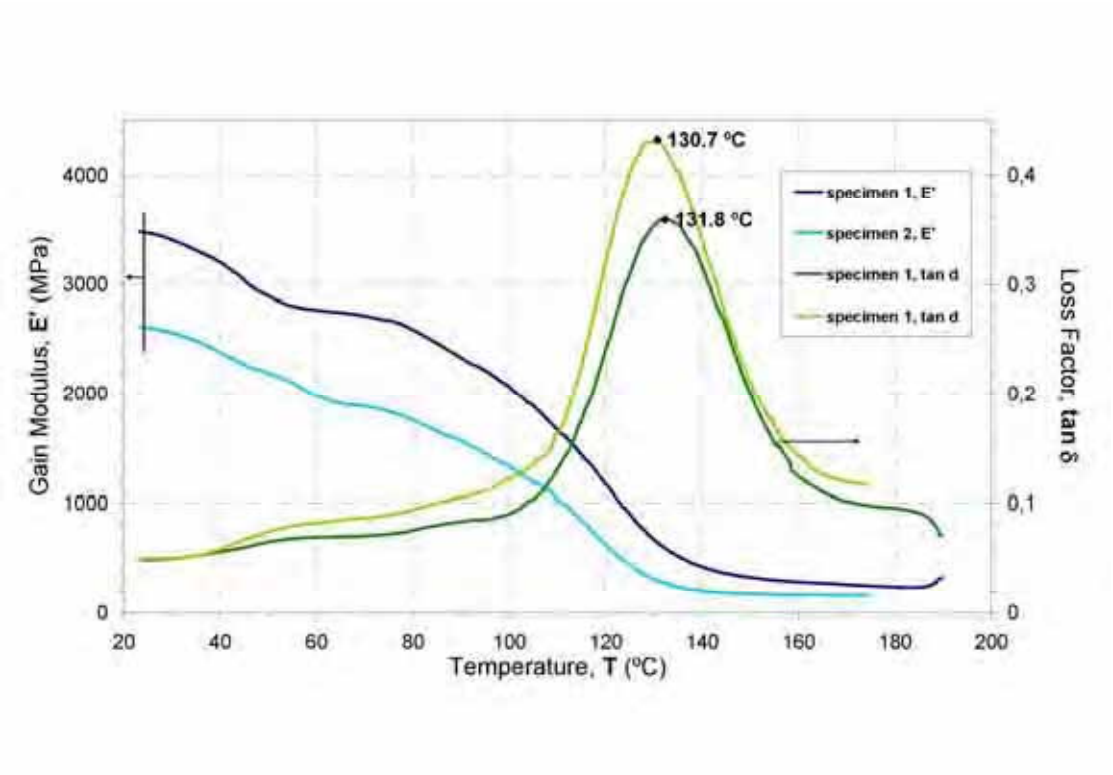

Figure 112. Glass transition temperature graph for Araldite 2021.

The Araldite 2021 Tg is higher than the substrate (PVC DECOM 1010), known to be near 75ºC - 85ºC from experimental testing done wile working in industry. Therefore the adhesive will not be a weak link in terms of temperature.

Chapter six

T-JOINT

6.1 Introduction

The major goal of this study is to develop an adhesive T-joint with a better performance than the existing fastened T-joint, in terms of mechanical behaviour, production and economical impact.

The T-joint geometry used industrially is represented in figure 113, where the transom (P2030/P2031) is joined to the base (P200/P2010) through a T accessory (P2090/P2091).

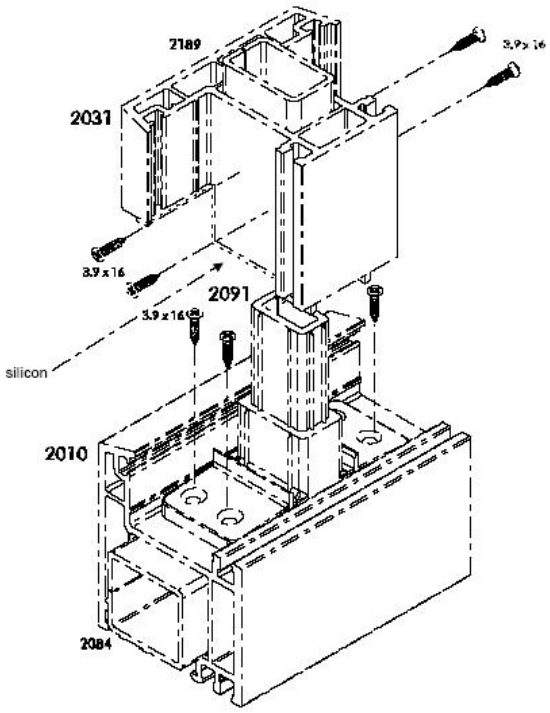

Figure 113. T-joint used in the windows framework industry.

6.2 Manufacture

The purpose of this thesis is to study the applicability of adhesive bonding in transom connection in an industrial context. Figure 115 describes the process of adhesive bonding. First, the adhesive is applied to the T accessory P2090 surfaces which will be in contact with the transom interior (a), after which it is placed inside the transom (b), and then the adhesive is applied to the T accessory P2090 bottom (c) which finally is glued to the exterior window frame P2000 (d). The adhesive is applied with a proper handgun, as seen in figure 114. After the process, that takes approximately five to ten minutes, the adhesive is already able to withstand the transom weight and can be moved if necessary to cure completely and achieve its best performance.

Figure 114. Araldite Eco Gun 50 ml.

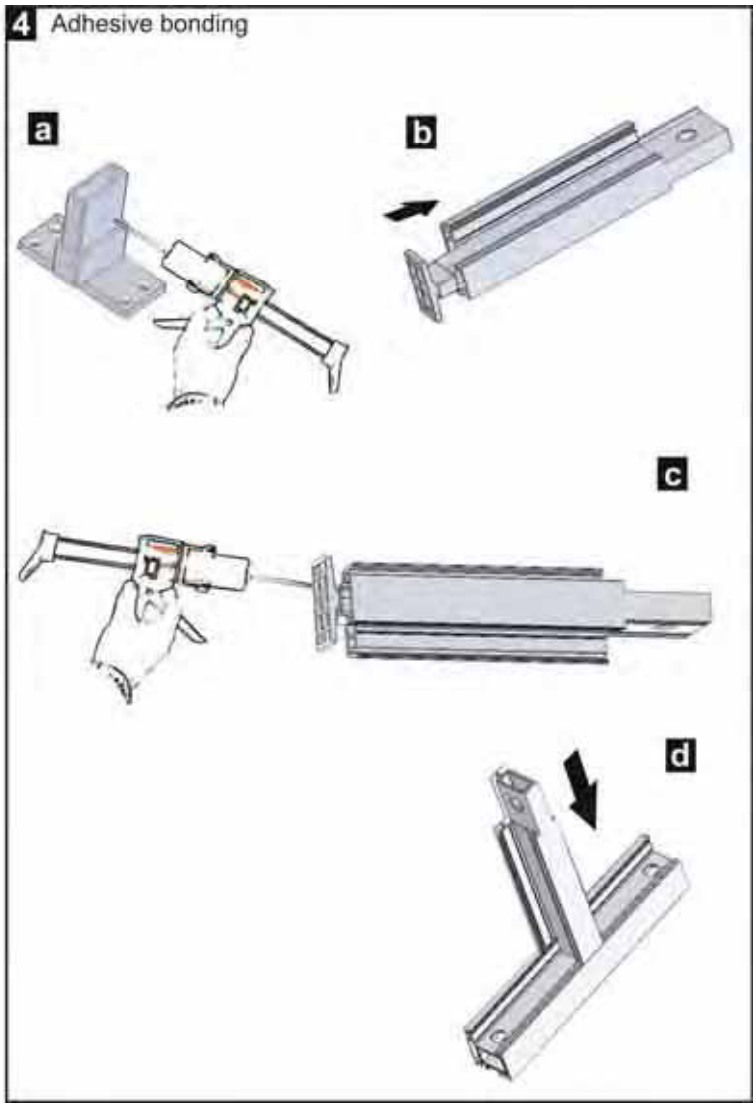

Figure 115. Transom connection by adhesive bonding.

In figure 116 the resulting T-joint specimen is shown.

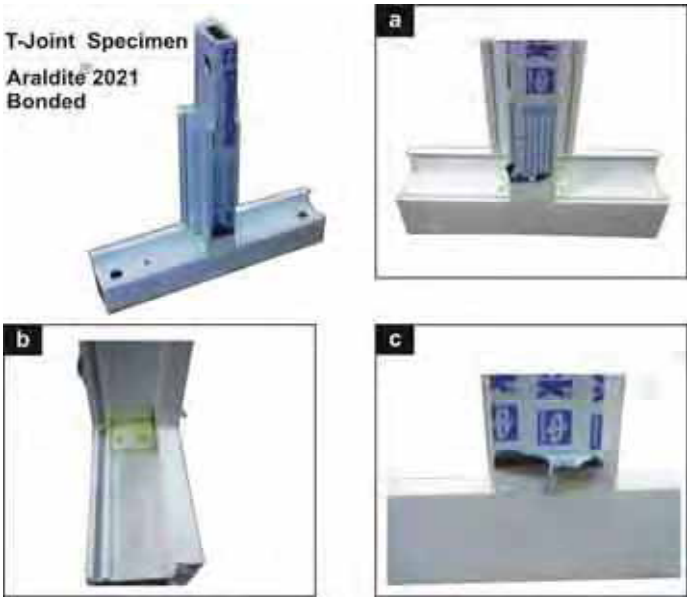

Figure 116. Different views of the adhesive bonded T-joint specimen.

Figure 117 shows the different parts composing the T-joint specimen.

Figure 117. Parts composing the T-joint specimen (P2000 and P2030 already reinforced).

6.3 Testing conditions

Two specimens were made to assess the effect of the type of loading. One of them (250 x 320 T – figure 118 left) is fastened to a reinforcement bar attached to the jig, simulating the case of a rigid base with no deformation. The other one is fastened directly to the jig (350x320 – figure 118 right) through two bolts at each end of the base. This set up is closer to reality where the window frame is allowed to deform. The drawings and specimens details are presented in Appendix IV.

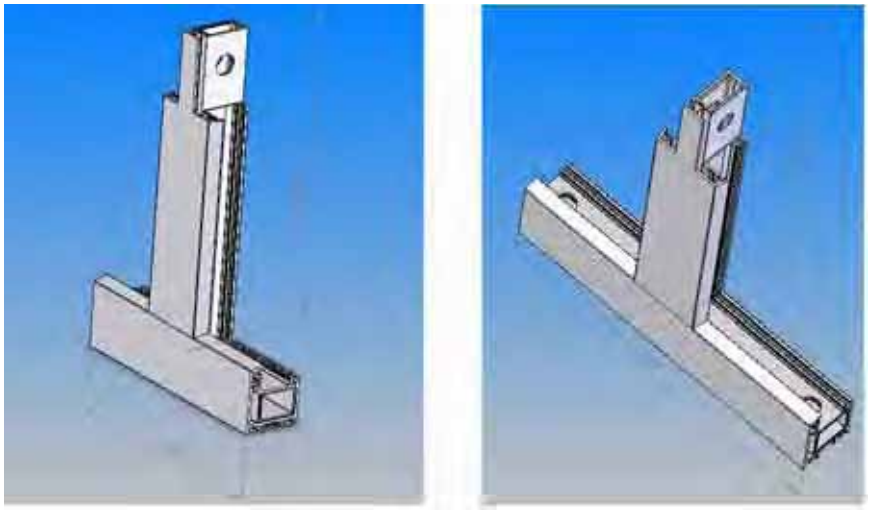

Figure 118. T-Joint specimens geometry – Fastened to the jig with a reinforcement bar (left). Fastened directly to the jig (right).

6.3.1 Jig

A jig was designed to test the two kinds of specimens (figures 119 and 120).

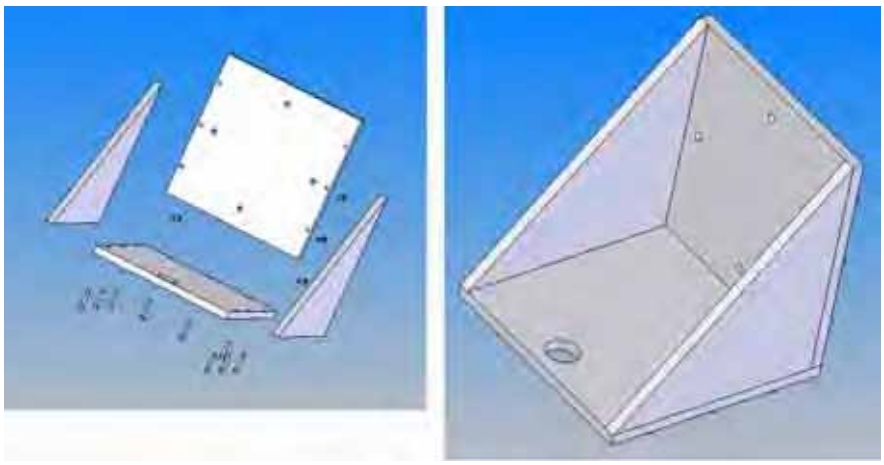

Figure 120. T- Joint test jig – Exploded view (left).

Figure 119. T-Joint test jig.

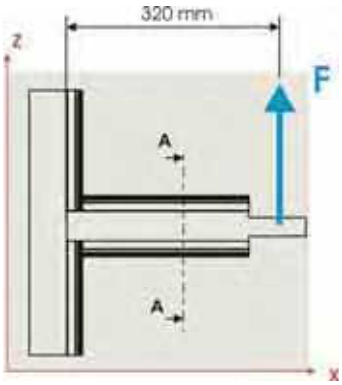

Figure 121. Static scheme of test position 1.

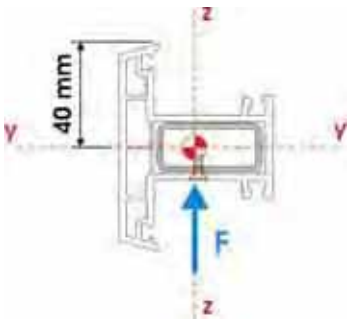

Figure 122. (**A-A**) Cross section of the horizontal transom of figure 106 with the force applied over the center of gravity.

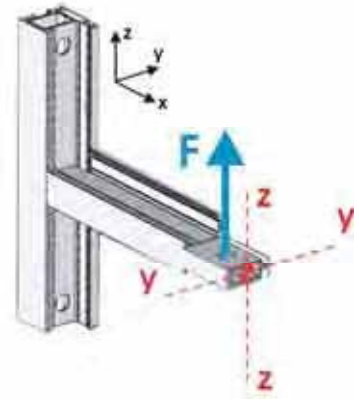

Figure 123. 3D representation of the joint.

To forecast the force that the jig can withstand, the following analysis was carried out.

The problem was assumed to be a simple bending case as shown in figure 121 and 123. The yield stress at the base of the transom can be expressed by :

$$\sigma_{yield} = \frac{M_f}{W_{yy}} \qquad \text{(Eq. 6.1)}$$

Where:

σ_{yield} $\Rightarrow$ PVC yield strength.

M_f $\Rightarrow$ Bending moment. (F x distance)

W_{yy} $\Rightarrow$ Bending resistance modulus along yy axis.

The PVC Decom 1010 yield strength is 45 MPa or 45 N/mm^2 (supplier data in appendix V).

The bending moment is :

$$M_f = F \times \ dist. \Leftrightarrow M_f = F \times 320 \ \left[N \cdot mm\right] \qquad \text{Eq. (6.2)}$$

.

The bending resistance modulus is determined by:

$$W_{yy} = \frac{I_{yy}}{z_{\max}} \qquad \text{Eq. (6.3)}$$

Where:

I_{yy} $\Rightarrow$ Cross section moment of inertia along yy axis.

$z_{\max}$ $\Rightarrow$ Most distant point in the cross section.

The moment of inertia of the PVC and steel assembly is $I_{yy} = 35 \ \left[cm^4\right] \Rightarrow 350000 \ \left[mm^4\right]$.

Figure 124 shows the transom profile (P2030) and reinforcement steel (P2063) and table 22 gives the inertia values. The inertia of the PVC profile and the reinforcement were considered to obtain the section inertia.

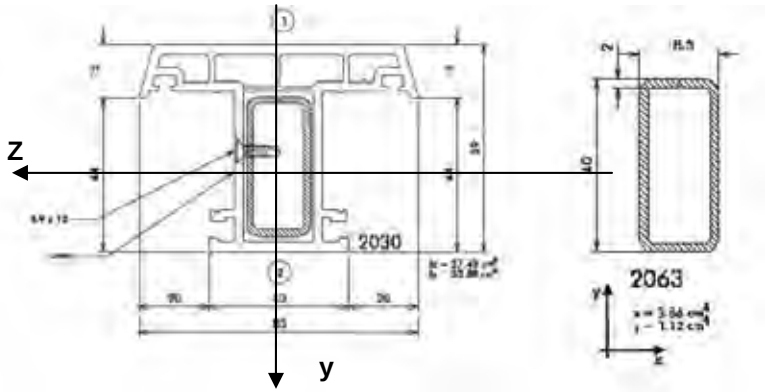

Figure 124. P2030 and P2063 inertias.

Table 22. Inertia values (transom and its steel reinforcement).

Position 1
Iyy = 35cm^4
Izz = 41.29 cm^4

According to figure 122, the most distant point in the cross section from the yy axis is 40 mm.

Substituting equation 5.2 and 5.3 in equation 5.1, results:

$$F_{yield} = \frac{\sigma_{yield} \cdot \left(I_{yy} / z_{\max}\right)}{dist} \qquad \text{(Eq. 6.4)}$$

which gives a yielding load of : $F_{yielding} = \frac{45 \cdot \left(350000/40\right)}{320} = 1231\ [N]$.

The jig was designed to resist a load higher than **1231 N**.

After some considerations, the test jig shown in figure 112 was used. Details of the construction and design can be found in Appendix III.

6.3.2 Test positions

The specimens were tested in three positions in order to simulate the three loading conditions defined in figure 10. The most critical position in practice is position 2 reflecting the window pressure (table 23). The test positions are shown in figure 125.

Table 23. Relation between figure 125 and figure 10.

Figure 125		*Figure 10*
Position 1	→	Weight
Position 2	→	Wind pressure
Position 3	→	Window closing force

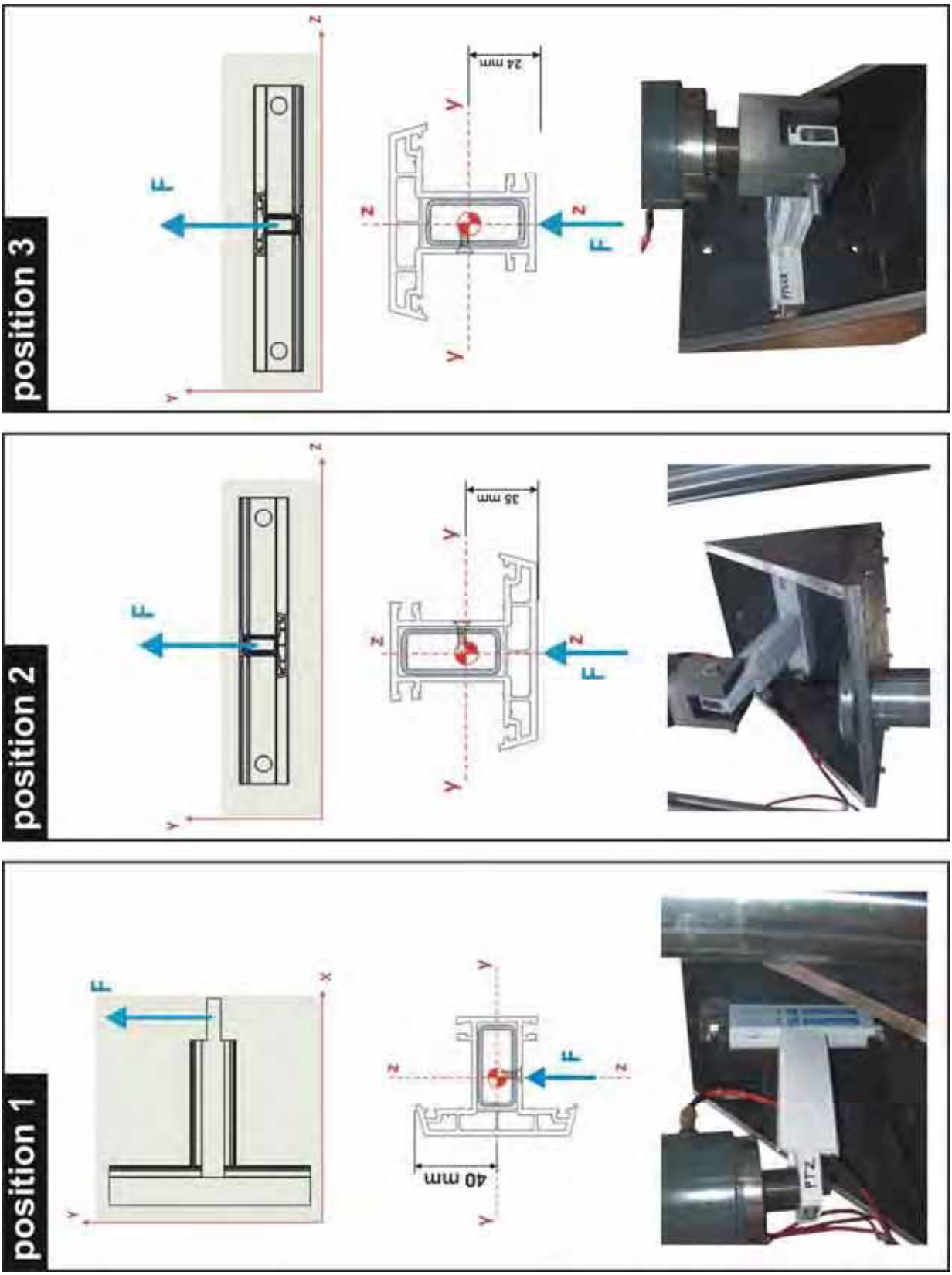

Figure 125. Scheme of the three positions for the T-joint test.

6.3.3 Specimen grip

Position 1 (figure 126a) is fixed directly to the load cell with a fastener. Position 2 (figure 126b) and position 3 (figure 129c) need a special fork shaped tool to fix the specimen in the tensile machine

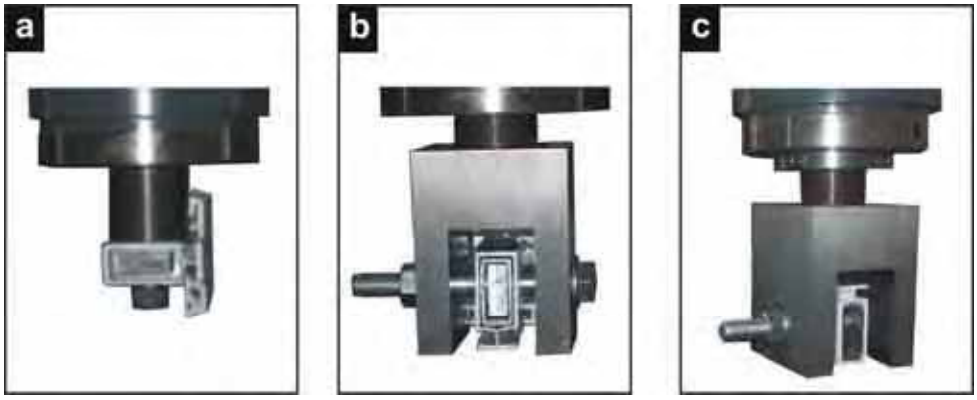

Figure 126. Gripping arrangement (a) position 1; (b) position 2 (fork tool); (c) position 3 (fork tool).

Over the grip area, steel packings were inserted inside the PVC to guarantee a proper grip of the specimen. This is shown in figure 127, with a single steel packing for the transom (P2030) and a double steel packing for the base (P2000)

Figure 127. Steel packings.

6.3.4 Reinforcement bar

To avoid the bending of the base profile (P2000), a reinforcement bar was placed inside this profile and the bar was bolted to the jig (figure 128 b). This loading gives a higher failure load because there is no bending of the base profile. However, in practice the base is allowed to bend.

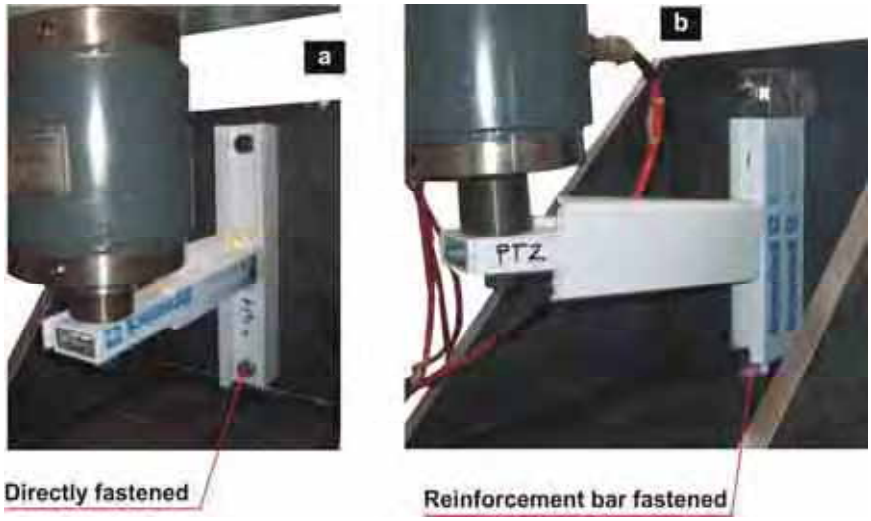

Figure 128. Specimens fastened to the jig. (a) Without reinforcement; (b) With reinforcement inside the base profile (P2000).

This situation was simulated by attaching the base to the jig without reinforcement as shown in figure 128 a.

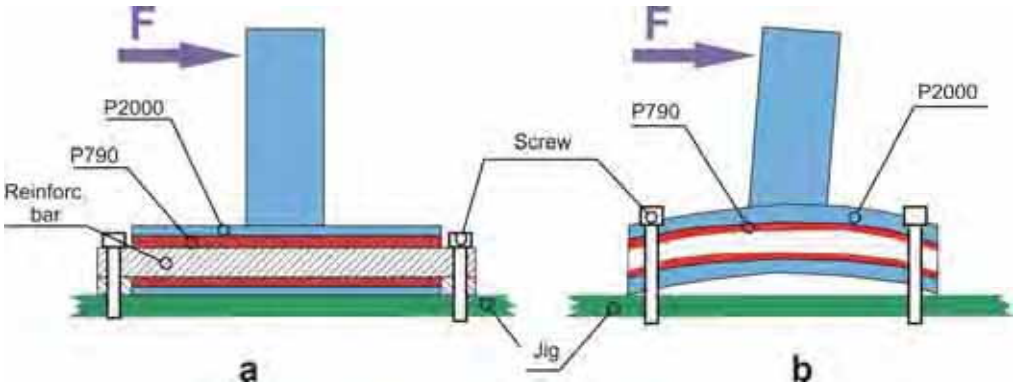

Figure 129. (a) Fastening test scheme with the reinforcement bar, avoiding the bending of the base (b) and without the reinforcement bar resulting in base bending.

6.4 Test results

6.4.1 Mechanism of failure

6.4.1.1 Joints fastened with screws

The load was applied and at some point, the T-joint accessory (P2090) started to lift from the basis profile (P2000), initiated a fracture and finally broke apart, as shown in figure 130 a and c. P2090 accessory clearly fractures near the base as shown in figure 130 b and d.

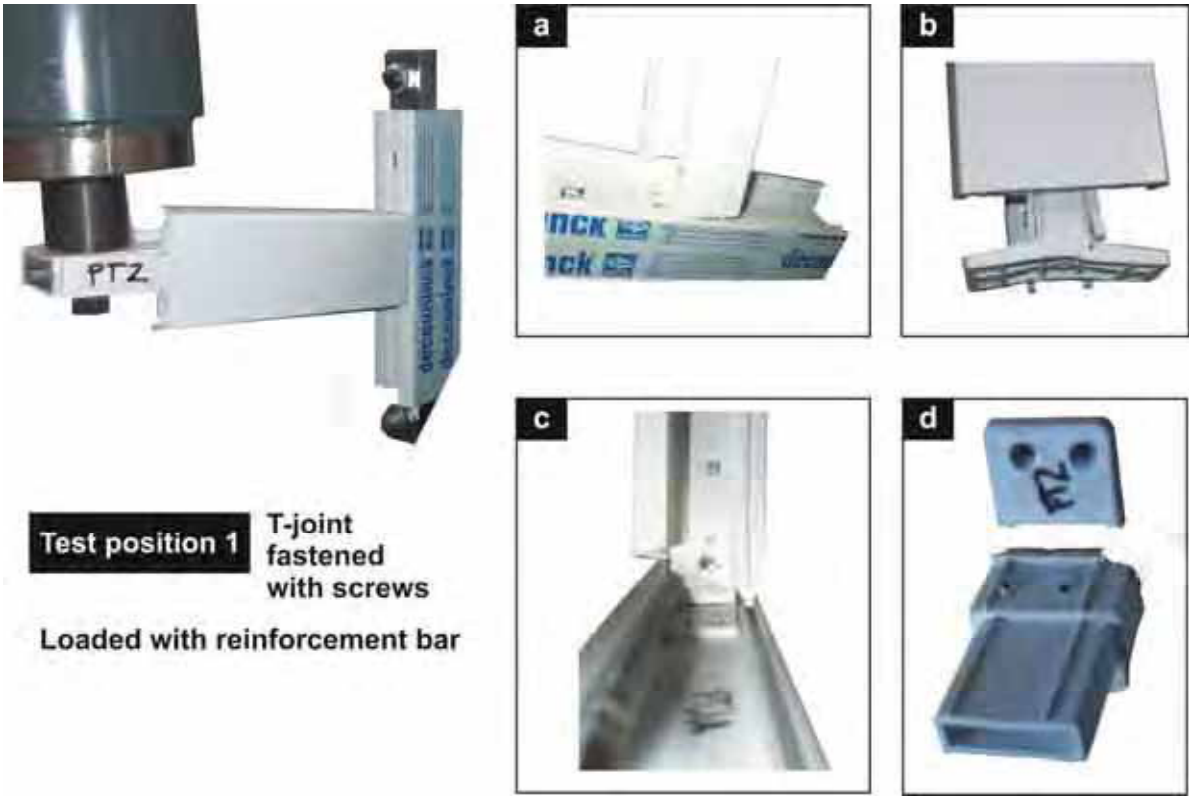

Figure 130. PT2A mechanically Fastened T-joint specimen (test position 1); (a) joint fracture and lifting; (b) P2090 fracture; (c) joint fracture side view; (d) P2090 fractured.

As the transom lifts from the base, it crashes the base profile on the opposite side as shown in figure 131.

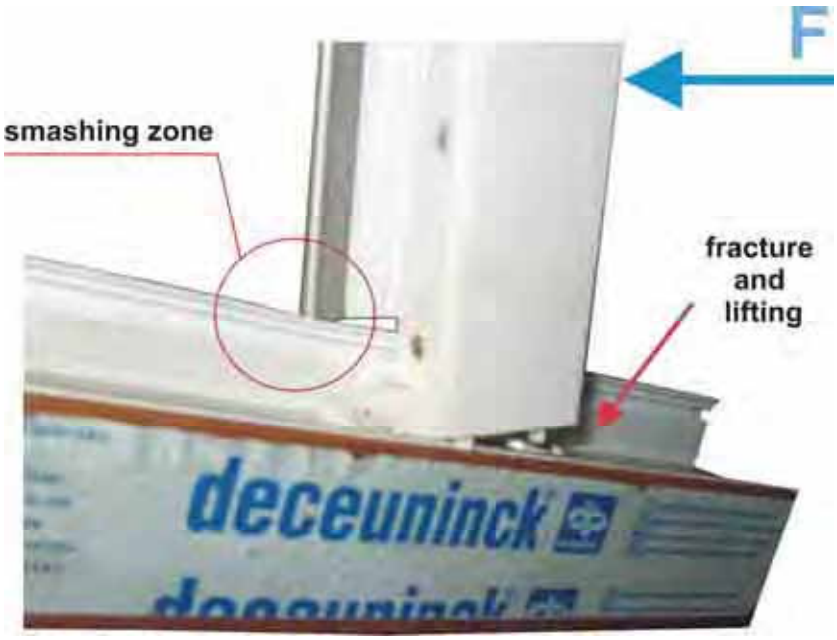

Figure 131. After fracture T junction in detail.

The T-joint accessory (P2090) final failure was identical for the three positions (figures 132 and 133) but the initiation was related to the test position. The registered fracture loads were different due to the different test positions, that lead to different stress distribution and resistant area.

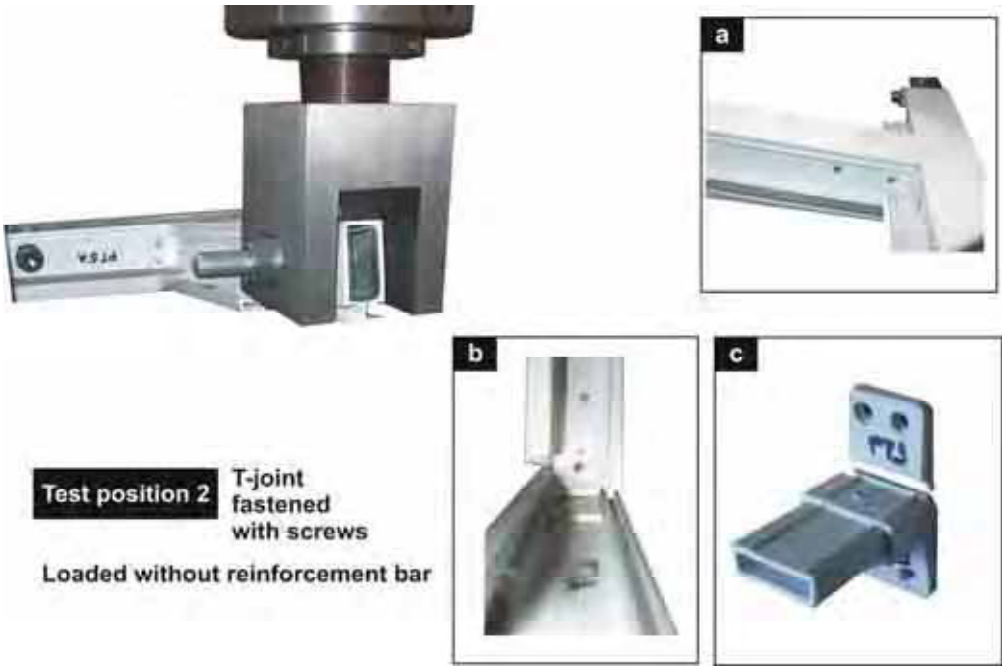

Figure 132. PT5A mechanically Fastened T-joint specimen (test position 2); (a) joint fracture and lifting; (b) joint fracture side view; (c) PT3A P2090 fractured.

Figure 133. PT4A mechanically Fastened T-joint specimen (test position 3); (a) joint fracture and lifting; (b) joint fracture side view; (c) joint fracture down view.

6.4.1.2 Adhesive joints

The bonded T- joint specimens (figure 116) were also tested with the same testing conditions as the fastened specimens.

Figure 134 shows the failure mechanism for position 1. In this case, P2090 accessory does not fracture. Instead, the joint suffers a cohesive failure where adhesive remains in each fracture surface – P2090 bottom and P2000 top faces. In some points the failure occurs in the PVC base (P2000).

The described failure occurs for the other two test positions (figure 134, 135 and 136), however the failure occurs at different stress values.

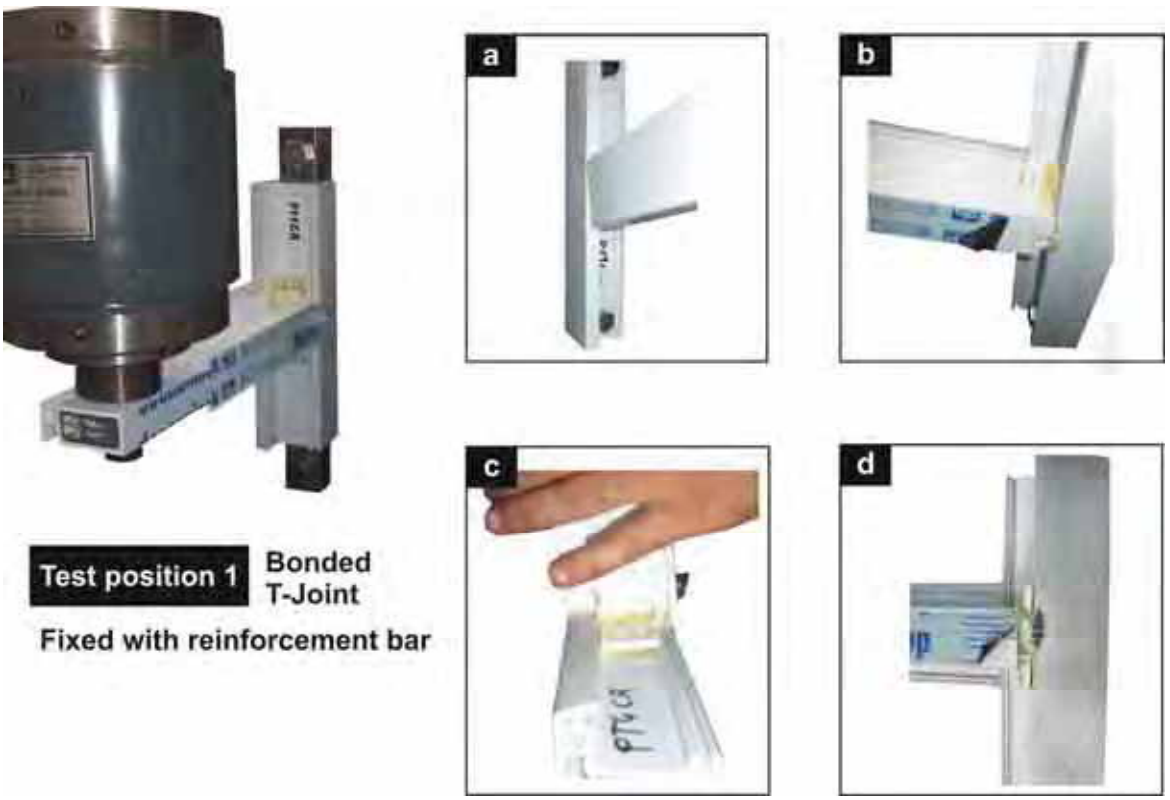

Figure 134. Bonded T-Joint specimen PT1CR (test position 1); (a) PT1C specimen being tested; (b) joint lifting and failure; (c) PT4CR joint failure side view; (d) PT4CR joint failure view.

Figure 134 shows PT4CR specimen tested in position 2. A detailed view of the joint area shows that P2090 accessory did not fracture. The failure occurs in the adhesive opposite to the load orientation.

Figure 135. Bonded T-Joint specimen PT4CR test position 2.

Figure 136. Bonded T-Joint specimen PT5C test position 3.

Figure 136 shows PT5C specimen tested in position 3. The failure detail shows that the P2090 does not fracture, and the failure is cohesive.

6.4.2 Load-displacement curves

The digital files of the tensile testing machine were referenced as follows:

Table 24. Digital file codenames.

PT#A.Dat	**P**rovete em **T** **A**parafusado (screwed T Specimen);
PT#C.Dat	**P**rovete em **T** **C**olado (adhesive T Specimen);
PT#AR.Dat	**P**rovete em **T** **A**parafusado **R**eforçado (screwed T Specimen reinforced);
PT#CR.Dat	**P**rovete em **T** **A**parafusado **C**olado (adhesive T Specimen reinforced).

é

The cardinal sign (#) is substituted by the test number from 1 to 6.

In the next table, the PT files and the testing condition can be related.

Table 25. Relation between testing condition and PT files.

file	Test position	Reinforced test	T-joint type of fastening
PT1AR.Dat	1	R	screws
PT2AR.Dat	1	R	screws
PT3AR.Dat	2	R	screws
PT4AR.Dat	2	R	screws
PT1C.Dat	1	-	Araldite 2021
PT2C.Dat	1	-	Araldite 2021
PT3C.Dat	2	-	Araldite 2021
PT4C.Dat	2	-	Araldite 2021
PT5C.Dat	3	-	Araldite 2021
PT6C.Dat	3	-	Araldite 2021
PT1A.Dat	1	-	screws
PT2A.Dat	1	-	screws
PT3A.Dat	2	-	screws
PT4A.Dat	3	-	screws
PT5A.Dat	2	-	screws
PT6A.Dat	3	-	screws
PT1CR.Dat	1	R	Araldite 2021
PT2CR.Dat	1	R	Araldite 2021
PT3CR.Dat	2	R	Araldite 2021
PT4CR.Dat	2	R	Araldite 2021

6.4.2.1 Test position 1 without reinforcement bar

The tensile testing machine data was imported into a spreadsheet and the following load-displacement curves were plotted.

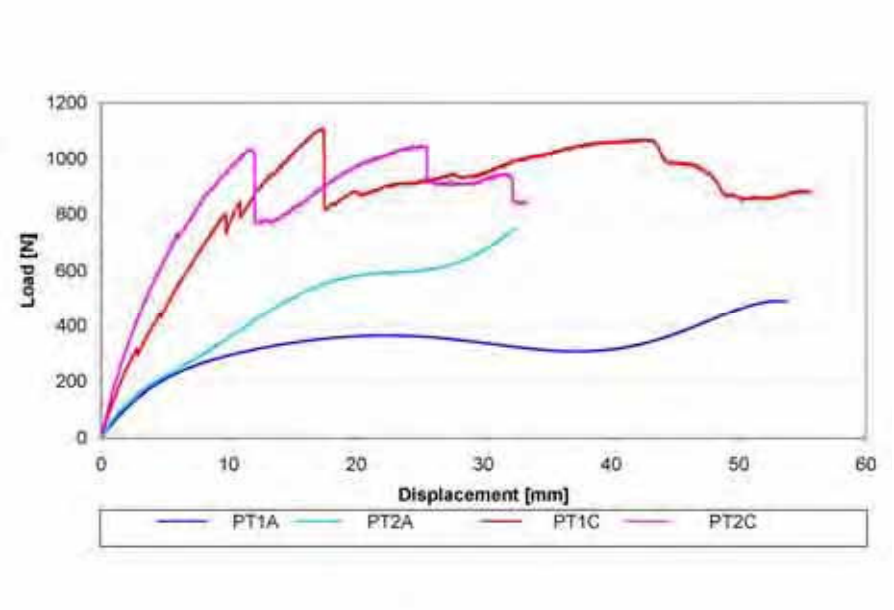

without reinforcement bar

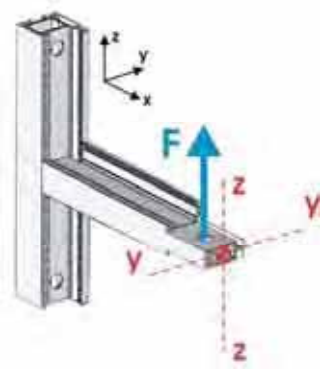

Figure 137. Load-displacement curves of PT1A, PT2A, PT1C and PT2C specimens (cross-head speed: 1 mm/min).

Test Position 1

Figure 137 registers the tests done with the screwed T-joint specimens PT1A (dark blue line) and PT2A (light blue line). At approximately 200 N a crack initiates in the T-joint accessory (P2090) and complete fracture occurs at 25 mm of displacement for the PT1A. The load keeps increasing because the base profile is still supporting the transom, but the T-joint failure load was considered to be the failure of P2090 accessory. T- joint accessory (P2090) failed at 550 N force value in the case of specimen PT2A and 300N for the PT1A.

Figure 137 also shows adhesive bonded specimens PT1C (red line) and PT2C (pink line). The red line has a first drop in load at 250 N and then at 800 N representing two distinct points of the T-joint accessory (P2090) lifting from the base (P2000). However the complete cohesive failure only occurs at 1100 N for a 20 mm displacement. The rest of the curve represents the bending of the transom supported by the base profile (being crushed). The pink line (PT2C) is very similar to the red, registering a cohesive failure at 1000 N for 10 mm of displacement.

6.4.2.2 Test position 1 with reinforcement bar

with reinforcement bar

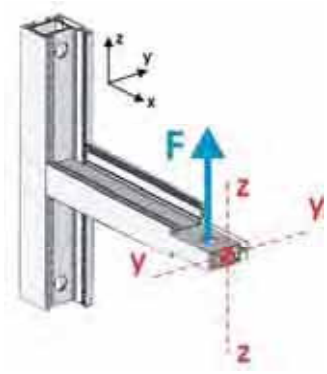

Test Position 1

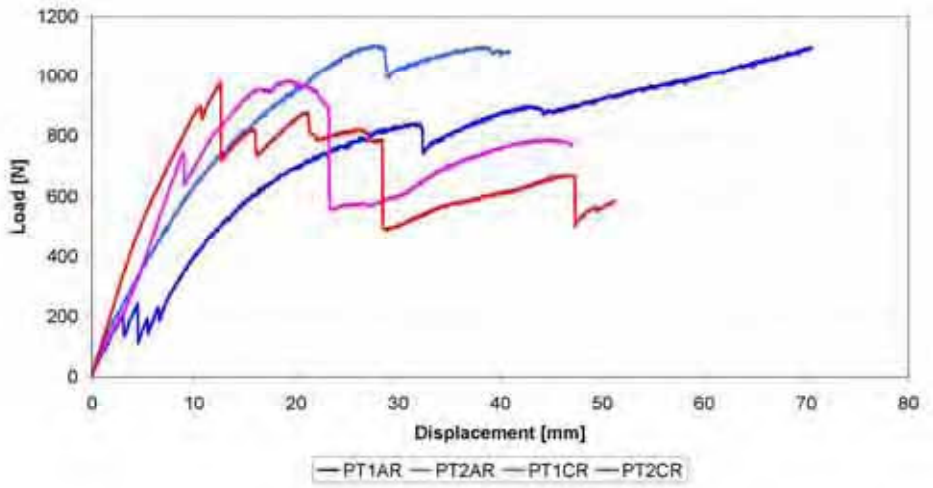

Figure 138. Load –displacement curves of PT1AR, PT2AR, PT1CR and PT2CR specimens (cross-head speed: 1 mm/min).

The blue lines in the graph of figure 138 are the joints fastened with screws (PT1AR and PT2AR). In PT1AR (darker blue), there is a first stage at 200 N corresponding to some instability mostly due to grip accommodation. It is only near 800 N that the T accessory (P2090) fractures. PT2AR (lighter blue) breaks at 1100 N for a displacement of 30 mm. The 1100 N failure load is very close to the one predicted earlier for the jig design (1231 N).

The adhesively bonded joint specimens (PT1CR and PT2CR) are the red and pink lines. They have a very similar behaviour. In PT1CR (pink) there is a first drop at 700 N that represents the T accessory (P2090) starting to lift from the base (P2000). However it remains bonded until the second drop at 800 N and a 20 mm displacement when the complete cohesive failure occurs. PT2CR (red) is very similar, with the first drop at 900 N and complete failure at 1000 N for a 30 mm displacement.

6.4.2.3 Test position 2 without reinforcement bar

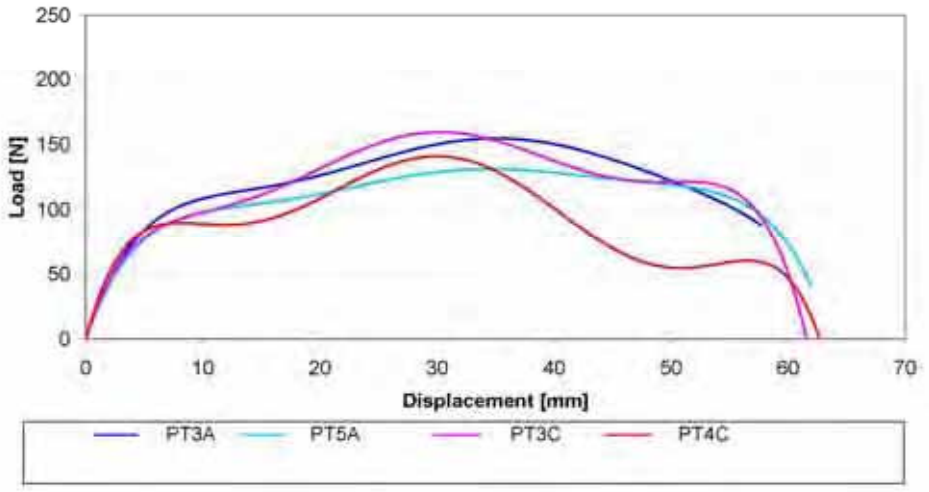

without reinforcement bar

Figure 139. Load-displacement curves of PT3A, PT5A, PT3C, PT4C specimens (cross-head speed: 1 mm/min).

Test Position 2

This test is representative of the wind pressure acting on the window.

For specimen PT3A the T-joint accessory (P2090) starts to fracture at 100 N and brakes completely for a 57 mm displacement (test stopped). Specimen PT5A is very similar; however, the P2090 fracture occurs for a slightly lower force and brakes completely at 62 mm of displacement.

The bonded T-Joint specimen PT4C (pink line) registers a load of 90 N when the T-joint accessory (P2090) starts to lift from the base (P2000) for a 7 mm displacement. The bond cohesive failure occurs at 150 N for a displacement of 30 to 35 mm. The red line representing PT3C specimen is very similar to PT4C, registering a lower load for the cohesive failure (125 N).

6.4.2.4 Test position 2 with reinforcement bar

with reinforcement bar

Test Position 2

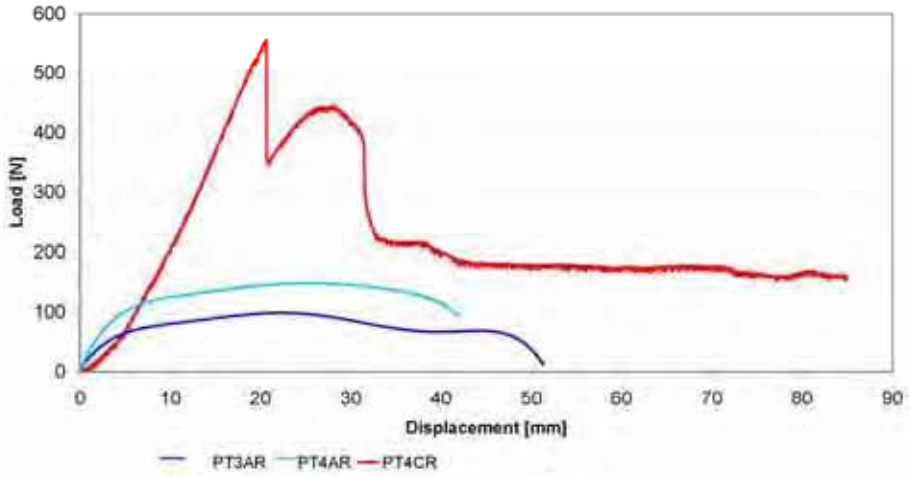

Figure 140. Load-displacement curves of PT3AR, PT4AR, PT3CR, PT4CR specimens (cross-head speed: 1 mm/min).

The dark and light blue lines in the graph of figure 144 represent the screwed T-joints (PT3AR and PT4AR). This figure shows that they start to deform between 60N and 100N and the T-joint accessory (P2090) fractures for a displacement of 35 mm.

The red line representing the bonded T-joint specimens is quite different. PT3CR test is not plotted due to data acquisition problems. The PT4CR test shows a first drop at 600 N, when the T-joint accessory (P2090) starts to lift from the base (P2000). The second drop occurs at 400 N with a 30 mm displacement and is due to the cohesive failure of the bonded joint.

6.4.2.5 Test position 3 without reinforcement bar

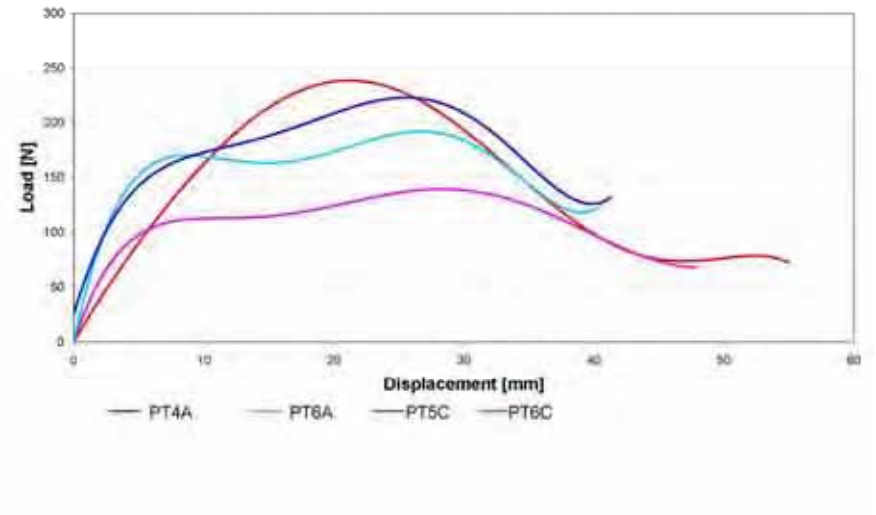

without reinforcement bar

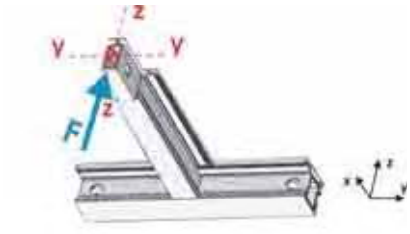

Figure 141. Load-displacement curves of PT4A, PT6A, PT5C and PT6C specimens (cross-head speed: 1 mm/min).

Test Position 3

The red and pink lines in the graph of figure 141 represent the adhesive bonded T-joints (PT5C and PT6C). The maximum load for PT5C occurs at 250 N and corresponds to the adhesive failure, for a displacement of approximately 20 mm. The same fracture occurs at 100 N for PT6C (pink line) for a displacement of 10 mm.

The mechanically fastened T-joints are plotted in dark blue (PT4A) and light blue (PT6A). The first drop occurs at 150 N when the T-joint accessory (P2090) starts to lift from the base (P2000). At 200 N (light blue – PT6A) or at 225 N (dark blue – PT4A), the T-joint accessory (P2090) fracture occurs for a displacement of 30 mm.

Test position 3 with reinforcement was not done because of a lack of time and its lower relevance when compared to the other tests.

Table 26. Failure loads for each test.

file	Test position	Reinforced test	T-joint type of fastening	Failure load [N]
PT1AR.Dat	1	R	screws	800
PT2AR.Dat	1	R	screws	1100
PT1CR.Dat	1	R	Araldite 2021	800
PT2CR.Dat	1	R	Araldite 2021	1000
PT3AR.Dat	2	R	screws	100
PT4AR.Dat	2	R	screws	100
PT3CR.Dat	2	R	Araldite 2021	-
PT4CR.Dat	2	R	Araldite 2021	400
PT1A.Dat	1	-	screws	200
PT2A.Dat	1	-	screws	550
PT1C.Dat	1	-	Araldite 2021	1100
PT2C.Dat	1	-	Araldite 2021	1000
PT3A.Dat	2	-	screws	100
PT5A.Dat	2	-	screws	100
PT3C.Dat	2	-	Araldite 2021	125
PT4C.Dat	2	-	Araldite 2021	150
PT4A.Dat	3	-	screws	160
PT6A.Dat	3	-	screws	200
PT5C.Dat	3	-	Araldite 2021	250
PT6C.Dat	3	-	Araldite 2021	100

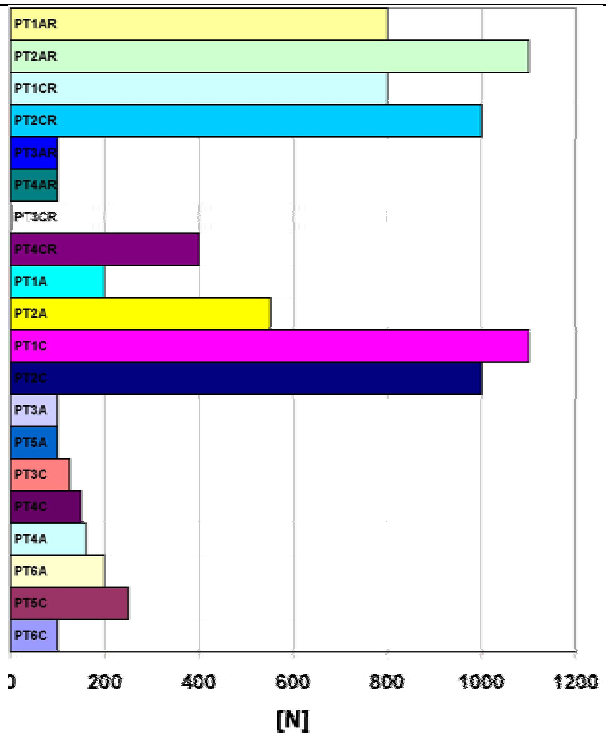

Table 26 summarizes the failure load for each case making it easy to compare.

Conclusions

This preliminary tests show that adhesive joints have a similar or better (position 1, without reinforcement for example) load bearing capacity than the fastened joints. Note that the design of the joint is not the best in terms of adhesive bonding. No alteration was made to the parts that are designed for a mechanical connection. If adhesion bonding was to be used, the T-joint accessory geometry could be optimised to reduce the stress concentrations in the adhesive. This is done theoretically in the next section with a finite element analysis.

It is also remarkable that complete structural rupture does not occurs in both kinds of joints (fastened and adhesive bonded). The T-joints are damage tolerant, having a very good performance in terms of safety.

5.5 Finite element analysis

At this point, the adhesive and adherend mechanical properties are known and the T-Joint specimen geometry is defined. A finite element analysis was carried out to obtain a predictive solution of the T-joints tested and optimize the stress distribution by changing the joint design.

The preprocessing program FEMAP v.8.3 was used to generate the geometry and the mesh. ABAQUS v.6.5 was used to compute the results and plot the stress distribution (post processing work).

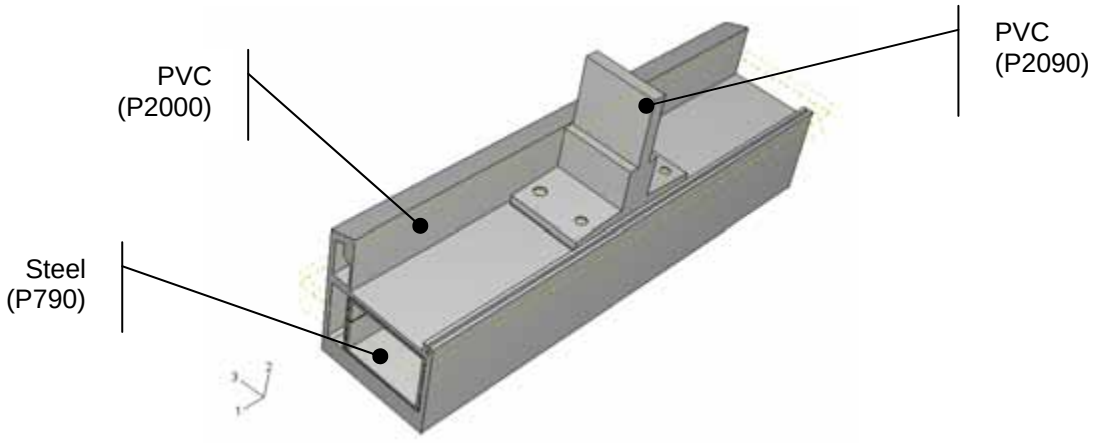

Figure 142. Model of the T-Joint specimen.

Figure 135 shows the 3D model of the T-joints. A three dimensional analysis was preferred because a two dimensional analysis was not realistic to simulate the complexity of the base profile. It is a complex problem, dealing with 3 different materials (PVC, steel and adhesive) in contact.

Two models were studied: the fastened T-joint and the adhesive bonded T-joint.

To obtain the best model for this study a contact pair was defined between P790 and P2000 as shown in figure 145. This contact pair was defined in the interaction menu (figures 144 and 145), with an adjustment tolerance of 0.2 mm between the red (master surface) and the pink (slave surface) surfaces.

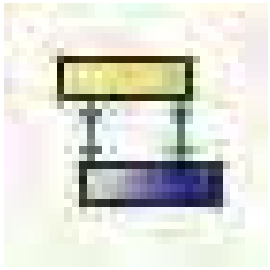

Figure 143. Surface Interaction tool icon

Figure 144. Model database with the interaction in display (ABAQUS).

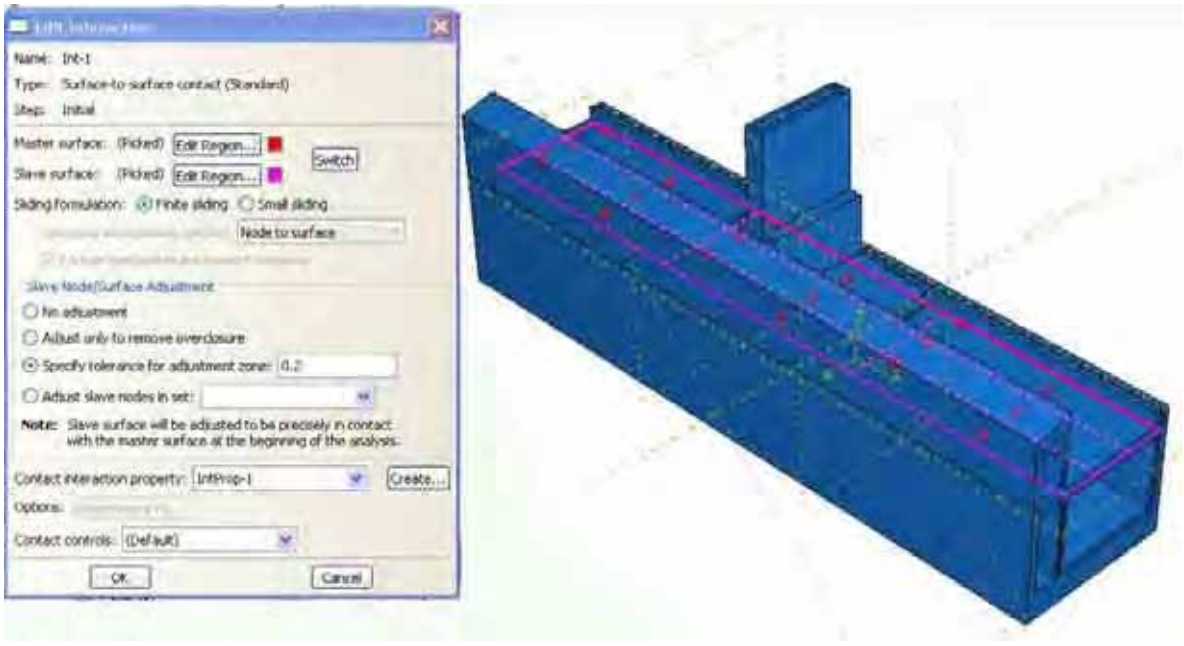

Figure 145. ABAQUS interaction contact pair (surface-to-surface) definition menu

Once again, nonlinear geometry (Nlgeom) was considered to include the nonlinear effects of large deformations and displacements.

An AMD Athlon 1300 Mhz processor with 512 MB DDRAM was used for the processing. The computing time took approximately 3 minutes for each case.

5.5.1 Fastened (with screws) model

The screws were modeled as beams, which is an option recommended by Abaqus to simplify the problem (figure 147). They were defined between two points joining three layers (P2090, P2000 and P790) as shown in figure 149.

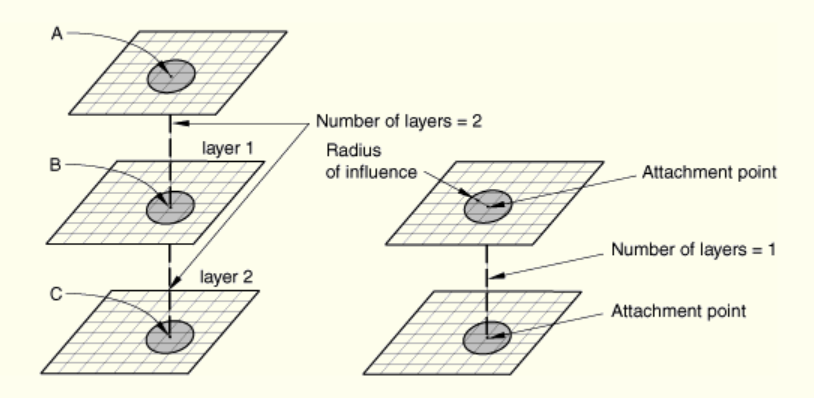

Figure 146. Fastening by layer scheme (ABAQUS Manual).

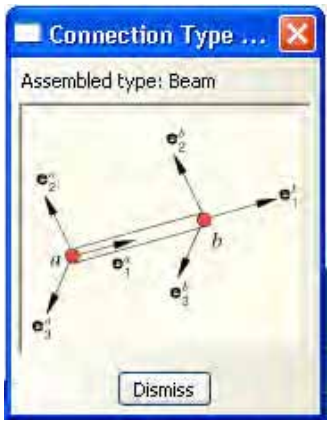

Figure 147. Screw modeled as a beam (ABAQUS).

Figure 148. ABAQUS conector property menu.

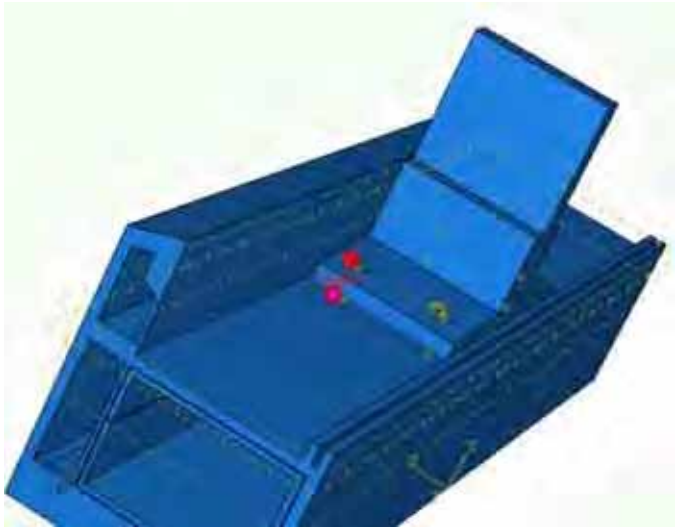

Figure 149. Beam connection between two points (through 3 layers).

Figure 148 shows the connector menu where three parameters should be introduced: the connector property (defining the type as beam) and the two points (sequence) to define the intended screw orientation.

Figure 150. Model database with the connectors in display (ABAQUS).

The previous definitions resulted in the fallowing joint geometry, where the fasteners are shown.

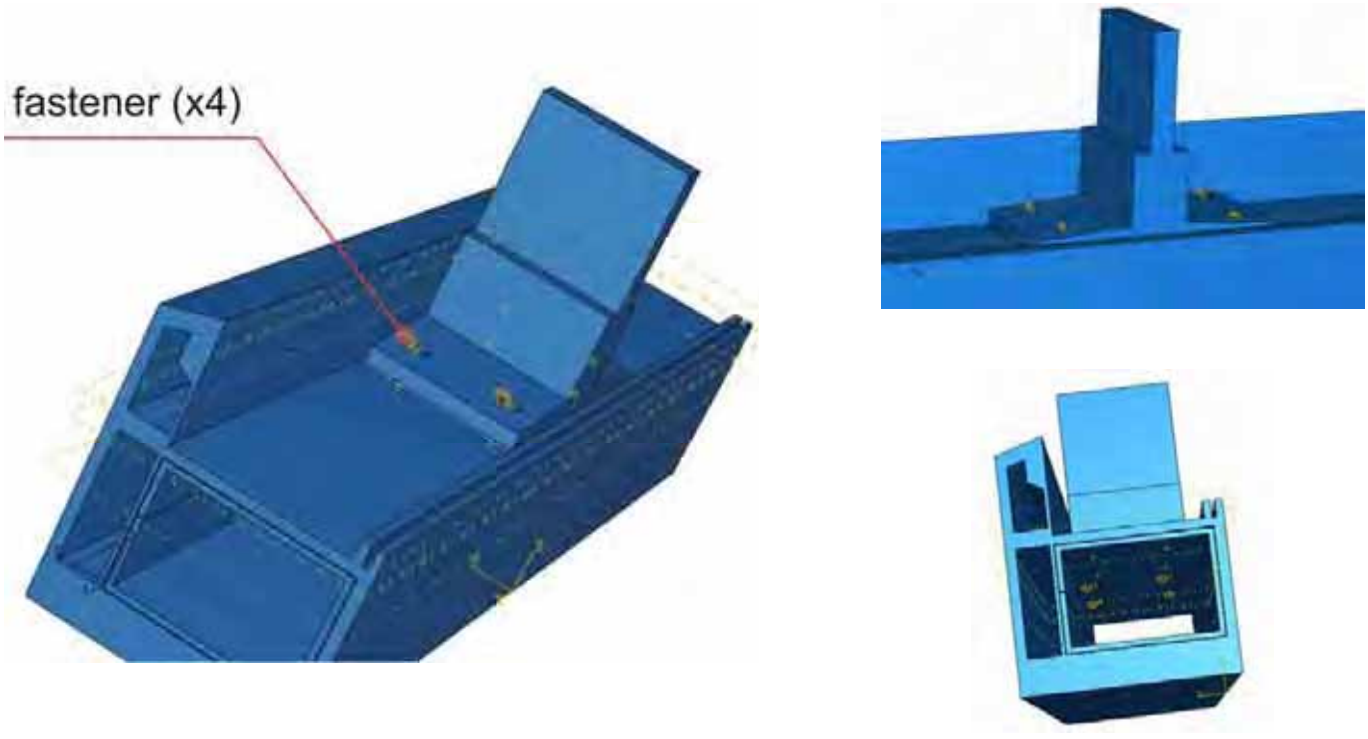

Figure 151. Several views for the T-joint fastened geometry.

5.5.2 Bonded model

Instead of the mechanical fasteners, the P290 accessory was adhesively bonded to the base profile (P2000). A partition was created as shown in figure 152. The adhesive was given the properties of Araldite® 2021™ , determined previously in chapter 5.

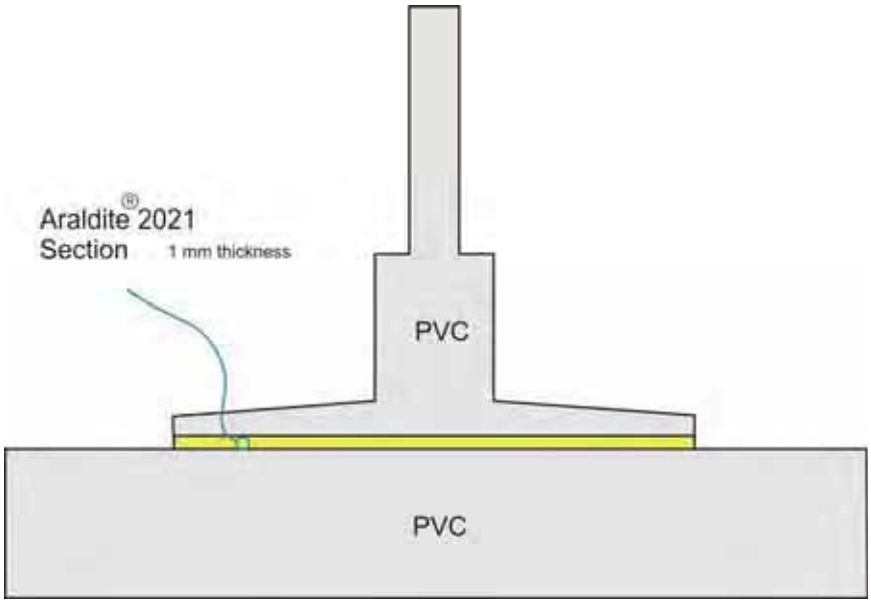

Figure 152. Section definition for the adhesive bonded model.

To simulate the load on the transom in position 1, a distributed load of $1\ N/mm^2\ \left(\frac{800\ [N]}{21\times 37\ [mm^2]}\right)$ was applied to the side of P2090 accessory, as shown in figure 153.

Position 1 was chosen because it allows creating a different T-joint design due to less geometrical constraints than positions 2 and 3.

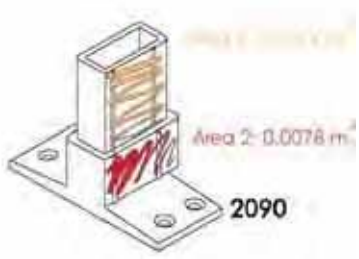

Figure 153. Areas of loading in P2090 accessory.

5.5.3 Mesh and boundary condition

After defining a Tet (tetrahedral) element shape (figure 154) with an approximate global seed size of 5, with curvature control and deviation factor of 0.1 (figure 155), the mesh was applied as shown in figure 157.

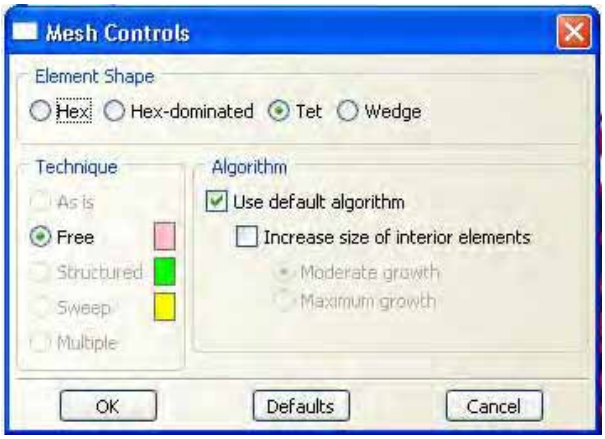

Figure 154. ABAQUS mesh controls menu.

Figure 155. ABAQUS Global Seeds menu.

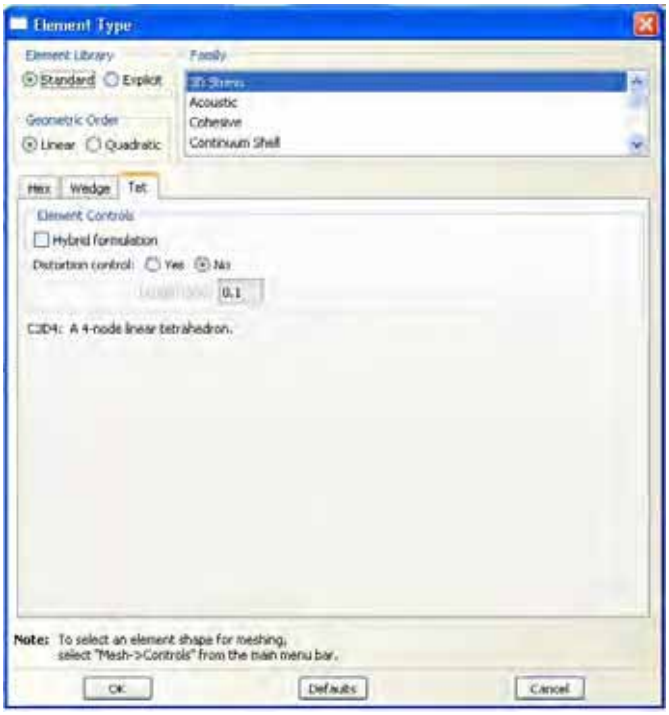

Figure 156. ABAQUS element type menu.

The element type was chosen from the 3D stress family as C3D4 – 4-node linear tetrahedron stress/ displacement element defined in figure 156.

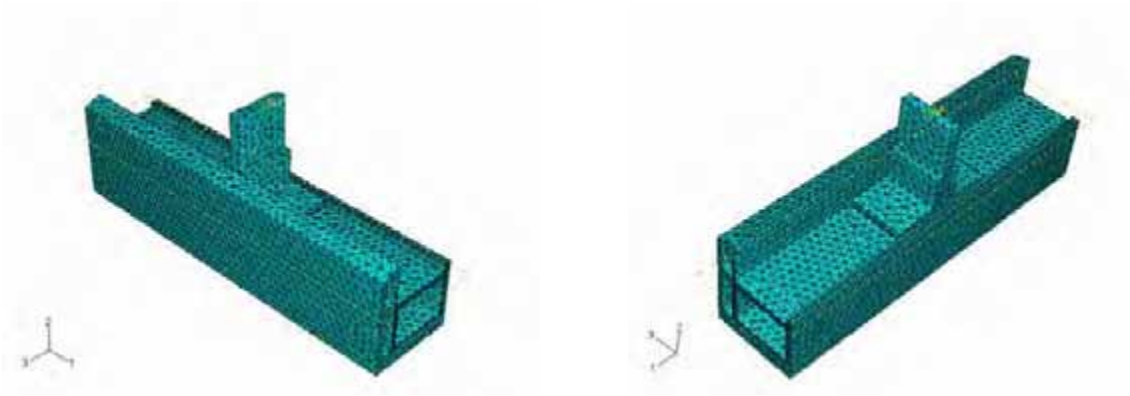

Figure 157. Mesh exterior and interior T-joint model views.

The boundary condition definitions are shown in the next figure. They simulate the case of a test with the reinforcement bar.

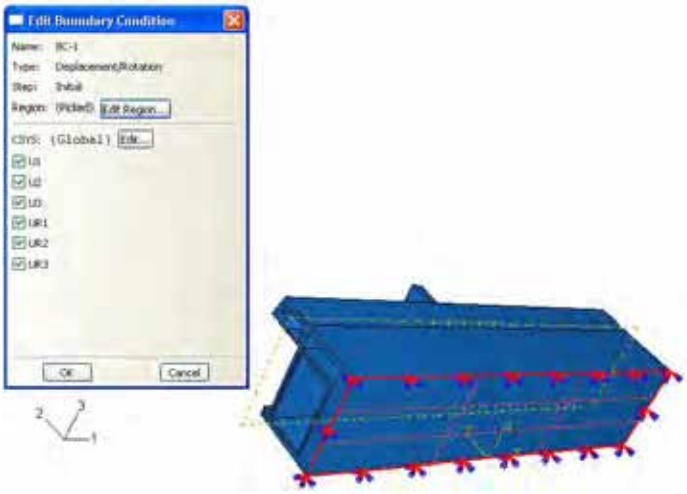

Figure 158. ABAQUS boundary condition.

5.5.4 Results

Contour plots of various components of stress are presented next for each model for comparison purposes.

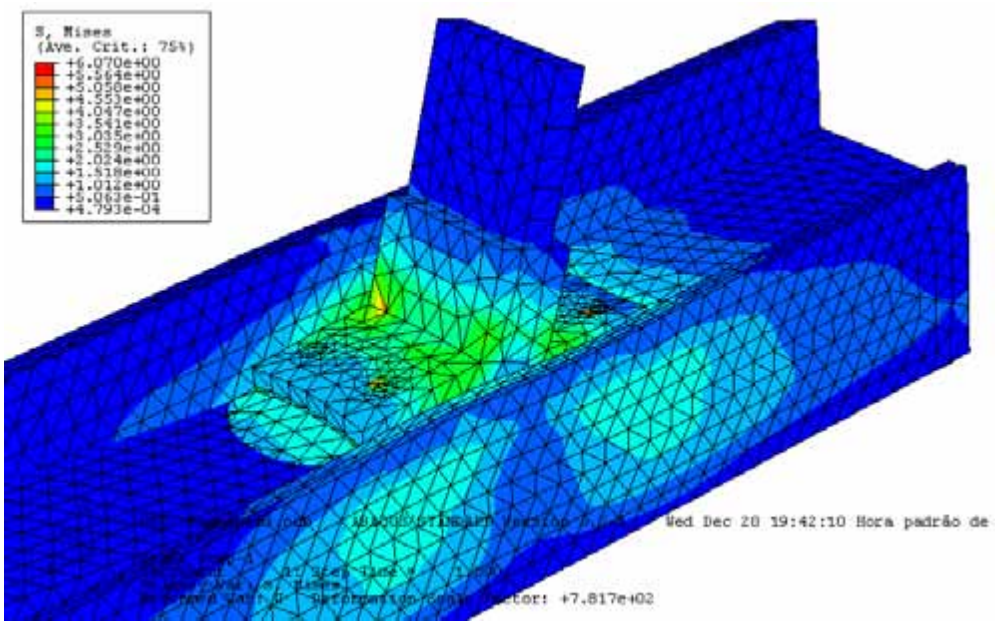

Figure 159. Fastened model stress distribution (Von Mises).

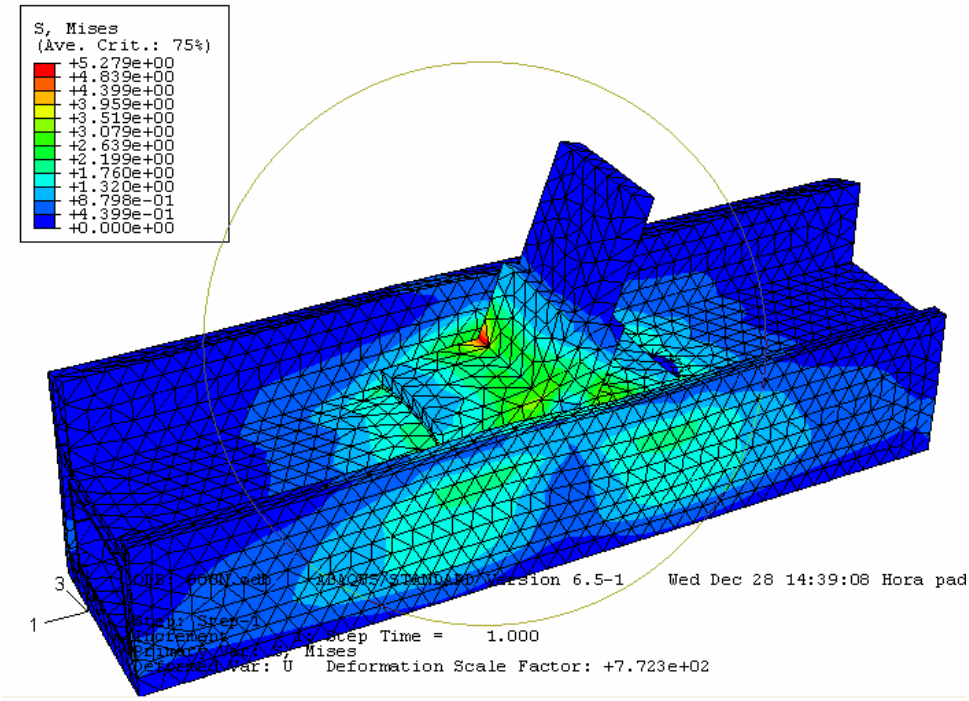

Figure 160. Bonded model stress distribution (Von Mises).

Figure 159 and 161 show that for the fastened joint, the T-joint accessory (P2090) is critically loaded at the base, which is in accordance with the experimental tests. The bonded joint (figure 160 and 162) also presents a stress concentration in the T-joint accessory (P2090). However, the experiments show that failure occurred in the adhesive. Therefore, the adhesive stress distribution should be analysed with more detail.

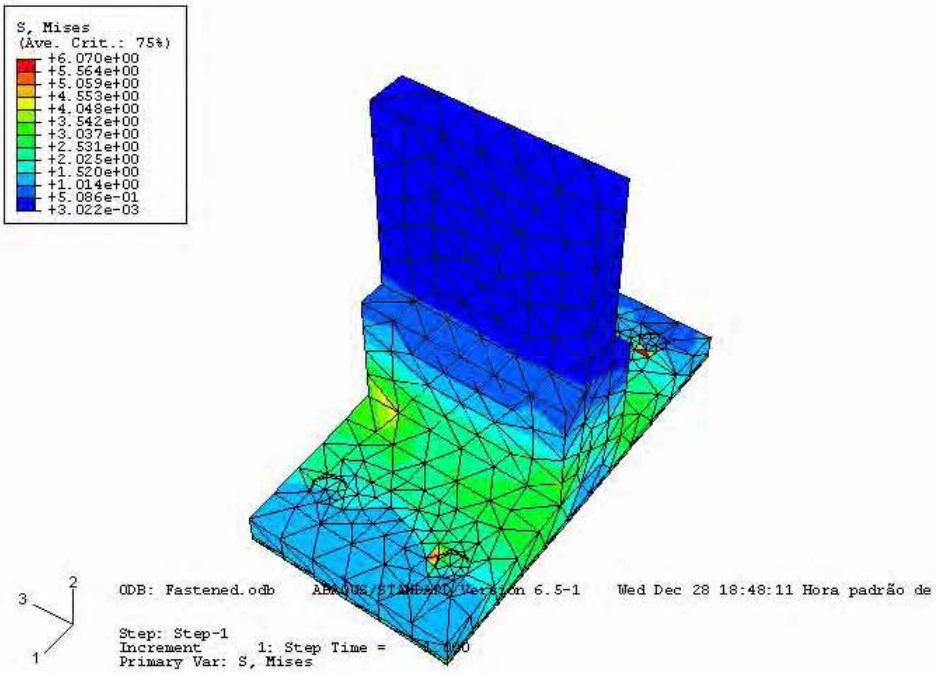

Figure 161. Fastened T-accessory (P2090) Von Mises stress contour.

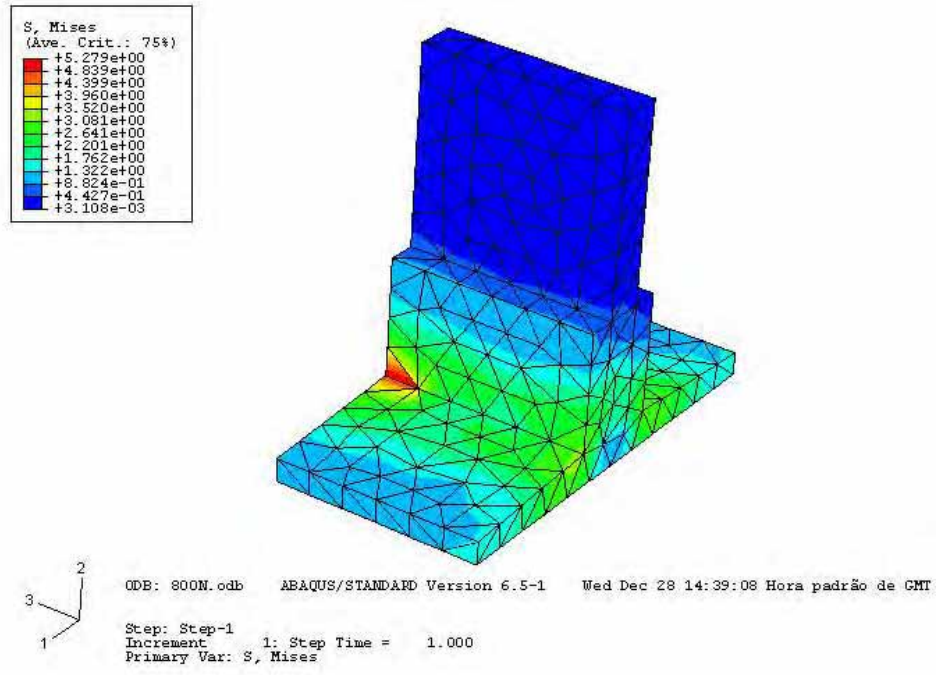

Figure 162. Bonded T-accessory (P2090) Von Mises stress contour.

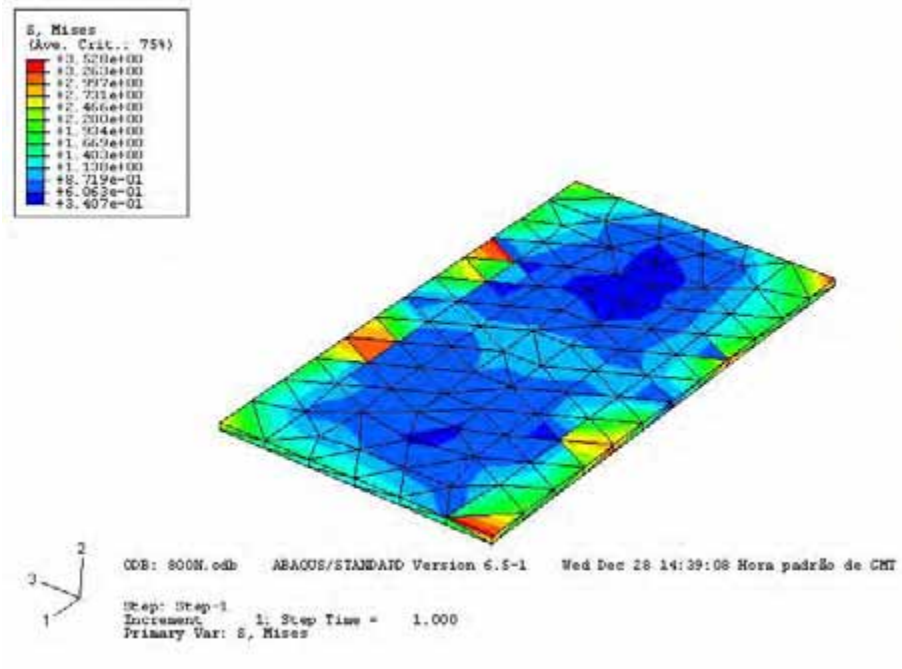

Figure 163. Adhesive Von Mises stress contour in the bonded model.

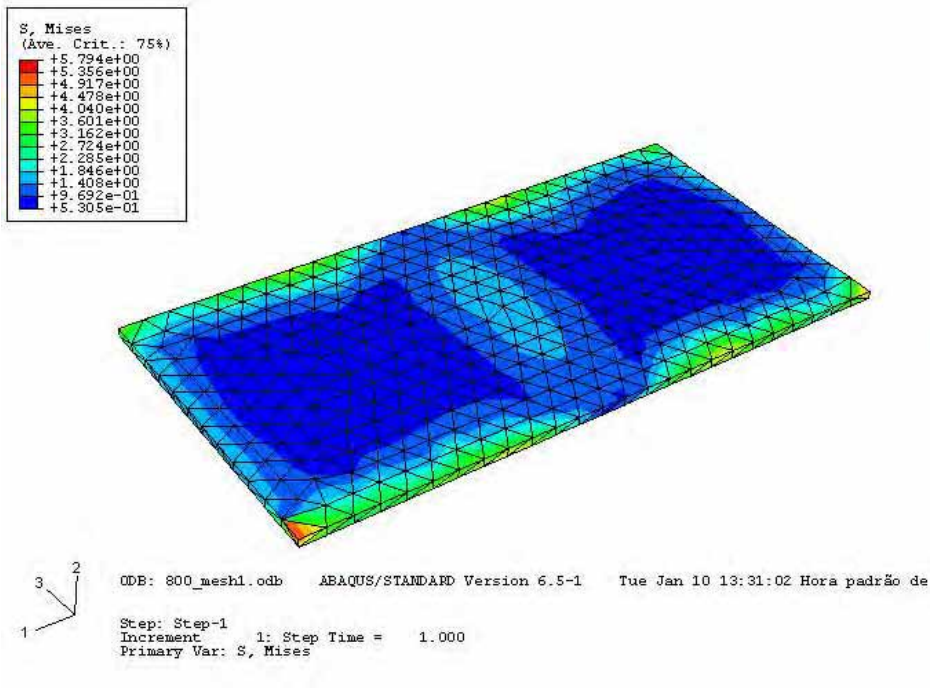

Figure 164. Adhesive Von Mises stress contour in the bonded model after mesh refinement.

Figures 163 and 164 show the Von Mises stress contour in the adhesive layer. A mesh refinement was carried out due to the high stress concentration as shown in figure 164. The maximum Von Mises stress in the adhesive is 5.80 MPa whereas in the PVC it is 5.30 MPa (see figure 162). Since the adhesive strength is 25 MPa and that of PVC is 45 MPa, the adhesive will break before the PVC. This confirms the experimental tests, where the failure

occurred in the adhesive. The experiments also indicated that the adhesive failed by peel, at the end of the T- joint accessory (P2090) base. Therefore, the normal stress distribution (σ_{22}) is an important stress component to analyse.

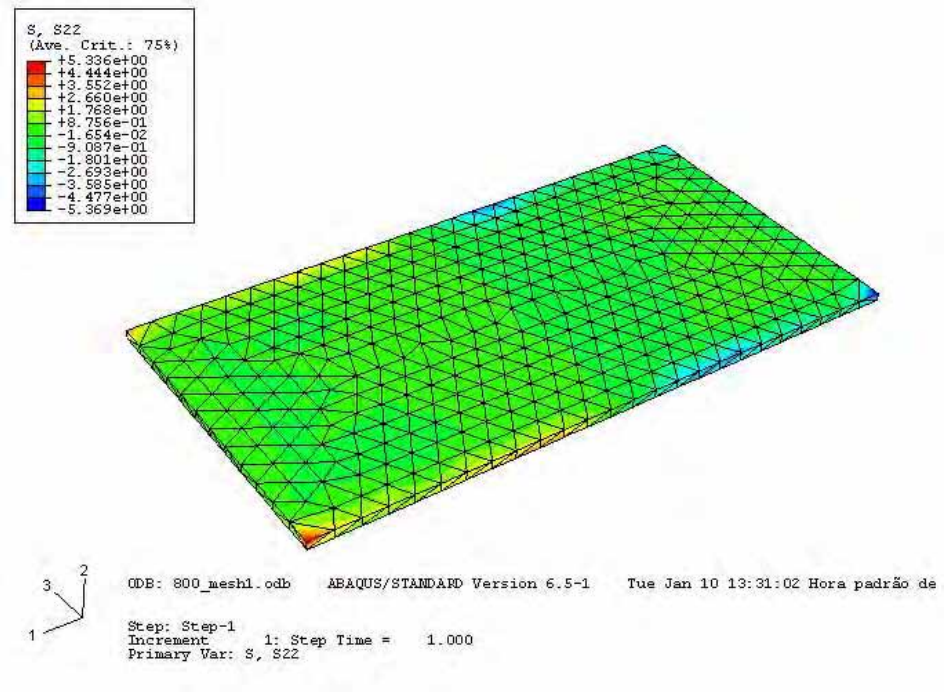

Figure 165. Normal stress (σ_{22}) contour in the adhesive layer.

Figure 165 shows the normal stress (σ_{22}) in the adhesive, where the peak occurs at the extremities with 5.34 MPa. This is in accordance with the experiments.

5.5.5 New design proposal

In order to reduce the adhesive stress concentration, the geometry of the T-joint accessory was modified as shown in figures 166, 167 and 168. These designs were proposed by Adams [50] to decrease the peel stress in the adhesive for lap joints.

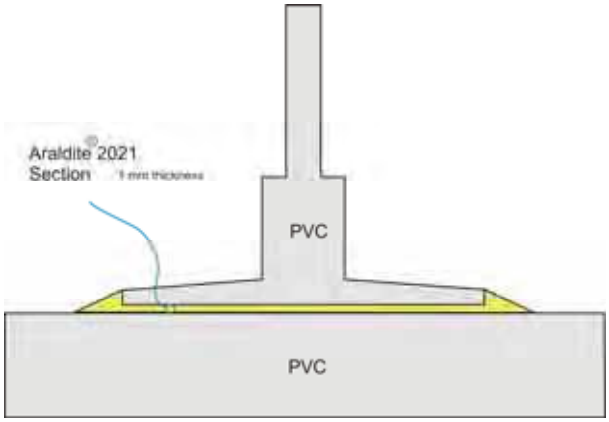

Figure 166. Design 1 – Adhesive fillet.

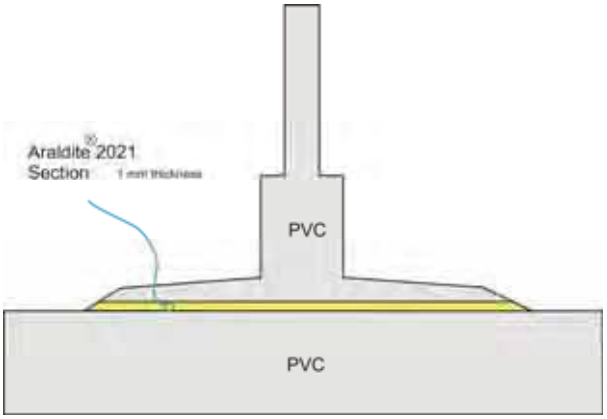

Figure 167. Design 2 – Adhesive fillet and outside taper in T-joint accessory.

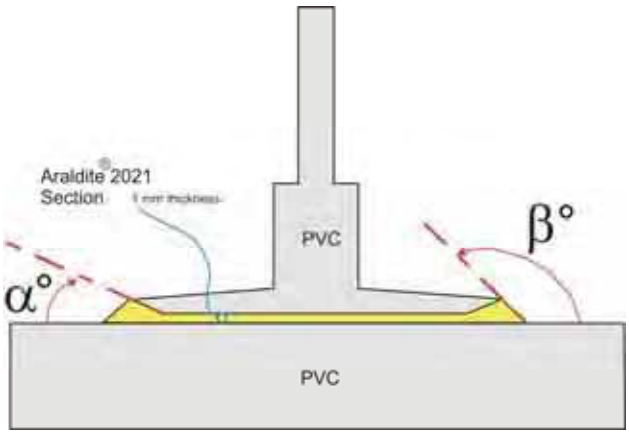

Figure 168. Design 3 - Inside taper in T-joint accessory and with adhesive fillet (β = 30º and α = 60º).

The adhesive fillet creates a smoother load transmission from the base profile to the T-accessory and the taper decreases the joint stiffness.

The mesh and boundary conditions are identical to the basic design described previously.

Running the computational calculus allowed to plot the following figures reflecting the stress distribution for the new design proposals.

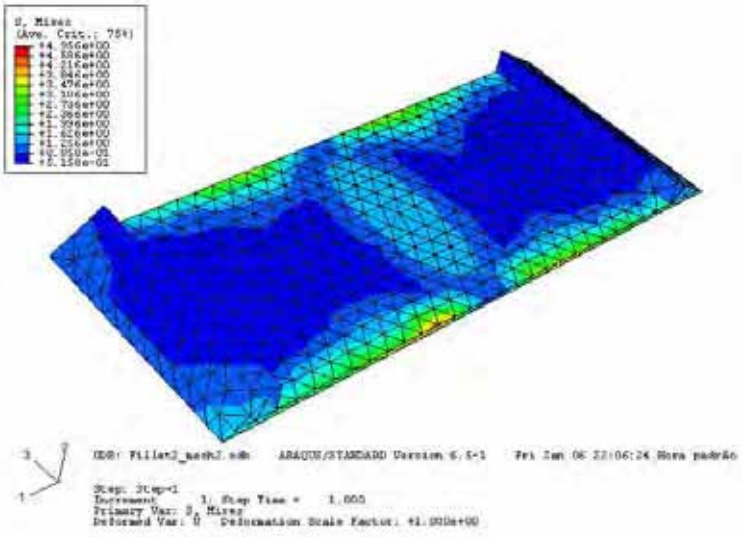

Figure 169. Adhesive Von Mises stress contour for design 1.

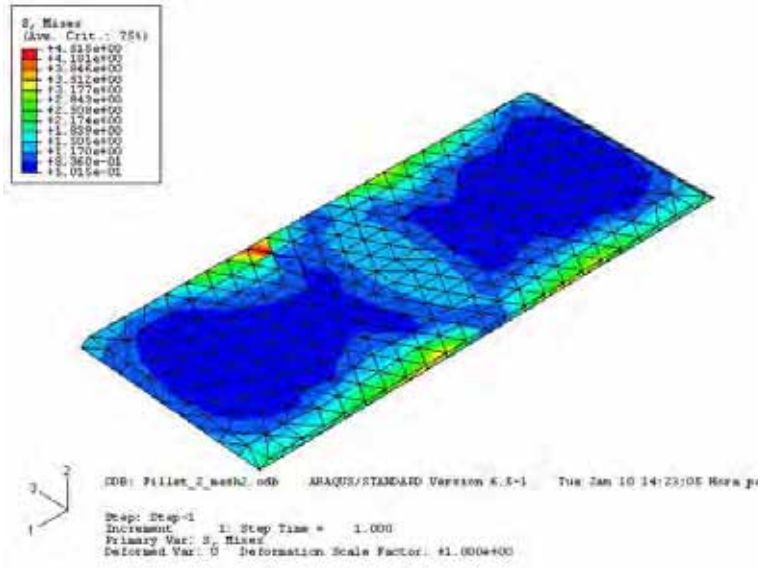

Figure 170. Adhesive Von Mises stress contour for design 2.

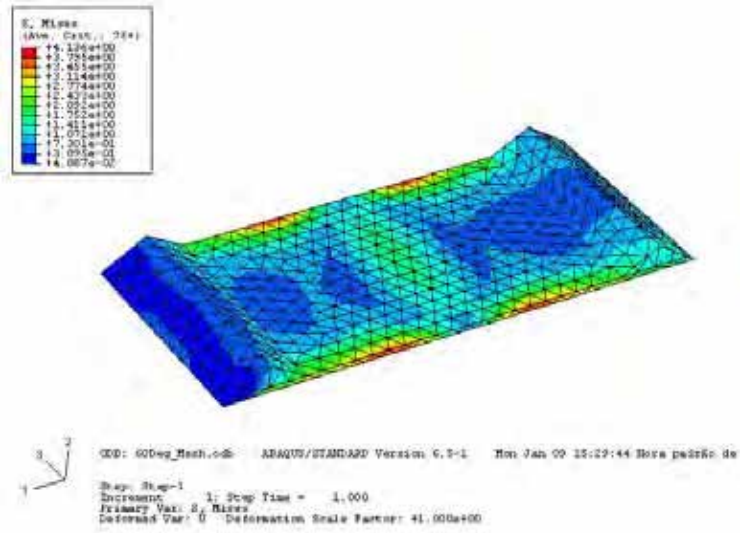

Figure 171. Adhesive Von Mises stress contour for design 3.

Figures 169, 170 and 171 show a progressive reduction in the maximal values of the Von Mises stress. This decrease from 5.80 MPa (initial design) to 4.14 MPa for design 3 (figure 171), represents a reduction of nearly 30%. The peel stress (σ_{22}) was also analysed and the results are presented in figures 172, 173 and 174.

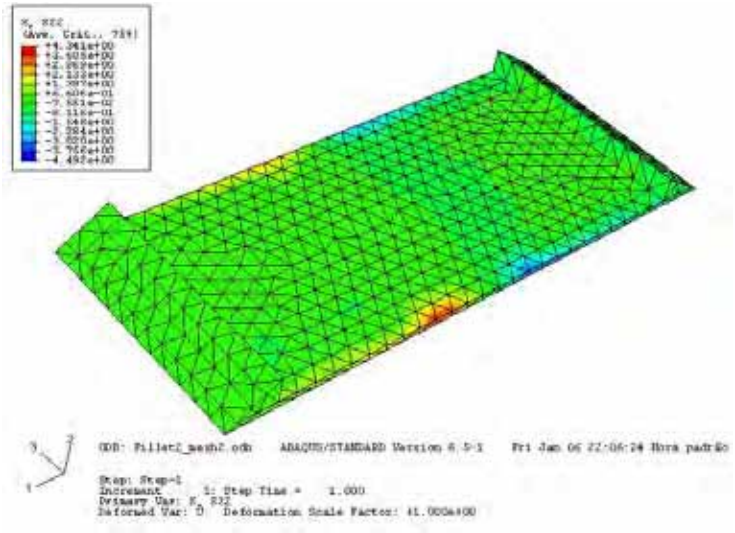

Figure 172. Normal stress (σ_{22}) stress contour for design 1.

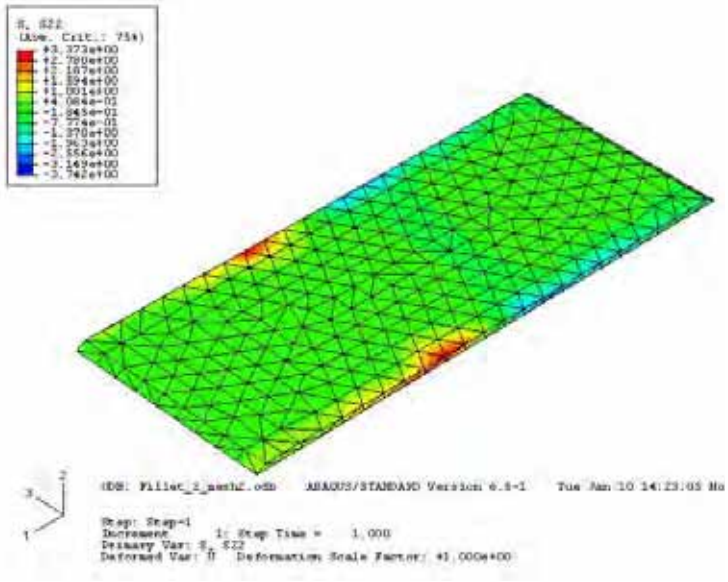

Figure 173. Normal stress (σ_{22}) stress contour for design 2.

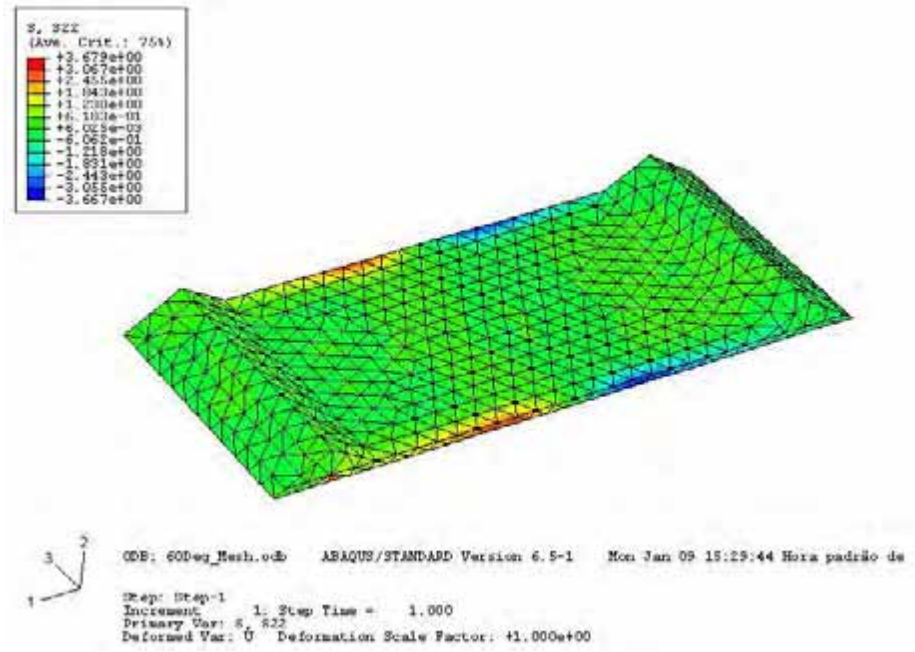

Figure 174. Normal stress (σ_{22}) stress contour for design 3.

As for the Von Mises stress, there is a reduction in the maximal values. When compared to the initial solution (figure 165), the normal stress (σ_{22}) reduction is approximately 30%.

Table 27 summarizes the results obtained for the basic design and the proposed designs for adhesive stress reduction.

Table 27. Stress values for each design and initial bond (in the adhesive layer)

FEM MODEL	Max Von Mises [MPa]	Max σ_{22} [MPa]
Initial (Bonded)	5.80	5.40
Design 1 (Bonded)	4.96	4.34
Design 2 (Bonded)	4.52	3.37
Design 3 (Bonded)	4.14	3.68

Table 27 shows that design 2 and design 3 provide an important improvement and will give an increased joint strength.The adhesive joint will have a clearly higher strength than the fastened joint and will therefore justify its use in terms of load bearing capacity.

Note that this finite element study was carried out only for position 1. The other positions should also be analysed to have an optimised solution for every type of loading.

Chapter seven

COST AND PROCESS ANALYSIS

7.1 Introduction

Nowadays, the industrial world is ruled by successful business rates and optimised profit margins. Production costs play a vital role and their reduction is a major goal.

This study would not be complete without a cost analysis for each solution (welded, screwed and glued) and a process comparison in industrial terms – time consumption, tools and workforce.

In this chapter, some considerations will be made about the industrial processes and then, the costs will be calculated for each technique.

7.2 Production Processes

There are at least four processes to produce this union (T-Joint) of profiles: welding, mechanical fastening with accessory (P2090), a mechanical attachment with accessory (P3270) placed with a tool (P3276 and 3278) and adhesive bonding.

There are several points to consider:

1. Time consumption;
2. Required tools;
3. Surface finish aspect;
4. Sealing properties;
5. Risk assessment.

7.2.1 Time consumption

In terms of the V welding process, there is the need to mill a V shape in the P2030 profile and also in the base profile P2000. Then the parts are welded in a special machine. The excess of material is removed after the part has cooled down to room temperature. This operation needs in total 8 minutes.

When fasteners and mechanical accessories are used, there is the need to mill the profile P2030 ends to fit P2000, place the accessory P2090 inside P2030 and screw 4 fasteners (see figure 176), and place it over P2000 and screw 4 other fasteners. This takes approximately 5 to 6 minutes. However, to obtain a good sealing, silicone must be applied over the joint perimeter, adding 1 or 2 more minutes. The overall process takes 6 to 8 minutes.

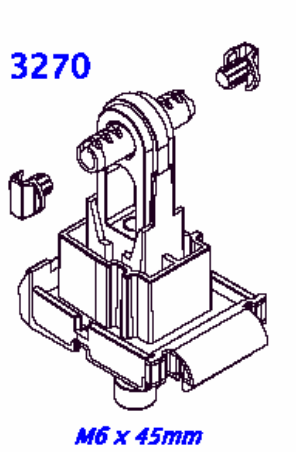

Figure 175. Accessory P3270.

The future solution with the accessory P3270 (figure 175), placed with a tool (P3276 and 3278) should take nearly the same time, because there is the need to mill, drill and then place the accessory with the tool and finally apply silicone.

With the structural adhesive joint the profile P2030 ends are milled and the adhesive is applied on the top. Adhesive is applied over the lateral surfaces of the accessory P2090 which is inserted in P2030. Then more adhesive is applied over the P2090 base. Finally P2030 and P2090 are placed over the P2000 profile. In the case of adhesive bonding, there is no need to apply silicone, due to the sealant properties of the adhesive. This process takes approximately 6 minutes.

7.2.2 Required tools

To weld the PVC, a specialized welding machine is necessary which is very costly, but profitable for big production rates. Mechanically fastened joints require common fastening screw machines, and silicone handgun for sealing. In the case of an adhesive joint, the cheapest solution is a handgun. For greater production rates a pneumatic handgun can be used.

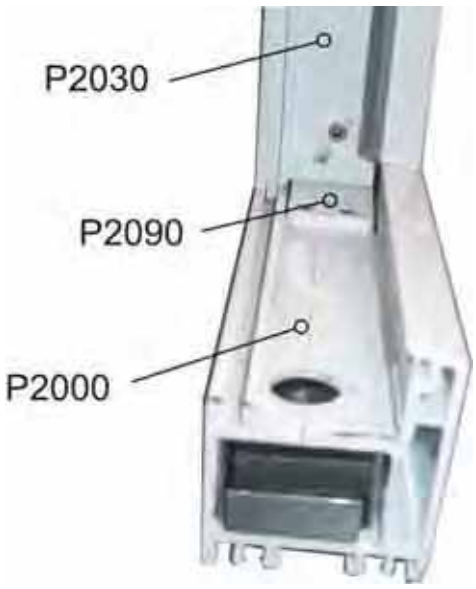

Figure 176. T-joint assembly (with screws).

Figure 177. Adhesive Joint without excess of adhesive removal.

7.2.4 Surface finish aspect

The welding option has a very good finish aspect (figure 178), but the mechanical fastening with screws leave the screws visible (figure 176), creating a joint finish with a raw aspect. The joint with adhesive has the best aspect once the adhesive excess have been removed. Figure 177 shows an adhesive joint before removing the excess of adhesive.

7.2.5 Sealing properties

This aspect is very important because the purpose of a window is to be a sealing element of the house perimeter.

Once again, welding is the optimal solution that guarantees material continuity and integrity. When screws are used, the profile is drilled and leaves a gap that must be sealed with silicone. Even so, this is not the best sealing solution.

An adhesive joint union does not imply drilling the profile, which represents an advantage, and its sealant properties are quite good because it is a methacrylate adhesive.

Figure 178. Welded joint.

7.2.6 Risk assessment

In an industrial environment, there are many risks at stake that should be noted and accounted to fairly compare the different options.

Welding is very safe in general, but there is always the possibility of burns because it involves temperatures near 250 ºC.

In the case of fastening solutions with screws, there is the danger to handle incorrectly the tools and cause some injuries, but it is improbable.

As regarding adhesive bonding, adhesives are chemical products that have some toxicity if ingested, skin absorbed or breathed and are often inflammable. Araldite® 2021™ is composed of two components and each one has its security sheet (see appendix VI). Basically, it is inflammable, it can cause eye and skin irritation as well as respiratory problems.

7.3 Cost analysis

The costs corresponding to manufacture the joint were calculated for each solution.

Welding technology involves the acquisition of a welding machine as seen earlier in the required tools, and implies a great amount of electric energy to maintain the temperature operational at nearly 250ºC. This compromises seriously the efficiency of this process and its environmental friendliness. The process needs cleaning after welding, which implies more machinery. However, it is the only process that requires no accessories.

Table 28. Welding process cost.

Tool/ machine investment	Welding machine	15000€ +
Energy consumption	Electricity	0.75€
Materials		0€
(cost for each joint*)	**Total**	**0.75€**

* Without the contribution of tool/machine investment

The mechanically fastened joint requires mostly screws, which nowadays are very cheap. To seal there is the need to use silicone, which introduces one more product and its associated costs. The mechanical joint also needs the accessory P2090. The machine used to fasten the screws is a pneumatic screw driver.

Table 29. Mechanical fastening cost.

Tool/machine investment		150€
Energy consumption	Electricity	0.25€
Materials	6 screws	0.2232€
	Silicone	0.25€
	P2090	1.54€
(cost for each joint*)	**Total**	**2.51€**

* Without the contribution of tool/machine investment

The future mechanical joint requires an initial investment in tools (P3278 and 3276) and a costly accessory (P3270) when compared to P2090. There is also the need to add silicone.

Table 30. Mechanical joint with P3270 cost.

Tool/machine investment	P3278 + P3276	56.61€ + 134.39€
Energy consumption	Electricity	0.25€
Materials	P3270	2.74€
	Silicone	0.25€
(cost for each joint*)	**Total**	**3.24€**

* Without the contribution of tool/machine investment

The adhesive joint requires the investment in tools, but it can be adapted to industrial production. In case of low production rates (characteristic of small factories) a cheap tool is used. For high production rates (characteristic of big factories) a pneumatic tool is used, which is a little more expensive.
Araldite® 2021™ is supplied in 50 ml or 400 ml cartridges. The 50 ml cartridges (costing 0.355 €/ml) are applied with the less expensive handgun while the 400ml cartridges (costing 0.133 €/ml) are applied with the pneumatic handgun.

Each joint requires nearly 12,5 ml of Araldite® 2021™ per joint (50 ml cartridge is enough for 4 joints). This value already contemplates the initial waste recommended by Huntsman®.

Table 31. Adhesive joint cost.

		50 ml	**400 ml**
Tool/machine investment	Handgun	20€	600€
Energy consumption	Electricity	0€	0.25€
Materials	Araldite® 2021™	4.43€	1.66€
	P2090	1,54 €	
(cost for each joint*)	**Total**	**5.97€**	**2.45€**

* Without the contribution of tool/machine investment

Notice that all the previous costs do not consider any waste that occur other than the advisable by the suppliers. Further studies should be done to assess the real cost for waste, contemplating a margin for it.

Table 32 summarizes the previous four tables.

Table 32. Joint costs summary.

	Welding	Mechanical (Screws)	Mechanical (P3270)	Adhesive Araldite 2021 50 ml / **400 ml**	
Costs	€				
Tool/machine investment	15000+	150	350	20	**600**
Energy consumption	0.75	0.25	0.25	0	**0.25**
Materials	0	2,31	2,99	5,97	**2.20**

To summarize this chapter, the next table aggregates all the major cons and pros of these processes.

Table 33. Comparison between the several joint processes.

	Welding	Mechanical (Screws)	Mechanical (P3270)	Adhesive Araldite 2021 50 ml / 400 ml	
Time consumption [min.]	8	6-8	6-8	6	
Required Tools	++++	++	+++	+	**++**
Surface finish aspect	ideal	bad	good	good	
Sealing properties	ideal	bad	bad	good	
Risk assessment	considerable	low	low	considerable	
Post-process	cleaning	silicone	silicone	cleaning	

+++	Extremely expensive	+++	Very expensive	++	expensive	+	cheap

Welding seems to be the best solution to join the transom with the base profile. However, residual stresses and the investment in machinery have been considered by the industry to be not practical, leading to the use of mechanical joining solutions. Comparing the mechanical solutions (screws fastening and P3270 mechanical fastening) with the adhesive bonding solution (when industrialized (400 ml)), proposed in this study, the last one proves to be a competitive solution.

Chapter eight

CONCLUSION AND FUTURE WORK

8.1 Conclusion

The tensile bulk adhesive tests and the single lap joint tests show that a toughened methacrylate is ideal for PVC application. The adhesive and cohesive properties of the adhesive are such that the failure takes place away from the joint area, in the PVC.

The weathering tests on SLJs and adhesive bulk specimens show that the adhesive has a better environmental resistance than the PVC. Therefore, the adhesive is not only adequate for initial strength but also for long term strength.

The preliminary static T-joint tests show that the adhesive joint is comparable or better to a fastened joint in terms of load bearing capacity. The optimization of the T-joint geometry for adhesive bonding indicates that strength can be increased. This reinforces the use of adhesive bonding in terms of mechanical behavior. However, this theoretical optimization needs confirmation with experimental tests.

The cost analysis comparison for the proposed adhesive T-joint solution proved to be in its favor. Therefore, it can be considered to have industrial application, and if so, it would certainly bring large scale economy savings.

This work as evolved from an industrial design point of view to an engineering approach, into the search for the best solution.

8.2 Future Work

Despite all the work done in this study, the research of the best solution for the PVC transom to windowframe T-Joint bonding is far from being complete.

1. Additional testing should be done to validate experimentally the T-joint optimization by FEA.
2. Position 2 and 3 should also be considered.
3. The weathering tests should be carried out with a longer timeframe in order to fully characterize the joint lifetime and the U.V. radiation should be included.
4. The adhesive application in the T-Joint should also be improved in order to minimize the adhesive waste and the cleaning of the joint.
5. The ultimate test will be the application of this adhesive joint in its work environment hopefully for several decades.

References

[1] Munari, B., (1981) *Da cosa nasce cosa*. Laterza.

[2] Deceuninck plastic industries technical catalogue (1999) , Deceuninck Plastic Industries, N.V..

[3] (undated) Règles de bonne pratique pour l'assemblage dês profilés par soudage au miroir chauffant, Solvay & Cie.

[4] Deceuninck Zendow Window catalogue (2004), Deceuninck Plastic Industries, N.V..

[5] ASEFAVE and AENOR, (2005) *Manual de producto Ventanas*, AENOR.

[6] Henkel Corporation - Loctite (2005, December – last update) [Online]. Available: www.loctite.com [undated] (Copyright © 2003 Henkel Corporation. All Rights Reserved).

[7] CSIRO Australia (2004, 10 June – last update). [Online]. Available: http://www.csiro.au/pubgenesite/research/human_health_nutrition/ frogGlue.htm [2004, 10 June].

[8] Edward, M. Petrie (2000), *Handbook of Adhesives and Sealants*. McGraw-Hill.

[9] Huntsman Users Guide to Adhesives (undated), Huntsman.

[10] Kinloch, A.J. (1987) *Adhesion and Adhesive*s. Chapman And Hall.

[11] Tabor, D., & RHS Winterton, (1969) The direct measurement of normal and retarded van der Waals forces, **Proc**. **Roy**. **Soc**., **A, 312**, pp. 435-450.

[12] Israelachvili JN, Tabor D (1972) The measurement of Van Der. Waals dispersion forces in the range 1.5 to 130 nm. **Proc R Soc. A 331**. pp.19–38.

[13] Johnson, KL Kendall, K. and Roberts, (1971) AD 'Surface energy and the contact of elastic solids'. **Proc**. **Roy Soc**., **A324**. pp. 301-320.

[14] DJ Arrowsmith, (1970) Adhesion of electroformed copper and nickel to. Plastic laminates," **Trans**. **Inst**. **Metal Finish., vol. 48**. pp. 88–92.

[15] Packam, D.E. (1981) *Developments in Adhesives*. Second edition. Applied Science Pub, London.

[16] Packam. D.E. (1983) *Adhesion Aspects of Polymeric Coatings*. K.L.Mitta Plenum, New York.

[17] Kusaksa, I. and W. Suetaka (1980) *Electromagnetic effect in Enhanced Infrared Absorption of absorbed molecules on thin metal films*. **Acta**. **36A** . p. 647

[18] Pritchard, W.H. (1970) *Aspects of Adhesion* . 6(ed. D.J. Alner), University of London Press, London.

[19] Rowell R. M., Banks W. B., 1987. Tensil strength and toughness of acetylated pine and lime flakes. **Brit. Polymer J., 19**. pp. 478-482.

[20] Klein, I.E., Sharon,J. Yaniv, A.E., Dodiuk, H. and Katz, D. (1983) Chemical interactions in the system anodized aluminum—primer—adhesive **Int. J. Adhes. Adhes**. **3**, p. 159.

[21] Whu, S. (1982) *Polymer Interface and Adhesion*. Marcel Dekker, New York.

[22] Crisp, S., Prosser, H.J. and Wilson, A.D. (1976) An infrared spectroscopic of poly(acry1ic acid) **J. Mater. Sci**. **11**, p. 36.

[23] Sugama, T.,Kukacka, L.E. and Carciello, N. (1984) Nature of interfacial and oxide metal surfaces **J. Mater. Sci**. **19**, p. 4045.

[24] Chu, H. T., Eib, N.K., Gent, A.N. and Henriksen, P.N. (1979) *Advances in Chemestry Series* **174** (ed. J. L. Koenig). American Chemical Society, Washington DC. p. 87.

[25] Deryaguin, B.V. (1955) ***Research 8***, 70.

[26] Deryaguin, B.V., Krotova, N.A., Karassev, V.V., Kirillova, Y.M. and Aleinikova, I.N. (1957) *Proceedings of the 2nd International Congress on Surface Activity-III*. Butterworths, London. p.417.

[27] Lin, C.B., Lee, S. and Liu, K.S. (1991) Microstructure of Solvent-Welding in PMMA **J. Adhesion**, **34**. pp. 221-240.

[28] Titow, W.V. (1978) Adhesion – 2 (ed. K.W. Allen). Applied Science Pub, London. p.181.

[29] Brewis, D.M. (1993) Adhesion to polymers: how important are weak boundary layers ? **Int. J. Adhes. Adhes**.., **13**. p. 251.

[30] Lord Corp. (undated). Chemical Product Div., Cary, NC.

[31] Loctite Corp. (undated), Rock Hill, CT.

[32] B.F. Goodrich General Products Bulletin, (1972), GPC-72-AD-3.

[33] Esteves, J.L. (1990) Estudo do comportamento de adesivos estruturais. MSc Thesis, FEUP.

[34] da Silva, L.F.M. (2003) Adhesive joints for high and low temperatures. PhD Thesis, Univeristy of Bristol.

[35] Volkersen O. (1938) Die nietkraftoerteilung in zubeanspruchten nietverbindungen konstanten loschonquerschnitten.***Luftfahrtforschung*** **15**. pp. 41-47 (in German).

[36] Goland, M., Reissner, E. (1944)*The stresses in cemented joints*. **J. of App. Mech. ,Transactions ASME**, **66**. pp. A17-A27.

[37] Hart-Smith, L. J. (1973) *Adhesive bonded double lap joints*. ***NASA CR-112235***.

[38] Hart-Smith, L. J. (1973) *Adhesive bonded double lap joints*. ***NASA CR-112235***.

[39] Renton, W. J. and Vinson, J. R. (1975) *The efficient design of adhesive bonded joints*, **J Adhesion, 7**. pp. 175-193.

[40] Allman, D.J. (1977) A theory for elastic stresses in adhesive bonded lap joints, **Q J. Mech. Appl. Math**, **30**. pp. 415-436.

[41] Adams, R.D. and Mallick, V (1992) A method for the stress analysis of lap joints, **J. Adhesion**, **38**. pp. 199-217.

[42] Ojalvo, I. U. and Eidinoff, H.L. (1978) Bond thickness effects upon stresses in single-lap adhesive joints, **AIAA Journal**, **16**. pp. 204-211.

[43] Frostig, Y., Thomsen, O.T. and Mortensen, F. (1999) Analysis of adhesive-bonded joints, square-end, and spew-fillet – high-order theory approach, **J Engrg Mech, ASCE**, **125**. pp. 1298-1307.

[44] Adams, R.D. and Peppiatt, N.A. (1973) Effects of Poisson's ratio strains in adherends on stress of an idealized lap joint, **J. Strain Anal**., **8**. pp. 134-139.

[45] Apalak, Z.G., Apalak, M. K., Davies, R. (1996) Analysis and design of tee joints with double support, **Int. J. Adhes. Adhes**., **Volume 16**, Number **3**.

[46] da Silva, L.F.M. and Adams, R.D. (2002) The strength of adhesively bonded T-joints, **Int. J. Adhes. Adhes**., **22**. pp. 311–315.

[47] Broughton, W. R., Crocker, L. E., Gower, M. R. L. and Shaw, R. M. (2004) Assessment of Predictive Analysis for Bonded and Bolted T-Joints, **NPL Report DEPC-MPR 002**.

[48] V.Marcadon, V. , Nadot, Y., Roy, A., Gacougnolle, J.L. (2005) Fatigue behavior of T-joints for marine applications, **Int. J. Adhes. Adhes**. In press.

[49] Adams, R.D., Comyn, J. and Wake, W.C. (1997) *Structural Adhesive Joints in Engineering Second Edition*, Chpaman & Hall.

[50] Adams, R.D., Atkins, R.W. , Harris, J.A. and Kinloch, A.J., (1986) Stress Analysis and Failure properties of carbon-fibre-reinforced-plastic/Steel Double-lap joints, **J. Adhesion** , **20**. pp. 29-53.

[51] Hildebrand, M (1994), Non-linear analysis and optimization of adhesively bonded single lap joints between fibre-reinforced plastics and metals, **Int. J. Adhes. Adhes.**, **14**. pp. 216-267.

[52] Groth, H.L. and Nordlund, P (1991), Shape optimization of bonded joints, **Int. J. Adhes. Adhes.**, **11**. pp. 240-212.

[53] Potter, K.D., Guild, F.J., Harvey, H.J., Winsom, M.R. and Adams, R.D., (2001) Understanding and control of adhesive crack propagation in bonded joints between carbon fibre composites adherends I. Experimental, **Int. J. of Adhes. Adhes.**, **21**. pp. 435-443.

[54] Kaye, R., Heller, M, (2005) Through-thickness shape optimisation of typical double lap-joints including effects of differential thermal contraction during curing, **Int. J. of Adhes. Adhes. 25**. pp. 227-238.

[55] Terry L. Gordon, Martin E. Fakley, (2003) The influence of elastic modulus on adhesion to thermoplastics and thermoset materials, **Int. J. Adhes. Adhes., 23**. pp. 95-100.

[56] The Loctite Design Guide for Bonding Plastics, (undated), **Volume 2**. Loctite Inc. pp. 14-67

[57] da Silva, L.F.M., Adams, R.D. and M. Gibbsb, (2004) Manufacture of adhesive joints and bulk specimens with high-temperature adhesives, **Int. J. Adhes. Adhes., 24**. pp. 69–83

[58] Standard specification for adhesive bulk specimen (1988). Designation **NF T 76-142**. Méthode de préparation de plaques d'adhésifs structuraux pour la réalisation d'eprouvettes d'essai de caractérisation.

[59] Standard Test Methods for Plastics (1976). Designation **BS 2782: Part3**. British Standard Methods of testing Plastics, Part 3. Mechanical Properties, Methods 320ª to 320 F. Tensile strength, elongation, and elastic modulus.

[60] Chousal , José Augusto Gonçalves, (1999) Processamento de Imagens Obtidas por Métodos Ópticos em Análise Experimental de Tensões. PhD Thesis, FEUP.

[61] Standard Test Method for apparent shear strength of single-lap-joint adhesively bonded metal specimens by tension loading (metal-to-metal). Designation **D1002-01**.American Society for the Testing of Materials, **Volume 15.06**, August 2002 Adhesives.

[62] Adams, R. Mallick,V, Davies,R., (1998) **V.C.Joint v.1.0** , University of Bristol.(Software)

[63] Wypych,G., Faulkner, T. (1990) *Basic Parameters in Weathering Studies -Testing to Mirror Real Life Performance*. William Andrew Publishing/Plastics Design Library. pp. 1-14.

[64] Summers and Rabinovitch, E.B. (1990) Weatherability of Vinyl and Other Plastics in Weathering of Plastics - *Testing to Mirror Real Life Performance, William Andrew Publishing/Plastics Design Library*. pp. 61-68.

[65] Trotignon, J.-P. , Verdu, J., Dobraczynski, A. , Piperaud, M. (1996) *Matières Plastiques, Les Précis AFNOR/Nathan*. Editions Nathan.

[66] Minsker, K. S. , Zaikov, G.E. , Zaikov, V.G. , (2005) Achievements and Research Tasks for Poly (vinyl chloride) Ageing and Stabilization, in ***Macromol. Symp**. **228**, pp.* 299-313.

[67] Gervat, L. *and* Morel, P. (1996) Analysis of the main parameters affecting the change of color and Physical Properties of weathered PVC profiles, ElfAtochem S.A.Centre d'Application de Levallois Levallois-Perret, France, **J. Vinyl Addit. Tech., Vol. 2**, No. **1**. pp. 37-43.

[68] H. Kondo, T. Tanaka, T. Masuda, A. Nakajima , (1992) Aging Effects in 16 years on mechanical properties of commercial polymers, **Pure &App*l*. Chern., Vol. 64, No. 12**, pp. 1945-1958.